Masters   Engineering

2014-2

Is Vehicle Characterization in Accordance With Standard Test Procedures a Necessary Prerequisite for Validating Computer Models of a Test Vehicle?

Michael Hall
Technological University Dublin, michael.hall@tudublin.ie

Recommended Citation

Is Vehicle Characterization in Accordance with Standard Test Procedures a Necessary Prerequisite for Validating Computer Models of a Test Vehicle?

A thesis submitted in partial fulfillment of the requirements for the award of the
Degree of Master of Philosophy of the Dublin Institute of Technology (DIT).

by

Michael Hall BSc BA

Department of Transport Engineering
School of Spatial Planning & Transport Engineering
Dublin Institute of Technology : Bolton Street.

Supervisors

Prof. Stephen Jerrams DIT Dublin
Dr Shaun McFadden TCD Dublin (formerly DIT)
Prof. Mike Blundell, Coventry University UK.

February 2014

Declaration

I certify that this thesis, which I now submit for examination for the award of Master of Philosophy of the Dublin Institute of Technology, is entirely my own work and has not been taken from the work of others, save and to the extent that such work has been cited and acknowledged within the text of my work.
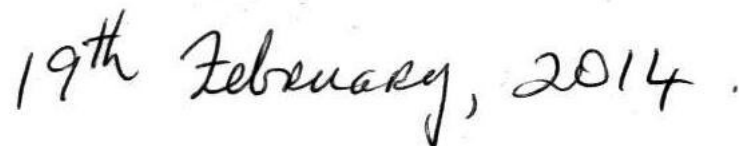
This thesis was prepared according to the regulations of the Dublin Institute of Technology for postgraduate study by research and has not been submitted in whole or in part for another award in any other third level institution.

The work reported on in this thesis conforms to the principles and requirements of the Dublin Institute of Technology's guidelines on ethics in research.

Signed: *Michael Hall*

Date: *19th February, 2014.*

Abstract

Vehicle characterization is the process by which a particular vehicle's inherent dynamic behavior is classified by measuring its response to certain command inputs under standard test conditions. Such information is required when comparing its performance to that of other vehicles in response to the same test event and it is also used to authenticate computer models of the test vehicle. The aim of this research was to determine whether vehicle characterization is possible using data from non-standard tests and to judge whether such data can also be used for the purpose of validating a computer model of the test vehicle.

The tests used as the benchmarking standard against which this proposition was appraised were those prescribed by the International Standards Organization (ISO), in particular, the *Steady State Cornering* test, the *Step Steer (J-turn)* test, and the *Power-off in a Turn* test. A suitably instrumented Ford Mondeo was prepared and subjected to basic versions of these tests that were not conducted in full compliance with the procedures and conditions laid down by the ISO standard, and a body of data was recorded.

This time history data was analyzed and, despite the suboptimal and disparate nature of the individual test runs, it generated two vehicle characteristic values that were shown to comply with expectations for the test vehicle and could be used as part of a validation process. These were the vehicle's understeer gradient of about 1deg/g and the yaw rate gain of 0.163 deg/sec per deg. In addition, the time history data from all of the non-standard tests performed was subjected to Fast Fourier Transform (FFT) analysis in order to identify the vehicle's natural frequencies of vibration and the results obtained were used to validate a modal or 'ride' model of the test vehicle.

By this means it was demonstrated that neither the process of vehicle characterization nor that of validating a computer model of the vehicle requires data obtained from standardized vehicle tests such as those prescribed by the ISO.

Acknowledgements

The author wishes to thank those who provided assistance, support or guidance in the period during which this work was undertaken. In chronological order:-

Contents

List of Figures

List of Tables

Nomenclature

The nomenclature used is in compliance with ISO 8855: 1991 *Glossary of Terms for Road Vehicle Dynamics and Road Holding Ability*.

a	acceleration (m/s^2)
acc	acceleration (m/s^2)
a1	Distance of Centre of Gravity from Front Axle (m)
a2	Distance of Centre of Gravity from Rear Axle (m)
a_c	Centripetal Acceleration (m/s^2)
a_X	Longitudinal Acceleration (m/s^2)
a_Y	Lateral Acceleration (m/s^2)
a_Z	Vertical Acceleration (m/s^2)
b1	Distance of Centre of Gravity from Vehicle Nearside (m)
b2	Distance of Centre of Gravity from Vehicle Offside (m)
deg	degrees
df	Front Axle Trackwidth (m)
dr	Rear Axle Trackwidth (m)
dZ(LF)	Vertical Displacement of Left Front Wheel
dZ(LR)	Vertical Displacement of Left Rear Wheel
dZ(RF)	Vertical Displacement of Right Front Wheel
dZ(RR)	Vertical Displacement of Right Rear Wheel
F	Force (newtons, N)
F_X	Longitudinal Force (newtons, N)
F_Y	Lateral Force (newtons, N)
F_Z	Vertical Force (newtons, N)
f	Frequency (Hz)
f_d	Damped Natural Frequency of Vibration (Hz)
f_n	Natural Frequency of Vibration (Hz)
g	Gravitational Acceleration (9.81 m/s^2)
h	Height of Vehicle's Centre of Gravity (metres, m)
i_S	Steering ratio (that is, $\delta_H : \delta_A$)
I	Inertia (kgm^2)
I_X	Moment of Inertia about the X axis (kgm^2)
I_Y	Moment of Inertia about the Y axis (kgm^2)
I_Z	Moment of Inertia about the Z axis (kgm^2)
kg	kilogramme
km/hr	Kilometre per hour

k_s	Suspension Spring Stiffness
k_w	
kRf	Front Anti-roll Bar Stiffness
kRr	Rear SAnti-roll Bar Stiffness
L	Vehicle Wheel Base
m	Mass (kg)
m_{spr}	Sprung Mass
m_{spr_Fr}	Front Sprung Mass
m_{spr_Rr}	Rear Sprung Mass
$m_{unsprung}$	Unsprung Mass
m_{Fr_unspr}	Front Unsprung Mass
m_{Rr_unspr}	Rear Unsprung Mass
r	Radius
$r_{gyration}$	Radius of Gyration
r_{wheel}	Wheel Radius
R_{Front}	Ground Reaction at Front Axle
R_{Rear}	Ground Reaction at Rear Axle
RotX	Rotation about the X axis
RotY	Rotation about the Y axis
RotZ	Rotation about the Z axis
SS	Steady State
T_{Fr}	Vehicle's Front Wheeltrack (m)
T_{Rr}	Vehicle's Rear Wheeltrack (m)
t	Time (sec)
t_0	Time at which an event is initiated
V	Volts
v	Velocity (m/s)
v_X	Vehicle Longitudinal Velocity (m/s)
v_Y	Vehicle Lateral Velocity (m/s)
W	Weight (N)
W_f	Weight on Front Axle (N)
W_{fl}	Weight on Front Left Wheel (N)
W_{fr}	Weight on Front Right Wheel (N)
W_r	Weight on the Rear Axle (N)
W_{rl}	Weight on Rear Left Wheel (N)
W_{rr}	Weight on Rear Right Wheel (N)
x	spring extension (m)
x	Deflection, change in length
α	Angular Acceleration (rad/s^2)
α	Wheel Slip Angle

α_f	Front Wheel Slip Angle
α_r	Rear Wheel Slip Angle
β	Vehicle Sideslip Angle
δ_A	Kinematic or Ackermann angle at a steerable wheel
δ_H	Handwheel (Steering Wheel) Angle (degrees)
λ	
μ	Coefficient of Friction between tyres and road
φ	Roll Angle (degrees)
$\dot{\varphi}$, $d\varphi/dt$	Roll Rate/Velocity (deg/sec)
θ	Pitch Angle (degrees)
$\dot{\theta}$, $d\theta/dt$	Pitch Rate/Velocity (deg/sec)
ψ	Yaw Angle (degrees)
$\dot{\psi}$, $d\psi/dt$	Yaw Rate/Velocity (deg/sec)
ω	Angular Velocity (rad/s)
ω_d	Damped Natural Circular Frequency (rad/s)
ω_n	Natural Circular Frequency (rad/s)
ζ	Damping Ratio

Abbreviations

ADAMS   Automatic Dynamic Analysis of Mechanical Systems

BS   British Standards

CAE   Computer Aided Engineering
CoG   Centre of Gravity

DAQ   Data Acquisition as in DAQ-Pac
DOF   Degree of Freedom

FFT   Fast Fourier Transform

ISO   International Organisation for Standards

LF   Left Front Wheel
LR   Left Rear Wheel
LHS   Left Hand Side
LMS   Engineering Computer Software
LPM   Lumped Parameter Mass

MATLAB   Matrix Laboratory (Numerical Computing Software)
MBF   Multi-body Formulation
MBM   Multi-body Model

NVH   Noise Vibration and Harshness

RF   Right Front Wheel
RR   Right Rear Wheel
RHS   Right Hand Side
RPM   Revolutions per minute

SAE   Society of Automotive Engineers
SS   Steady State

YRG   Yaw Rate Gain (or yaw velocity gain)

Chapter 1: Introduction

1.1   Research Question and Aim of the Research

The research described here was conducted in order to address the following question:

*Is Vehicle Characterization in Accordance with Standard Test Procedures a
Necessary Prerequisite for Validating Computer Models of a Test Vehicle?*

To provide an answer to this question the primary aim of this research was to field test a Ford Mondeo saloon car and assess the test results for the purpose of validating computer models of the vehicle.

1.2   Objectives

In order to complete this programme of research and achieve its primary aim the following strategic objectives were identified at the outset:-

(1) To complete a Literature Survey in order to identify and study the work of relevant researchers in the field of vehicle dynamics and vehicle testing;

(2) To decide on a programme of tests for the test vehicle;

(3) To instrument and prepare a test vehicle and subject it to various road tests designed to obtain data for use in the validation of computer models of the vehicle;

(4) To prepare, post-process and plot the time history data obtained from these tests;

(5) To assess the tests conducted with respect to the recommended ISO standard tests;

(6) To analyse the time history data obtained from the tests in order to determine the characteristic values of the test vehicle as prescribed by the ISO standards;

(7) To assess these characteristic values, and the test data generally, in light of their possible use for the validation of computer models of the test vehicle;

(8) To establish how rigorously such tests need to be conducted for this purpose;

(9) To create a representative rigid-body ride (or modal) model of the test vehicle and validate it by reference to the test data collected.

1.3   Research Facilities and Support

An instrumented test vehicle was made available through the Wolfson School of Mechanical and Manufacturing Engineering, Loughborough University. This was a Ford Mondeo 2 Litre Zetec Saloon car which was used for research purposes by post-graduate students studying vehicle dynamics and was on loan from the Automotive & Aeronautical Department of the same university. In addition, support was provided by technical staff that assisted with the preparation of the vehicle for testing. The Mondeo already came equipped with eleven sensors together with an onboard data acquisition system. Some of the sensors needed servicing and recalibration, and four new wheel vertical deflection sensors were installed on the vehicle and calibrated.

Testing was conducted on the Loughborough University campus, in car parks and in other public places because state-of-the-art test sites and facilities were unavailable or could not be laid out due to a lack of space, funding, time or manpower. The vehicle was driven by one of the university staff who was not a professional test-driver.

1.4   Methodology

In order to successfully achieve the overall aim and objectives that have been set out it was necessary to obtain particular characteristic information about the test vehicle and assess its quality both in terms of its intrinsic value and as a basis for any future validation of a computer model. Vehicle characterisation is the process by which vehicle behaviour in response to input commands is quantitatively determined using information recorded during testing and then subsequently analysed. The result is a set of characteristic values unique to that vehicle which may be used to compare it with other vehicles that have been subjected to exactly the same test procedures.

One aspect of the research undertaken was to explore the requirements for the successful validation of a relatively simple computer model, although the same requirements would also be relevant to the validation of more complex models. What are the procedures needed to satisfactorily validate a model? What criteria ought to be

applied and why? One particular objective was to investigate the use of ISO standard tests as a means of characterising the dynamic behaviour of the vehicle and also, in the light of the problems encountered, to explore how rigorously such standard tests need to be conducted in order to provide acceptable data for model validation purposes. Are properly conducted ISO vehicle tests necessary or even sufficient for such a purpose? Are the ISO standards a suitable template for validating a computer model? All that is claimed by the ISO standard is that the tests provide repeatable and discriminatory results that enable the characterisation of a vehicle's dynamic properties. Any given test aims to focus on particular repeatable vehicle behaviour under controlled conditions. These tests are therefore designed to replicate as closely as possible the conditions under which a particular vehicle is tested in order to eliminate as many uncontrolled variables as possible. Ultimately such tests not only enable the characterisation of an individual vehicle but they also allow meaningful comparisons to be made between it and other vehicles that have performed the same test.

In most of the introductions to the ISO standards literature – for example, the International Standard ISO 9816 (2006) *Passenger Cars: Power-off of a Vehicle in a Turn* – it is quite reasonably stated that because test conditions and tyres have so strong an influence on the results obtained only vehicle characteristics determined under identical test and tyre conditions are comparable one with the other. They further state that because insufficient knowledge exists concerning the correlation between the dynamic properties of vehicles and accident avoidance, test results cannot be used for regulatory purposes and can only be considered significant for a very small part of a vehicle's overall dynamic behaviour. So, even though all of the ISO standards attempt to prescribe repeatable and controllable test conditions while at the same time recognising the complexity of the vehicle's total dynamic behaviour, they declare that the results only have limited significance to a relatively narrow aspect of the vehicle behaviour and then only if the test standards are met.

It is important to note that when using such tests and their results for validating a computer model of a vehicle the issue of control and repeatability can hardly be said to be of major concern. Model validation and vehicle characterisation do not have the same objectives. A particular computer model is always custom built to model a

specific vehicle operating in well defined simulation conditions. It is also going to be a simplification of the real thing and because it is numerically based it is always going to give the same results (outputs) for the same inputs. Certainly, this is true of a deterministic approach to modelling. The problem associated with validation is not about the reproducibility of results from one test to another in order that meaningful comparisons can be made between vehicles, but concerns the ability of a model to faithfully reproduce the same results as those obtained from a particular test of the real vehicle given the same conditions and command inputs. If reproducibility were a problem then a stochastic approach incorporating a full statistical analysis of the results may be required. However, all that is necessary to prove a deterministic model is a valid set of test results or test vehicle characterizations that can then be sought from a test simulation of the model. All models, owing to the simplifications built into them, cannot be absolutely faithful in this regard. Complex engineering systems like motor vehicles may be modelled using the lumped parameter approach – as described, for example, by Happian-Smith (2001) – and in which the subcomponents of the system are represented by discreet masses concentrated at certain points connected by massless elastic and damping elements. The number of lumped masses and their degrees of freedom (DOFs) determine the accuracy of the model and the aim is to capture with as little computing power as possible the essential characteristics of the real vehicle. There is an ongoing controversy over the benefits of unnecessary model complexity compared to those of simpler models that provide equally reliable results. *'Models do not possess intrinsic value. They are for solving problems. ... The ideal model is that which with minimum complexity is capable of solving the problems of concern with an acceptable risk of the solution being 'wrong''* [Sharp (1991)], quoted in Blundell & Harty (2004). That would not be a sufficient basis for testing a vehicle in accordance with ISO standards where the emphasis is on a particular vehicle's response to an accurately repeatable input command applied under the same repeatable test conditions. The distinction lies in the difference to which the results are being put. To make a comparison between the dynamic behaviour of a range of different vehicles, the characterisation process in each individual case requires a common test standard as a benchmark. This is what the ISO test standard provides.

Validation of a computer model is a much more intrinsic process involving only a comparison between a particular vehicle and its computer model and no benchmark is necessary.

The research conducted for the present work attempted to test a vehicle in accordance with ISO standards and assess the results for validation purposes. A suitable test vehicle, a Ford Mondeo, was instrumented and a series of tests were conducted but due to certain instrument failures and other shortcomings these tests could not be said to have complied fully with ISO repeatability standards. However, valid results were obtained from these tests which could be subsequently used as part of a credible validation process. The key point is that these results can be used with a numeric model that is subjected to a virtual test that mirrors the one which the Mondeo actually underwent. If the computer model is a good representation of the physical vehicle and its environment and if it is supplied with the same command inputs as the real vehicle then one might expect that the model will give similar results. Modern computer simulations tend to produce acceptably accurate results if they are reasonably accurate models embodying an appropriate level of simplification.

Although data from a range of tests was obtained for the purpose of this research only that from the steady state cornering (ISO 4138), the step steer or j-turn (ISO 7401) and the power-off in a turn (ISO 9816) test was analysed in depth and in accordance with the requirements and procedures laid down by the ISO standards.

Tests were chosen not merely because they were standard tests commonly applied to vehicles but also because they were the kinds of tests that would readily excite various natural frequencies and modes of vibration in the vehicle. Some of the tests conducted introduced steering and braking command inputs into the vehicle that provoked bounce, pitch and roll responses. A modal model of the vehicle, for example, could then be validated by comparing the natural frequencies observed in the tests to those calculated within the model. To facilitate this Fast Fourier Transform (FFT) analysis was applied to the test data and the results are presented in Appendix D.

1.5   Summary and structure of this Report

This report consists of seven chapters with four appendices and is summarised and structured as follows:

Chapter 1:   Introduces the research undertaken by stating the main question addressed and the aim and objectives of the research before putting it in its wider context and summarising the remainder of the thesis and the work presented in it.

Chapter 2:   Provides an overview of vehicle dynamics and a literature review that references the work of relevant researchers in the field of vehicle dynamics, testing and modelling, including a discussion of the standard tests used as the basis for the research conducted in this thesis.

Chapter 3:   Outlines the tests conducted and describes the test vehicle, explains the nature of the sensors and other instrumentation employed on the vehicle, and describes the test data acquisition system.

Chapter 4:   Explains the data preparation and post-processing conducted as part of the test programme, describing the reference voltages, gains, biases and the polarity issues with regard to the sensor data, and the issues involved with noise and filtering.

Chapter 5:   Presents the results from the tests conducted, analyses the data in accordance with the procedures laid down in the ISO standards, and discusses the results obtained by comparison with these standards. Any shortcomings are outlined and any assumptions made in overcoming these are explained.

Chapter 6:   Describes a MATLAB ride or modal model of the Mondeo that was created using vehicle specifications obtained via Ford UK. An attempt at validation by comparing a fast Fourier transform analysis of the Mondeo's test data to the natural frequencies of vibration given by this model is described.

Chapter 7:   Summarises the work done, restates the aims and objectives and assesses to what extent these were successfully achieved. Conclusions are drawn and some recommendations for future work are made.

Appendix A: Supplies information regarding the Mondeo's specifications; mass, geometry, etc.

Appendix B: Gives information concerning the Mondeo's unladen or kerb weight and the weight distribution when being tested.

Appendix C: Provides the governing equations derived in generating the MATLAB modal model and gives the MATLAB m-file code used to solve these equations.

Appendix D: Presents the results of the FFT analysis of the time history data from the tests undertaken by the Mondeo.

Chapter 2: Literature Review

2.1　　Vehicle Dynamics Overview

Vehicle dynamics is concerned with the way forces acting on a vehicle effect its motion. Although the processes involved are governed by well-known physical laws the interaction between vehicle design, human agency and the environment is so complex that it continues to be the subject of research. For this research the initial problem was to decide upon the kinds of tests that ought to be conducted and what kind of test information should be gathered for use in a model validation process. Much of the literature that provides an answer to these questions is concerned with the ride and handling qualities of a vehicle and how it responds to environmental disturbances and driver control inputs (e.g. Dixon (1996)). Most testing is mainly concerned with assessing the handling behaviour of a vehicle. In this respect there are two response modes or states: transient and steady state. The initial response of a vehicle is characterised by a transient state in which '*either the applied external forces and moments, the control positions or the vehicle motion responses are varying with time*' (International Standard ISO 8855: 2011 *Road Vehicles – Vehicle Dynamics and Road-holding Ability – Vocabulary*). Eventually this settles into a steady state where '*the sum of the applied external forces and moments and the inertial forces and moments which balance them form an unchanging force and moment system*' over an arbitrary period of time. According to one group of researchers in this field, Wade-Allen et al (2002), a thorough validation process should be based upon test manoeuvres involving steady state and transient vehicle behaviour with data comparison involving time histories and frequency response. Research engineers have developed many types of tests for assessing the ride and handling qualities of vehicles in transient and steady conditions, a process known as vehicle characterisation. One set of standard tests used for this purpose are those devised by the technical committees of the International Organization for Standardisation (ISO) and it was

decided for this research, where possible, to use these as the basis for a test programme.

These tests, which are open loop in nature, are described in appropriate detail later. Open loop refers to a vehicle's behavioural response to a specific command input. Gillespie (1992) notes that a vehicle and its driver are a closed loop system in which the driver uses sensory feedback to correct deviations from some desired motion. However, for the purposes of vehicle characterisation and in order to obtain what are called the characteristic values of the vehicle, only open loop tests are used as this allows a precise correlation to be made between a specific input command and the resulting measurable vehicle response. With this information specific comparisons can be made between different vehicles experiencing the same command input and important insights may be gained into the dynamic interplay between engineering design and vehicle behaviour.

In the particular case of the Ford Mondeo employed in this research the characteristic values obtained were not being used to compare it to other vehicles in similar test circumstances but rather to underpin the veracity of computer models of the vehicle. That change in purpose has important implications for the outcome of this research. In this regard it was only necessary to demonstrate that the results obtained from the tests, even if they were of insufficient quality for orthodox comparison purposes, were usable to prove the integrity of a computer model of the vehicle.

The sensors on board the test vehicle will be described in the next chapter and obviously have a role to play in recording the kind of information that engineers require for the purpose of characterizing vehicle performance. However, because of recent trends in research into the elasto-kinematics of suspension components the test vehicle was fitted with linear transducers that recorded the vertical deflections of the wheels. These are important not only for analysing pitch and roll behaviour but also because large vertical deflections of the suspension affect the loads acting on the suspension bushings. Some researchers (Watanabe & Sayer, 2004) have shown that for large suspension deflections, linear models provide a poor representation of behaviour and non-linear models give better and more reliable results. Such non-linear

models incorporate elasto-kinematic effects due to compliance deformation in the suspension components.

The whole area of vertical wheel displacement is more directly concerned with the ride comfort and ride safety of a vehicle, although it also has a major impact on handling. Many factors influence the handling of a vehicle by affecting cornering forces developed by tyres in the presence of lateral acceleration. For virtually all pneumatic tyres, the cornering forces are dependent upon, and non-linear with, vertical load (Gillespie, p.210ff.). Theoretically, the vertical deflections (dZ) in the wheel suspension can be related to the normal loads (F_Z) on the wheels. These in turn, via the coefficient of friction, are related to the maximum possible lateral (F_Y) and longitudinal (F_X) forces acting in the tyre contact patch. Knowing the static trim state of the vehicle and the wheel and suspension spring rates, it should be possible to determine the dynamic changes in the normal loads on the wheels by measuring their instantaneous bump/rebound position. The Mondeo's static load distribution was calculated as shown in Appendix B and so the changing wheel loads should be calculable using the calibration information from the wheel deflection sensors. It should be quite straightforward to write an algorithm in MATLAB to calculate the associated vertical forces acting at each wheel using the wheel deflection data.

Of course, this approach best suits a quasi-static analysis and would not be suitable for situations where there are high acceleration rates. In such cases the forces acting do not solely involve the suspension spring deflection and any calculation of force based on spring deflection alone ignores the presence of frictional (damper) and acceleration forces. Tests performed on rough ground would certainly involve high accelerations associated with small vertical wheel deflections and reversals. Based on a summation of forces in accordance with Newton's Second Law, the classic dynamic equation for a single DOF mass-spring-damper system is given by equation (2.1):

$$\sum F = ma \quad \Rightarrow \quad m\ddot{x} + c\dot{x} + kx = F(t) \qquad (2.1)$$

19

Where $\ddot{x}$, $\dot{x}$ and x represent the system's instantaneous acceleration, velocity and displacement from its static equilibrium position respectively. Applied to a wheel suspension, the other parameters in this equation are the mass (m) supported by the system, the rate of viscous damping (c) and the spring stiffness (k) respectively. For a vehicle suspension that is oscillating vertically from its static equilibrium position, F(t) would represent the instantaneous change in the vertical loading on the system. The vertical deflection (x) is the instantaneous distance from the rest position. Knowing this deflection, MATLAB can be used to determine the corresponding derived values for the instantaneous velocity and acceleration. From this it should be possible, knowing values for the mass (m), damping rate (c) and spring stiffness (k), to calculate the instantaneous vertical load on individual wheels.

According to ISO Directive 2631 (1997) root mean square (r.m.s.) values of the vehicle body acceleration are crucial to determining the effects of vibration on health and comfort. Soft suspensions reduce r.m.s. acceleration values but require larger vertical suspension travel. As a result, ride comfort is inevitably a compromise between these two conflicting phenomenon and, therefore, body acceleration and suspension travel must be used as objective criteria in making any judgement about ride quality (Rill, 2012). Consequently, information regarding the vertical wheel displacements of a vehicle undergoing various test manoeuvres must be a requisite for a better analysis of its behaviour and for understanding its general dynamics, and this is especially the case when this information can be correlated in time with other vehicle parameters like acceleration.

Two aspects of a vehicle's characterisation have been alluded to: vehicle ride and vehicle handling. These may seem to be two separate aspects of a vehicle's behaviour but in reality they are inextricably connected: those design features that produce 'good ride' and those that produce 'good handling' are not necessarily or even usually compatible with each other. It is generally the case that soft suspensions provide a more comfortable ride but impact adversely on handling. Good handling requires that the driver has feedback through the steering system and can feel the road, and a stiffer overall suspension offers a more positive and responsive steering.

Ride quality refers to the vibrational feel of a vehicle and deals with passenger comfort. Because a vehicle is essentially a sprung mass and its various components have some degree of elasticity, vibrations can be excited by any source of disturbance and can be transmitted to the occupants. In many respects ride quality is subjective but studies have been done to establish objective criteria for use by vehicle designers. Early analysts suggested that vibrations with frequencies that correspond with natural human activities - walking, trotting or running – were mostly acceptable; i.e. $1.5\text{Hz} \le f_n \le 2.5\text{Hz}$ in bounce. Certain low frequency motions in pitch, roll or bounce, $0.5 \le f \le 0.75\,\text{Hz}$, were found to be uncomfortable and tended to induce motion or sea-sickness. Fenton (1998) explains that as frequency increases, tolerance to vibrational displacement decreases. The Janeway comfort criterion as outlined in the SAE's *Ride and Vibration Data Manual J6a* (quoted in Wong, p.683) gives parameters for this relationship. These recommend that in the 1-6Hz range jerk, the rate of change of acceleration, should be the criterion and should be approximately no greater than 12.6m/s^3. At a ride frequency of 1Hz this corresponds to an amplitude limit of 50mm. Ride comfort is a quality of the sprung mass and is related to body bounce but is also influenced by body pitch and roll. The most comfortable frequency is generally in the range 1.0 to 1.5Hz (Gillespie, 1992). The natural frequency of the suspension itself, which is an unsprung mass, is another important vibration. It is usually at least an order of magnitude higher than that of the sprung mass to avoid the possibility of resonance.

The handling characteristics of a vehicle are as equally important to human comfort as they are to its stability and directional control. Most handling manoeuvres occur at speeds that involve some level of lateral acceleration. Accelerations of any kind, lateral or longitudinal, have their greatest effect at the level of the head where sensitivity to stiffening of the suspension, for example, is most pronounced (Bastow *et al*, 2004). These effects are given greater effect when a vehicle occupant is secured by seatbelts. In such circumstances, the body is held relatively rigid and sideways motion is restricted except for the upper body and head. Not only is the head more affected by accelerations than the rest of the body but also by jerk, the rate of change of acceleration. Characterisation of a vehicle's handling capability involves analysing the sideslip, yaw and steering command with respect to the lateral acceleration

experienced in a turn (Dixon, 1996). Characteristic values like yaw velocity gain - the rate of change of yaw velocity with respect to handwheel angle under steady state conditions –are important yardsticks not only for assessing vehicle handling behaviour but also for understanding what is best from the perspective of the vehicle occupants.

Any manoeuvre that is executed by a steer command will involve body roll to some extent. Ride dynamics – roll, pitch and bounce – affect suspension and steering geometry which, in turn, has an impact on the handling response of the vehicle. Bump and roll steer, for example, are phenomenon induced by changes in the steering kinematics caused by body roll. Body roll due to the lateral inertia force generated when cornering changes the normal forces acting on the wheels because of load redistribution and this in turn alters the lateral forces on the wheels (Gillespie, 1992). These changes in the normal forces acting on the wheels can be correlated with the vertical wheel deflection relative to the sprung mass of the car body. Front wheel camber generates understeer (Ellis, 1994) and roll also causes cambering of the wheels. Tyre contact surfaces are displaced laterally (scrubbing) and, in conjunction with the forward speed of the car, this can cause increased slip angles at the tyres. On independent suspensions, camber thrust can play an important role in cornering even though the forces involved are not as severe as those associated with slip angle (Gillespie, p.218).

Modern vehicles are designed with all of the above issues in mind so it was expected that the characteristic values of the Mondeo as determined from the test data would conform to modern best practice. A number of tests were conducted on the Ford Mondeo (Table 1, p.34) which was instrumented with sensors intended to record the information required by the ISO standards. In addition, because of the importance of vertical wheel deflections as previously described, wheel displacement sensors were also fitted. The tests included not only standard open loop tests but also subjective tests such as single and double lane changes. However, for this work, only the steady state cornering, j-turn (step steer) and power-off in a turn tests were analysed in depth, mainly because they were open loop tests and their data was suitable for analysis.

2.2   Steady State Cornering

How a vehicle handles while undergoing a cornering manoeuvre is an important aspect of vehicle behaviour from the point of view of the driver. Gillespie (1992) states that the most commonly used measure of open loop response is the understeer gradient which evaluates the performance under steady state conditions. One might imagine that, for a particular radius of turn, no matter what the vehicle speed, a driver need only input a fixed steer angle at the handwheel. However, owing to a number of factors, this is not the case. As explained by Heisler (1999) the wheels do not go where they are pointed because of the effect of lateral acceleration ('centrifugal force') on the elastic response of the tyres. Depending on the vehicle's speed, the position of the centre of gravity and the stiffness of the tyres, the elastic compliance of the tyres will have an appreciable effect on the steering behaviour of the vehicle. The greater the elastic deflection of the front tyres compared to the rear, the greater the tendency of the vehicle to steer out of a turn; that is, to understeer. The opposite behaviour where the rear wheels steer out of the turn more than the front is called oversteer.

A vehicle's response to a handwheel command may be categorized as either neutral steer, understeer or oversteer. Understeer, which is the preferred condition for the general motorist because it is inherently safer (Heisler, 1999), occurs when the handwheel steer angle has to be increased the faster one tries to take a turn of a given radius; i.e. as lateral acceleration increases the front end steers out of the turn more than the rear end. An understeering vehicle, therefore, needs a greater steer command angle from the driver to make it follow the same radius of turn at a faster speed. The opposite is the case with an oversteering vehicle where the vehicle turns into a corner more sharply than anticipated because the rear end steers out of the turn more than the front. This condition is better suited to a professional race- or rally driver where reflexes and better vehicle control are necessary.

The ISO standard cornering manoeuvre is outlined in the International Standard ISO 4138: 2004 *Passenger Car – Steady State Circular Driving Behaviour*. A steady state condition while cornering requires a controlled equilibrium between vehicle speed, handwheel steer angle and turn radius. This standard allows for three types of test

procedure in which one or other of these three parameters is kept constant while another is varied and the third is measured. Both left and right hand turns should be made as part of the test. The ISO standard stipulates that the vehicle's longitudinal velocity (v_X), handwheel angle (δ_H) and lateral acceleration (a_Y) should be recorded. In addition, the standard states the desirability of recording the yaw velocity ($d\psi/dt$), longitudinal acceleration (a_X), roll angle (φ), and sideslip angle (β) and/or lateral velocity (v_Y).

As noted by Dixon (1996), the vehicle's forward velocity (v), lateral acceleration (a_Y) and yaw velocity ($d\psi/dt$), as well as the radius of turn (R) or the path curvature (ρ), are related via equation (2.2) and equation (2.3):

$$a_Y = \rho v^2 = \dot{\psi} v = \frac{v^2}{R} \qquad\qquad (2.2)$$

where $\qquad \rho = \dfrac{1}{R} \qquad$ and $\qquad \dot{\psi} = \rho v = \dfrac{v}{R} \qquad (2.3)$

These equations ignore transient effects. Ellis (p. 40-42), however, provides a more comprehensive analysis from first principles of the motion of a vehicle performing a turning manoeuvre on a flat smooth surface (XY plane). Using Ellis' notation a vehicle travelling at a velocity *v* on a curved path has initial body longitudinal, lateral and yaw velocity of U, V and r respectively. [Note: the yaw velocity r, which is the rate of change of yaw angle, may also be written as $(d\varphi/dt)$ or $\dot{\varphi}$]. If the centre of gravity of the vehicle coincides with the global origin then the vehicle's longitudinal and lateral accelerations in the global reference plain may be expressed using Equation 2.4):

$$a(x) = \dot{U} - Vr$$
$$a(y) = \dot{V} + Ur \qquad\qquad (2.4)$$

$$\frac{1}{R} = (d^2 y / dx^2) / \left[1 + (dy/dx)^2 \right]^{3/2} \qquad\qquad (2.5)$$

Using Equation 2.5, the standard mathematical expression for curvature, Ellis (1994, pp.143-146) recasts it in terms of the vehicle velocity and acceleration components and derives Equation 2.6.

$$\frac{1}{R} = \frac{Ua(y) - Va(x)}{v^3} \quad \text{where } v = \sqrt{U^2 + V^2} \qquad (2.6)$$

This equation clearly indicates that the path curvature (1/R) is a function of both the lateral and the longitudinal vehicle acceleration and is composed of both steady state and transient terms. It is equally clear, by transposing this equation, that the lateral acceleration (a_y) has transients components associated with it. When the vehicle is travelling on a curved path of large radius at a steady forward speed (v) the velocities, U and v, are approximately equal to each other and Va(x) is negligible. In that case the path curvature may be simplified as

$$\frac{1}{R} = \frac{a(y)}{v^2} \qquad \text{or} \qquad a(y) = \frac{v^2}{R} \qquad (2.7)$$

Radt & Pacejka (1963) in a seminal study demonstrated that vehicle cornering dynamics remains linear up to lateral accelerations of about 0.3g. Dixon (1996), describing lateral accelerations within this range as the primary handling regime of a typical car, states that below 0.3g the steering angle of the handwheel changes linearly with lateral acceleration at a given radius. However, he states (p. 271) that for a modern high-performance car the linear regime is perhaps as high as 0.45g. On the theoretical side, some computer modelling studies (Willumeit et al, 1992) show linearity up to about 0.4g or even a little more. In this investigation Willumeit et al created a 5 DOF model incorporating non-linear formulations for the springs, shock absorbers, tyres, and suspension kinematics. Their plot of handwheel angle against lateral acceleration remained linear with increased loading of the vehicle model up to and beyond 0.4g. This has relevance for the current work because the Mondeo experienced a centripetal acceleration in its steady state cornering test of the order of 0.4g and the analysis that follows assumes linearity up to that level.

According to Dixon (1996) and Rahnejat (2000) any possible cornering manoeuvre will involve lateral accelerations of the vehicle body up to a maximum of approximately $0.8g = 7.85 \text{m/s}^2$. A lateral acceleration $a_Y = 0.8g$ is possible in cornering manoeuvres involving turns of various radii taken at different vehicle speeds. High lateral acceleration ('high g') turns are probably more telling in terms of the vehicle's transient dynamic behaviour but are inherently more dangerous and not likely to be normally experienced by road users. The lateral acceleration is based upon – though as we shall see, not exactly the same thing as – the centripetal acceleration and is calculated in accordance with equation (2.8):

$$a_Y = v^2/R \qquad (2.8)$$

where v is the vehicle velocity in m/s and R is the turn radius in metres. The kinematic (Ackermann) steer angle (δ_A), in radians, for a vehicle with wheelbase L metres negotiating a turn of constant radius R metres at very low speed, as would be the case in a car-park manoeuvre, is given by the elementary expression of equation (2.9):

$$\delta_A = \tan^{-1}(L/R) \qquad (2.9)$$

For small values of δ_A (in radians) the assumption can be made that $\delta_A \approx \tan \delta_A$. Hence, and based on this approximation, equation (2.10) is usually written:

$$\delta_A = L/R \qquad (2.10)$$

For cornering speeds at higher velocities this angle must be modified by consideration of the effect of the slip angles, α_f and α_r, that arise at the front and rear tyres due to the rubber deforming side forces generated by lateral acceleration. A slip angle, α, is the angle between the direction in which the hub of a wheel is pointing (or being steered) and the direction in which the wheel is actually travelling. This is explained fully in many standard texts, for example Gillespie (1992) and Dixon (1996), where the expression for the characteristic steer angle, equation (2.11), is derived:

$$\delta = \frac{L}{R} + Ka_Y \qquad\qquad (2.11)$$

The term 'Ka$_Y$' in equation (2.11) represents the adjustment that must be made to the Ackermann angle, L/R, in order to accommodate the effect of slip angle. Within the linear handling regime of the vehicle as described previously – up to say 0.4g lateral acceleration – this equation represents a straight line with intercept L/R and a slope K. The value of L/R is equivalent to the Ackermann angle associated with a turn of constant radius and corresponds to the neutral steer angle: the value K is the characteristic steer gradient (Rill, 2012, p.295) which is sometimes also referred to as the stability factor (Jazar, 2008). For a given vehicle under test there are three variables associated with equation (2.11): the handwheel angle (δ), the radius of turn (R) and the velocity (v) at which the test is performed. The ISO 4138 standard states that the nature of any stable steady state is independent of the method by which it is achieved and that, therefore, to obtain a state of steady equilibrium any one of these three variables may be held constant while a second is varied and the third is measured. The commonest form of the steady state cornering test is the constant radius test where the speed is varied and the handwheel angle is measured.

Figure 1 illustrates the three possible forms this linear equation can take for a left-hand turn depending on whether the vehicle's handling characteristic is neutral steer, understeer or oversteer. The same plots for a right-hand turn would appear in the third quadrant of this graph by central symmetry in the origin. The ISO standard requires that the handwheel angle be plotted against lateral acceleration. In this case the steering ratio (i_S), which is defined by the International Standard (ISO 8855, 2011) as the rate of change of the handwheel angle with respect to the mean kinematic (Ackermann) angle, $\delta_{m,kin}$, of a pair of steered road wheels, has to be taken into account. This means that the mean steer angle on the road wheels must be multiplied by the steering ratio to obtain the handwheel angle indicated in Figure 1. In modern vehicles this rate of change usually varies and so the steering ratio is not constant. This has implications in Chapter 5 of the current work for the analysis made of the steady state test data.

Linear Handling Regime (Left-hand Turn)

Understster: L/R + kA : k > 0

Neutral Steer: L/R : k = 0

Oversteer: L/R + kA : k < 0

Handwheel Angle (deg)

Lateral Acceleration (m/s^2)
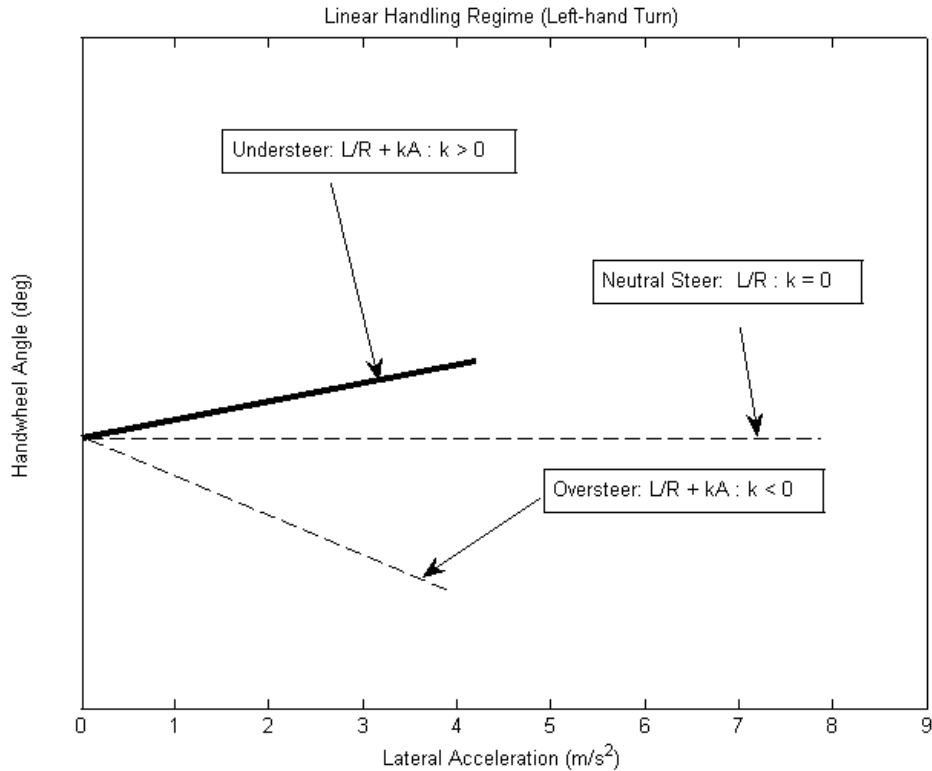
Figure 1: Vehicle Steering Characteristic (Constant Turn Radius)

As most vehicles are designed with inbuilt understeer, the stability factor K is invariably referred to as the understeer gradient (Dixon, p.275). Gillespie states that the most common measure of open-loop response is an 'understeer gradient' where K > 0. It is the estimated value of this understeer gradient that will be determined from the results obtained from the steady state cornering test on the Ford Mondeo.

2.3   Step Steer (J-turn) Manoeuvre

Whereas the steady state cornering manoeuvre provides characteristic information about the vehicle's steady state dynamics in a turn, the step steer (J-turn) manoeuvre provides useful information on the transient response to a handwheel steer input. Theoretically a true step steer command at the handwheel is inputted instantaneously although in practice it is a ramped input having a finite rise time. Dixon (1991) states that '*the step steer response is perhaps the most fundamental transient because it*

corresponds to simple corner entry or exit conditions' (p.370). Following such a steer command, and depending on the natural frequency and damping in yaw, the vehicle will achieve a new equilibrium state after the completion of a transient phase. Rill (2012, p.315) states that the handwheel angle (δ_H) is the salient factor in determining the cornering behaviour although the angle at the steered wheels will be different to this due to the steering ratio (i_S). However, the effect of compliance due to steering system elasticities, friction and possible servo support will also have an influence on the transient behaviour.

The step steer is one of three types of steer command described in the international standard ISO 7401: 2011 *Road Vehicles – Lateral Transient Response Test Methods* and is equivalent to a simple cornering manoeuvre or J-turn. The two other types of steer test described are the impulse steer and the sinusoidal steer input. The ISO standard stipulates that the handwheel angle (δ_H), the lateral acceleration (a_Y), the yaw velocity ($d\psi/dt$) and the longitudinal velocity (v_X) should be recorded. In addition, it states that it is desirable to record the roll angle (φ), the sideslip angle (β), the lateral velocity (v_Y) and the handwheel torque (M_H).

The tests described should be conducted on the test vehicle under minimum and maximum loading conditions. Minimum loading is the kerb weight of the vehicle plus the test driver and the test equipment. Maximum loading is stated to be the vehicle's kerb weight plus the equivalent of 68 kg per passenger seat. Any load over and above this, up to the vehicle's maximum authorized total load, should be evenly distributed over the luggage compartment.

According to Rill (2012) this test is designed to provide an objective assessment of the vehicle's yaw, roll and sideslip behaviour as excessive responses in these areas are subjectively perceived as annoying. The results obtained from the test are presented in the form of three time histories for the handwheel angle (δ_H), the lateral acceleration (a_Y) and the yaw velocity ($d\psi/dt$). Based on an analysis of these time histories the following values were recorded and used to characterise the test vehicle's transient behaviour:

Steady State	Yaw Vel. Gain	$(\dot{\psi}/\delta_H)_{SS}$
Lateral Acceleration	Response Time	T_{aY}
	Peak Response Time	T_{aYmax}
	Overshoot	U_{aY}
Yaw (Rate) Velocity	Response Time	$T_{\dot{\psi}}$
	Peak Response Time	$T_{\dot{\psi}\,max}$
	Overshoot	$U_{\dot{\psi}}$

Both yaw velocity and understeer gradient are related. Blundell & Harty (2004) state that an understeering vehicle is one in which the yaw velocity is less than expected whereas for an oversteering vehicle the yaw rate is greater than anticipated. Dixon (1996) claims that a neutral steer vehicle gives the best yaw velocity response with no yaw velocity overshoot. The more usual understeering vehicle will exhibit a yaw velocity response overshoot due to the lower yaw damping and this gets worse with increasing speed. The oversteering vehicle has good yaw damping but its response takes longer to reach steady state. Rill presents time histories that show that for a vehicle with increased sprung mass – for example, the fully laden Ford Mondeo test vehicle – whose damping remains relatively unchanged, the overshoot in yaw velocity, lateral acceleration and sideslip becomes more pronounced than when unladen. Dukkipati et al (2008) give typical yaw velocity overshoots ranging from 12% to 65% (1.12 – 1.65) for vehicles tested in conditions where velocity v = 30m/s and lateral acceleration a_Y = 0.4g.

In order to express a useful vehicle characteristic value from the myriad possible combinations of speed and steer angle, the notion of a yaw rate (velocity) gain (YRG) is used, this being a correlation between a measured output and the input that caused it (Blundell & Harty, 2004). This will be looked at again in Chapter 5 when the results from the j-turn (step steer) tests are analysed.

2.4 Power-off in a Turn

The power-off in a turn test is described in ISO 9816: 2006 *Power-off Reaction in a Turn*. The stated purpose of the test is to determine the effect of powering off on the course holding and directional behaviour of a vehicle operating in steady state circular motion. The test requires that power-off be effected by a sudden releasing of the accelerator pedal while the vehicle is following a circular path of given radius (r) at a constant forward or longitudinal velocity (v_X). As the ISO standard notes, this test is designed to characterise vehicle response behaviour when powering off on typical bends on secondary rural roads or on exit ramps from high-speed roadways. In such situations there is an obvious possible effect of power-off on vehicle stability and directional control and this test is designed to measure the vehicle's characteristic response to a power-off disturbance.

The constant radius test method involves initial conditions where the vehicle is being driven on a constant radius and the lateral acceleration is incrementally increased by increasing the initial speed for each test run. A radius of 100 metres (minimum permissible, 30m) and an initial lateral acceleration of about 4m/s^2 are recommended. This latter value will determine the forward or longitudinal velocity (v_X) of test vehicle on a particular turn radius. This test requires a skilful test driver who must achieve the initial steady state cornering conditions while following a circular path of fixed radius.

The test variables that must be determined are the moment of power off (t_0), the handwheel angle (δ_H), the yaw velocity ($d\psi/dt$), the longitudinal velocity (v_X), the lateral acceleration (a_Y), and the sideslip angle (β). The longitudinal acceleration (a_X) is also a desirable parameter to be recorded. The ISO standard notes that this is not intended as a complete list so additional test variables may also be recorded.

The test data obtained is then used to characterise the vehicle's transient response to the power-off command. The ISO standard claims that throttle-off behaviour in modern passenger vehicles is normally designed in such a way that the vehicle slightly decreases the radius of curvature of the driving path after the initiation of power-off.

The characteristic values derived from the test should be determined and presented as functions of the vehicle's initial steady state lateral acceleration. During the test the vehicle's characteristic steady state condition is defined using the mean values that are obtained during the time interval between 1.3 and 0.3 seconds before the initiation of throttle-off at time t_0. Other vehicle characteristic values are determined from an analysis of the period beginning at t_0 and ending 2 seconds later at t_n; i.e. $t_n = t_0 + 2s$.

The ISO standard admits that because of the current state of understanding of the dynamic response of vehicles to command inputs in relation to the subjective reaction of the driver, it can only suggest a set of fourteen separate calculations that may be made in order to evaluate the test data. The resulting characteristic values should be determined and presented as functions of the initial steady state lateral acceleration.

2.5   Other Tests and Test Parameters

Only those tests whose recorded data was considered useable for comparison against standard ISO test data were subjected to an analysis in accordance with ISO vehicle characterisation procedures. These were the *Steady State Cornering* (ISO 4138) test, *Step Steer (J-turn)* test (ISO 7401) and the *Power-off in a Turn* (ISO 9816) test. Other tests were also performed. These included the *Braking in a Turn* (ISO 7975), the *Pulse Steer* (ISO7401) test and the single and *Double Lane Change* (ISO 3888) tests. The data from the braking in a turn and the pulse steer tests was not analysed for the purpose of this work, and the single and double lane change manoeuvres are generally considered subjective tests not amenable to objective analysis because they are two influenced by driver performance. Therefore, although part of the vehicle testing programme, a theoretic discussion and the review of literature regarding these last three tests are not included here.

As will become clear in the next chapter, test parameters other than those required by the ISO and already alluded to, were recorded – in particular, the throttle position. Dixon (1996) notes that for steady state handling tests throttle or accelerator position ought to be treated as a control input in full computer simulations. He argues that

together with handwheel angle and gear ratio, throttle position would constitute a third independent variable where vehicle speed and path curvature are the dependent variables. He states that although the handwheel is regularly considered as a control input in handling theory, he is not aware of the throttle position being used in a like manner. It will be seen that the throttle position was used in this research to assist in the analysis of the data obtained in the power-off tests (Chapter 5). Here it was used to determine the moment of power-off, that is, t_0, the time of test initiation.

2.6   Summary

The first objective given in Chapter 1 (p.10) was to complete a literature review in which the work of relevant researchers in the field of vehicle dynamics would be identified and presented. Drawing on the works of these researchers – notably Dixon, Gillespie, Rill and Bastow – this chapter has outlined the relevant theory that forms the basis of any analysis of the dynamic behaviour of vehicles in general. Experimental testing of vehicles provides empirical data from which a vehicle's particular characteristic responses to given driver commands may be determined.

A second objective was to decide upon which vehicle tests would be used to verify the hypothesis that vehicle characterisation based on standard tests is a necessary prerequisite for validating computer models of the test vehicle. This literature review has presented, and discussed at some length, three types of vehicle test – the steady state cornering test, step steer (J-turn) and the power-off in a turn – that have been chosen for this purpose. The procedures and assessment criteria recommended by the International Standards Organisation (ISO) for these tests have been described and analysed in relation to the relevant vehicle dynamic theory. In particular, two important vehicle characterisation values, understeer gradient (K) and yaw velocity gain ($(\dot{\psi}/\delta_H)$), both associated with the handling response of a vehicle, have been identified in this context. In addition, a set of suggested values characterising the transient response of the vehicle during a power-off in a steady state turn have been identified.

Table 1 presents a summary of all of the tests that were conducted on the vehicle including those tests that were not subsequently analysed for the purposes of this work. The table distinguishes between those variables that the various ISO standards recommend as necessary (**N**) and those that are desirable (**D**) to be recorded. These are all detailed together with their respective symbols as prescribed by the International Standard ISO 8855: 2011 *Road Vehicles – Vehicle Dynamics and Road-holding Ability – Vocabulary*, Second Edition (2011).

In addition, the table is colour-coded to indicate which vehicle or test variables were directly recordable using the vehicle's onboard sensors and which were not recorded at all. It also indicates information that can be indirectly derived from information that was recorded.

Vehicle Parameter, ISO Symbol	Steady State Corner-ing ISO 4138	Pulse Steer Input ISO 7401	Step Steer or J-Turn ISO 7401	Power-off in a Turn ISO 9816	Brake In a Turn ISO 7975	Double Lane Change ISO 3888
Test Initiation Time, t_0	—	N	N	N	N	—
Steering/Handwheel angle, δ_H	N	N	N	N	N	—
Longitudinal Velocity, v_X	N	N	N	N	N	N
Lateral Velocity, v_Y	D	D	D	N	N	—
Longitudinal Acc., a_X	D	—	—	D	N	—
Lateral Acc., a_Y	N	N	N	N	N	—
Vertical Acc., a_Z	—	—	—	—	—	—
Roll Angle, φ	D	D	D	D	D	—
Pitch Angle, θ	—	—	—	D	D	—
Yaw Angle, ψ	—	—	—	—	—	—
Roll (Velocity) Rate,	—	—	—	—	—	—
Pitch (Velocity) Rate	—	—	—	—	—	—
Yaw (Velocity) Rate	D	N	N	N	N	—
Sideslip Angle, β	—	D	D	N	N	—
Radius of Turn, r	N	—	—	N	—	—
Handwheel Torque, M_H	D	D	D	—	—	—
Brakeline Pressure, pB	—	—	—	—	N	—
Brake Pedal Force, Fp	—	—	—	—	N	—
Brake Pedal Travel, sp	—	—	—	—	N	—
Stopping Distance,	—	—	—	—	D	—
Throttle Opening (deg)	—	—	—	—	—	—
Engine Speed (RPM)	—	—	—	—	—	—
Drive Wheel Speed (km/hr)	—	—	—	—	—	—
Front Left Wheel Deflections (dZ)	—	—	—	—	—	—
Front Right Wheel Deflection (dZ)	—	—	—	—	—	—
Rear Left Wheel Deflections (dZ)	—	—	—	—	—	—
Rear Right Wheel Deflections (dZ)	—	—	—	—	—	—

Legend: **N** = Necessary ISO Test Variable   **D** = Desirable ISO Test Variable

Recorded Data ☐   Derivable Data ☐   Unrecorded Data ☐

Table 1: Summary of All Test Data to be Recorded

Chapter 3: Vehicle Instrumentation and Data Acquisition

3.1   Introduction: Testing, Modelling and Model Validation

The primary aim of this research was to test a Ford Mondeo in the field under sufficiently controlled test conditions that the quality and suitability of the vehicle characterisation information obtained could be assessed for the purpose of validating a numerical model of the test vehicle. Whenever possible, vehicle testing was conducted in accordance with ISO standards and all testing was compared to ISO requirements as a benchmark.

In any vehicle modelling exercise, the intention of the researcher is that the model faithfully reproduces the characteristics and behaviour of the actual vehicle as close as possible. Achieving a faithful model like this is fraught with difficulty because there are so many variables and parameters involved that they cannot all be modelled and even those that are may be limited by other factors such as the level of complexity involved and the quality and accuracy of the information available for them. As part of the preparation for the research associated with this thesis, information about the test vehicle was obtained from Ford UK and this is contained in Appendix A.

On the validation side, the accuracy of a model depends on equally many factors to do with the testing of the vehicle being modelled. Such factors include the type and cost of the sensors used to monitor and record vehicle behaviour, the type of vehicle behaviours chosen to be recorded, environmental testing conditions, the positioning of sensors, etc. These are crucial considerations since they will determine whether the research methods and assumptions employed in creating and validating the model can produce sensible outputs from the model to be used for further research work.

The remainder of this chapter outlines the test vehicle coordinate frame of reference, the tests conducted, the vehicle instrumentation and the data acquisition system.

3.2   The ISO Axis System

The axis system and terminology used to describe and analyze the behaviour of the test vehicle is that defined by the International Organisation for Standards (ISO) and laid down by them in their publication ISO 8855: 1991: '*Road Vehicles – Vehicle Dynamics and Road Holding Ability – Vocabulary*' and shown in Figure 2. This represents a right-handed orthogonal system of axes and determines the sense or orientation of the various vehicle motions; e.g. longitudinal (x), lateral (y) and vertical (z) translations, and roll (φ), pitch (θ), and yaw (ψ) rotations. Viewed from the perspective of the driver the following convention ('right hand curl rule') applies:
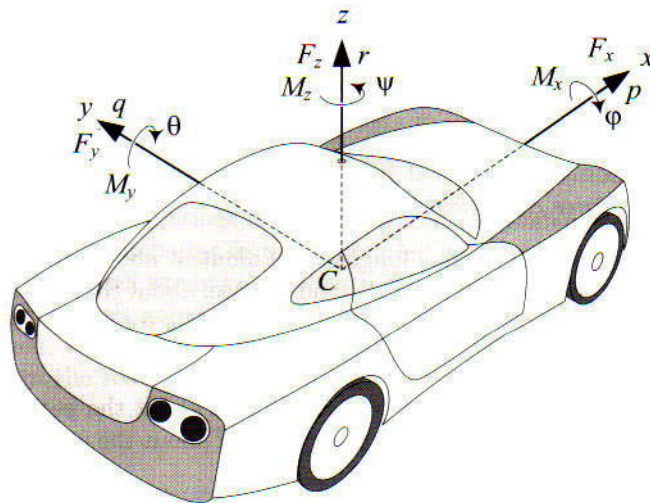
[Ref.: Jazar, Reza N., *Vehicle Dynamics: theory and application* (Springer, 2008)]

Figure 2: The ISO Axis System

1. The positive X axis extends forward in the direction of travel of the vehicle which has forward positive velocity and acceleration, v_X and a_X, respectively;

2. The positive Y axis extends outwards to the near- or left-hand side of the vehicle with positive lateral velocity, v_Y and acceleration a_Y, in that direction;

3. The positive Z axis extends upwards through the roof of the vehicle: the negative Z axis extends downwards through the floor;

4. Positive roll (φ) corresponds to the vehicle leaning out of a left-hand turn (rolling clockwise to the right): negative roll to its leaning out of a right-hand turn (rolling anticlockwise to the left);

5. Positive pitch (θ) corresponds to front end dive: negative pitch to rear end squat;

6. Positive yaw (ψ) corresponds to a turn to the left: negative yaw to a turn to the right.

Besides the nomenclature associated with this axis system other terms are commonly used for identification purposes; for example, *nearside* and *offside*. The nearside, or passenger side of a vehicle is the side nearest the kerb; the offside, or driver's side of the vehicle is the side furthest from the kerb. The test vehicle, a Ford Mondeo (Figure 3), was a right-hand drive with independent suspension on all four wheels, employing a Macpherson strut at the front and independent quadralink arrangement at the rear.

.

Figure 3: The Ford Mondeo Test Vehicle

3.3   The Test Vehicle

A considerable body of raw data has been acquired from actual testing of a Ford Mondeo 2 litre V6 Zetec. This test car belonged to the Automotive & Aeronautical Department of Loughborough University and was already instrumented with several existing sensors and equipped with a data logging system. Since the car had already been used as a test vehicle over many years all the sensors were recalibrated and checked by technical support staff. The only new sensors that were installed on the

vehicle were a set of four wheel vertical displacement sensors. These were installed by the same supporting technical staff and calibrated by the author.

3.4   Tests Conducted

The Ford Mondeo was subjected to a series of tests over a period of three days. Some were conducted on the college campus, some in an empty car-park and others on the public roads. The particular tests conducted on the Mondeo are listed in Table 2:

<u>Type of Test Conducted</u>

Steady State (Constant Radius) Turn

Pulse Steer to the Left

Pulse Steer to the Right

J-turn (Step Steer) to the Left

J-turn (Step Steer) to the Right

Power-off in a Turn to the Left

Power-off in a Turn to the Right

Brake in a Turn to the Left

Brake in a Turn to the Right

Single Lane Change to Left

Single Lane Change to Right

Single Lane Change to Left

Single Lane Change to Right

Single Lane Change to Right

Double Lane Change (Left then right)

Double Lane Change (Right then left)

Table 2: Tests Conducted using the Ford Mondeo

3.5   Sensors

A total of 66 individual test trials were conducted and for each of them data was recorded for 15 different vehicle parameters (Table 3).

MEASURED PARAMETER	SENSOR
1 Throttle Position (deg)	Potentiometer on Accelerator
2 Engine Speed (rpm)	Taken from Vehicle CPU
3 Handwheel* Angle turned through (deg)	Potentiometer on Steering Column
4 Rear Left (Kerb/ Nearside) Wheel Speed (km/hr)	Speed sensor on the wheel
5 Rear Right (Driver/Offside) Wheel Speed (km/hr)	Speed sensor on the wheel
6 Longitudinal Acceleration, a_X (m/s^2)	Accelerometer at Vehicle C of G
7 Lateral Acceleration, a_Y (m/s^2)	Accelerometer at Vehicle C of G
8 Vertical Acceleration, a_Z (m/s^2)	Accelerometer at Vehicle C of G
9 Roll Rate (or Roll Angular Velocity), $\dot{\phi}$ (deg/s)	Gyro at Vehicle Centre of Gravity
10 Pitch Rate (or Pitch Angular Velocity), $\dot{\theta}$ (deg/s)	Gyro at Vehicle Centre of Gravity
11 Yaw Rate (or Yaw Angular Velocity), $\dot{\psi}$ (deg/s)	Gyro at Vehicle Centre of Gravity
12 Left (Nearside) Front Wheel Vertical Deflection, (cm)	String potentiometer fixed at wheel
13 Right (Offside) Front Wheel Vertical Deflection, (cm)	String potentiometer fixed at wheel
14 Left (Nearside) Rear Wheel Vertical Deflection, (cm)	Linear Transducer fixed at wheel
15 Right (Offside) Rear Wheel Vertical Deflection, (cm)	Linear Transducer fixed at wheel

Table 3: Ford Mondeo – Onboard Sensors

3.5.1 Accelerometers and Gyroscopes

The accelerometers and gyroscopes were all positioned together on the floor behind the vehicle's handbrake lever and between the front seats (Figure 4). This location was originally chosen as being as close as practicable to the vehicle's centre of gravity (see Appendix B) and still allow unimpeded operation of the vehicle.

Three accelerometers were employed to record vehicle motions along the X, Y and Z vehicle axes; that is, longitudinal, lateral and vertical acceleration rates. These were

---

*The commonly used 'steering wheel' is too ambiguous a term as it can refer to either a vehicle's steerable road wheel or to the driver's hand-controlled steering wheel. Following the recommendation of M. Blundell & D. Harty, *The Multibody Systems Approach to Vehicle Dynamics* (2004), p.4, the term 'handwheel' will be used henceforth to denote the driver's hand operated steering wheel.

Figure 4: Location of the accelerometers and gyroscopes

Schaevitz DC operated A-220 Series accelerometers (Figure 5) capable of measuring accelerations of ±2g. Their recalibration involved pointing them downwards and then upwards in order to take a reading of ±1g for the acceleration due to earth gravity. The result was found to be accurate to within ±0.05%.

Figure 5: Schaevitz A220 series DC operated linear servo accelerometer

The gyros used to detect and record the vehicle's roll, pitch and yaw motion were BAE Systems Solid State Vibrating Structure Gyroscopes (VSG) with a rate range up to 100°/s (Figure 6).

Figure 6: Bipolar type single axis vibrating structure gyroscope
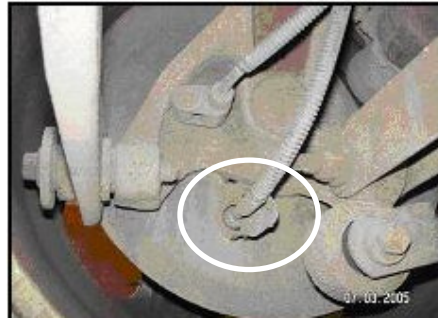
Figure 7: Wheel Speed Sensor (circled)

3.5.2 Wheel Speed Sensors

Wheel speeds were monitored using magnetic pick-up sensors at each rear wheel (Figure 7). Using a toothed wheel these sensors generate pulses whose frequency is converted to an analogue voltage signal. Knowing the angular velocity (ω) of a wheel in radians per second (rad/s) and its rolling radius (r) in metres (m) the forward or longitudinal velocity (v_X) is given by the formula:

$$v_X = \omega r \tag{3.1}$$

3.5.3 Engine Speed Sensor

A similar magnetic pick-up sensor located at the flywheel of the engine (Figure 8) engaged with its 135 teeth to generate a pulse frequency that was also converted to an analogue voltage, thus providing a means of measuring engine speed.

Figure 8: Engine Speed Sensor (circled)

3.5.4 Throttle Pedal Sensor

Movement of the throttle (accelerator) pedal was recorded by means of a linear potentiometer installed as shown in Figure 9. This device could measure movement up to 50mm. All that was required was that the voltage output at the extremes of pedal travel be recorded and a calibration factor calculated on the basis that the relationship between travel and output voltage was linear.

Figure 9: Throttle Pedal Sensor (circled)

**Figure 10: Rotary Potentiometer (circled)
for sensing steering angle**

3.5.5   Handwheel (Steering Wheel) Angle Sensor

A belt operated rotary potentiometer was fixed to the steering column (Figure 10). This device, which had to be recalibrated (Figure 11) before taking the vehicle out to test, provides a linear relationship between angle turned through and voltage output. It could record handwheel angles up to ±500°, or nearly one-and-a-half turns of the steering wheel to the left or to the right. This calibration has been included here because it is referred to again later when the steady state cornering data is being analysed in Chapter 5.

Handwheel Angle (deg)	Potentiometer Voltage (Volt)
500	0.12
450	0.39
360	0.75
270	1.14
180	1.48
90	1.88
0	2.23
-90	2.62
-18-	2.96
-270	3.37
-360	3.73
-450	4.13
-500	4.31
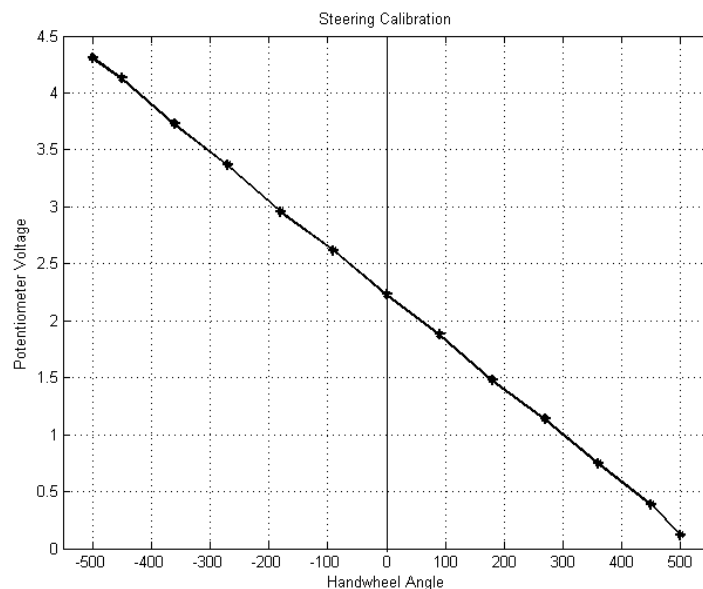
Figure 11: Handwheel Angle Sensor Calibration

3.5.6   Wheel Vertical Displacement Sensors

Linear transducers on each wheel were attached to the vehicle body at one end and to the hub carrier at the other. Due to difficulties involving their fitting and mounting it was necessary to chose different types of sensor for the front and rear suspensions. ASM WS10 string pots capable of recording displacements up to ±250mm were fitted at the front wheels (Figure 12) and conventional wiper-type Vishay linear transducers, capable of measuring displacement up to 100mm, were fitted at the rear (Figure 13).

Figure 12: ASM WS10 Position Sensor ('String Pot')
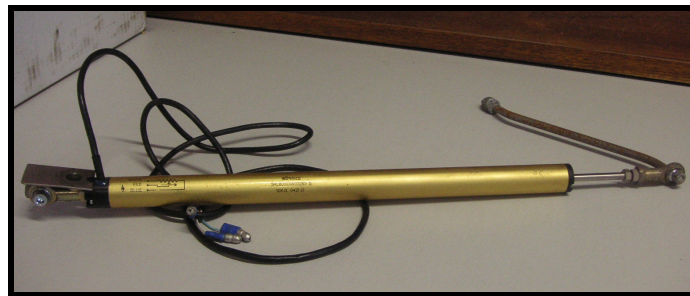
Figure 13: Vishay Linear Transducer
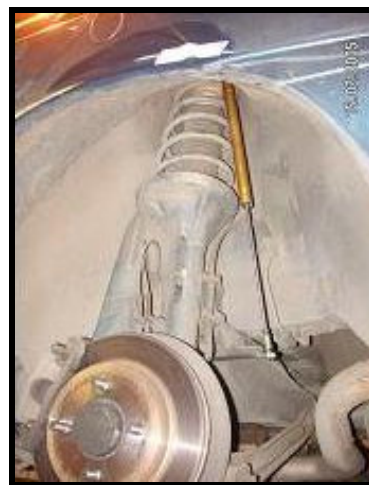
(a) Front   (b) Rear

Figure 14: Suspension Displacement Sensors in situ

Figure 14 shows these sensors in situ on the vehicle. Whereas it was possible to position the front wheel deflection sensors in such a manner as to record true vertical movement at the point of attachment, this proved too difficult with the rear wheel sensors which are out of the true vertical position by approximately 10°. This

introduced an error in the recorded vertical displacement that was slightly greater than the true value by about 1.5%. In the case of the rear wheels, this inaccuracy is counterbalanced by the fact that the sensors are positioned inboard of the wheel centres where the measured deflection is less than that actually experienced by the wheel. A further source of error is due to the wheels following an arc when vertically displaced rather than a true linear path, but this is so small that it may be ignored.

3.6   Test Data Acquisition

Aside from the sensors themselves and their associated wiring all of the data acquisition equipment was located in the rear boot of the vehicle. (Figure 15). The real time data acquired from each of the onboard sensors was in the form of a raw voltage signal output which was downloaded via a 16 Channel National Instruments DAQ-Pac using Labview 5.1 software. A sampling rate of 200 Hz was employed and the data was saved in a simple text file format for post-processing.

As will be explained later, the highest frequency of vibration of interest was that associated with wheel hop and this was erroneously thought to be about 30-35 Hz based on misinformation obtained about the test vehicle. All other frequencies of interest would be well below this value. Furthermore, the data recovered through some of the sensors was quite noisy and it was thought desirable to filter it. So, in order to avoid removing the wheel hop frequency, a corner or cut-off frequency of 40 Hz was selected.

The Nyquist sampling criterion as explained by Liu & Huston (2011) requires that the rate at which a signal is sampled be at least twice that of the highest frequency of the signal being sought (p.438). However, Ramirez (1985), p.130, recommends that a margin of safety be used. Since it takes at least two points per cycle to uniquely define a sinusoid of given amplitude and frequency it is not prudent to rely solely on this minimum but, instead, a much higher sampling rate should be employed to ensure that three or more points per cycle are sampled. In the present case, the 200 Hz sampling

frequency that was employed was high enough to avoid any possibility of losing genuine information due to the problem of aliasing.

Figure 15: Data Acquisition Equipment in Car Boot

Before finally closing this chapter it should be noted that calibration curves for all of the test vehicle's sensors are available but it was deemed unnecessary to include them here when Table 4 (p.48) provides the essential calibration information in the form of base or reference output voltages and their gain or scale factors. The exception made was that of the potentiometer fitted to the handwheel steering column which will play a direct role in the calculation of the steering ratio in Chapter 5.

3.7 Summary

This chapter has presented details regarding the test vehicle, its instrumentation and the tests to which it was subjected. In particular, the nature and type of the onboard sensors, and their position, have been described, and the parameters they measured and recorded have been outlined. In doing so it has demonstrated that the third objective outlined in Chapter 1 (p.10) – to instrument and prepare a test vehicle – has been successfully completed.

Chapter 4: Data Preparation and Post-processing

4.1   Signal Reference Voltages, Gains and Polarity

The text files of raw road test data were imported into MATLAB and post-processed. A sample of the raw data is given in graphical form in Figure 16 and Figure 17. These plots show the baseline (quiescent) voltage output from some of the sensors when the vehicle was either stationary or not undergoing a dynamic response to an input disturbance.

DAQ-Pac Channel	Measured Variable	ISO Symbol	SI Units	Quiescent or Base Reference Voltage	Gain (Scale or Calibration Factor)
0	Longitudinal Acceleration	a_X	m/s^2	-0.045	2.51 V/g
1	Lateral Acceleration	a_Y	m/s^2	0	2.49 V/g
2	Vertical Acceleration	a_Z	m/s^2	-0.08	-2.49 V/g
3	Roll (Velocity) Rate	$d\varphi/dt$	°/s	0	0.1 V/°/s
4	Pitch (Velocity) Rate	$d\theta/dt$	°/s	5.2	-0.1 V/°/s
5	Yaw (Velocity) Rate	$d\psi/dt$	°/s	0	-0.026 V/°/s
6	Handwheel (Steer) Angle	δ_H		2.23	0.0042 V/°
7	Engine Speed		rpm	1.05	0.001V/rpm
8	[Empty]	-	-	-	-
9	Throttle opening		%	0.4	0.033V/%
10	Near-side Rear Wheel Speed		km/hr	0.105	0.022 V/km/hr
11	Off-side Rear Wheel Speed		km/hr	0.095	0.022 V/km/hr
12	Left Front Wheel Displacement (dZ)		cm	2.321	0.091 V/cm
13	Right Front Wheel Displacement (dZ)		cm	3.095	0.087 V/cm
14	Left Rear Wheel Displacement (dZ)		cm	2.461	0.44 V/cm
15	Right Rear Wheel Displacement (dZ)		cm	1.887	0.33 V/cm

Table 4: Sensor Calibration Data – Base Reference Voltages & Scale Factors

For each sensor the recorded voltage values required the application of the relevant sensor gain in order to convert them to the appropriate engineering unit for the vehicle parameter being measured (Table 4). For example, the handwheel potentiometer voltages had to be divided by -0.0042V/degree to render the result into degrees of handwheel rotation. It was also necessary to decide, depending on the polarity of the raw signal, whether the gain applied should be positive or negative in order to ensure that the processed signal matched the sense, orientation or direction of the vehicle's behaviour within the reference frame of the ISO axis system.
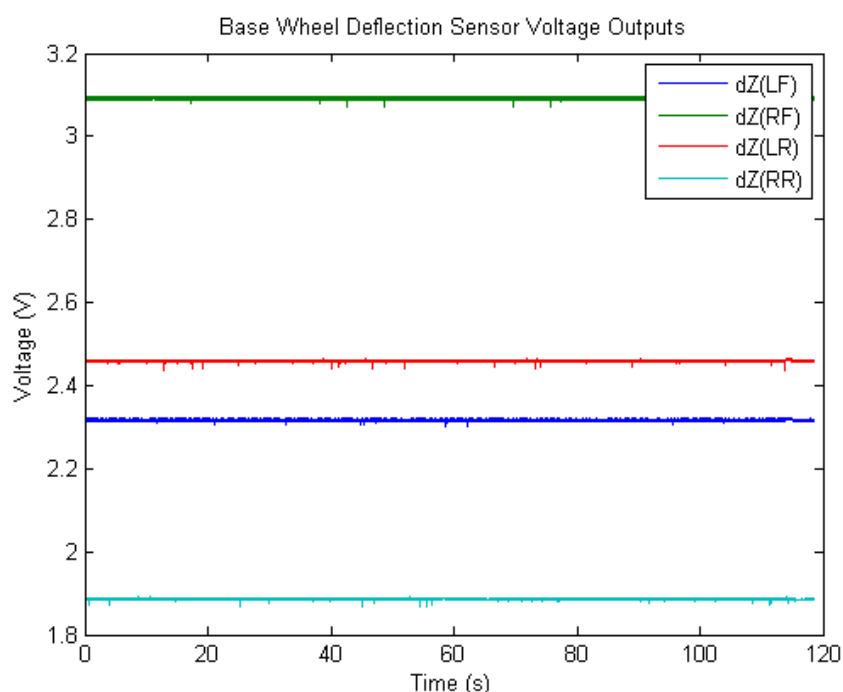
Figure 16: Wheel Sensors Raw Voltage Data

Some sensors exhibited bias baseline values (Table 4, Figures 16 and 17) and did not output a zero reference voltage in their quiescent or neutral state. For example, the steer or handwheel angle sensor (Figure 17) recorded a value of 2.23 volts when the handwheel was at zero degrees in its neutral, straight ahead, position. In order to clearly and unambiguously interpret the plotted raw data it was necessary to remove these bias values. An exception can be made in the case of the output from the four linear transducers that recorded the vertical deflections (dZ) of each of the road

49

wheels (Figure 16). Because these are all invariably plotted together on the same graph it aided interpretation to separate them on occasion, each from the other, by deliberately adding bias values.
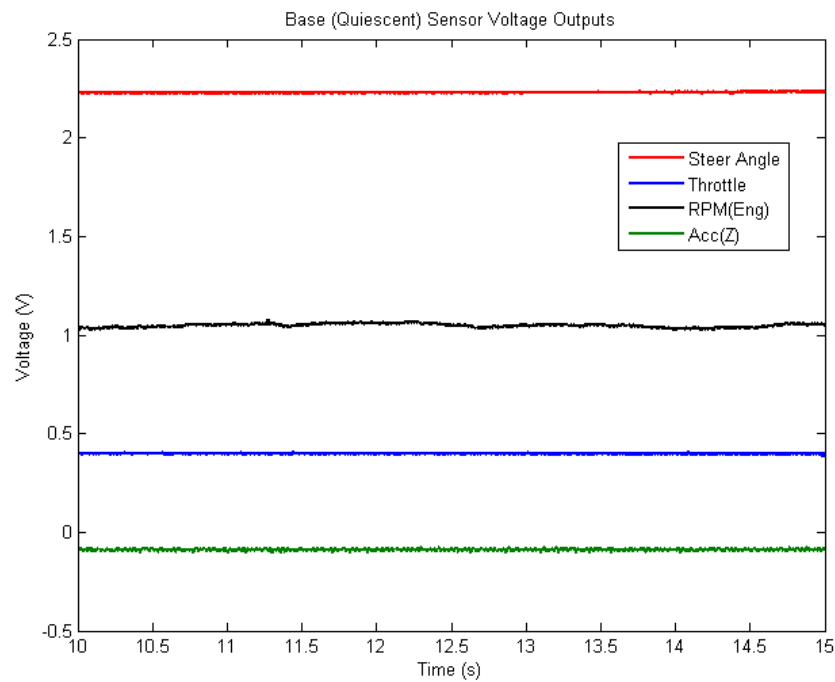
Figure 17: Other Raw Voltage Sensor Data

4.2   Noise and Filtering

In addition, the output from some sensors, notably the gyros and accelerometers, proved to be quite noisy. Whenever possible and depending on which were the important parameters that needed recording for any given manoeuvre, faulty or noisy sensors were swapped for properly working ones. However, this was not always possible because of constraints due to time or personnel. The test vehicle was only available for a short period and there were problems with the equipment. The data recorded during the Double Lane Change (Obstacle Avoidance) manoeuvre executed by the Mondeo provides a good example of the noisy data – in this case, the yaw and roll signals (refer to Figure 18 and Figure 19). The question arises: to what can this noise be attributed? Was it a genuine dynamic response from the vehicle or just an instrument problem? The double lane change manoeuvre was executed on a motorway

at 112 km/hr (70 mph). Both the yaw and roll sensors could have been recording real vehicle behaviour due to road surface variations, engine vibration, bearing and bushing wear or aerodynamic effects. Note that the noise was evident in the yaw and roll signal prior to the introduction of the handwheel disturbance and it continued
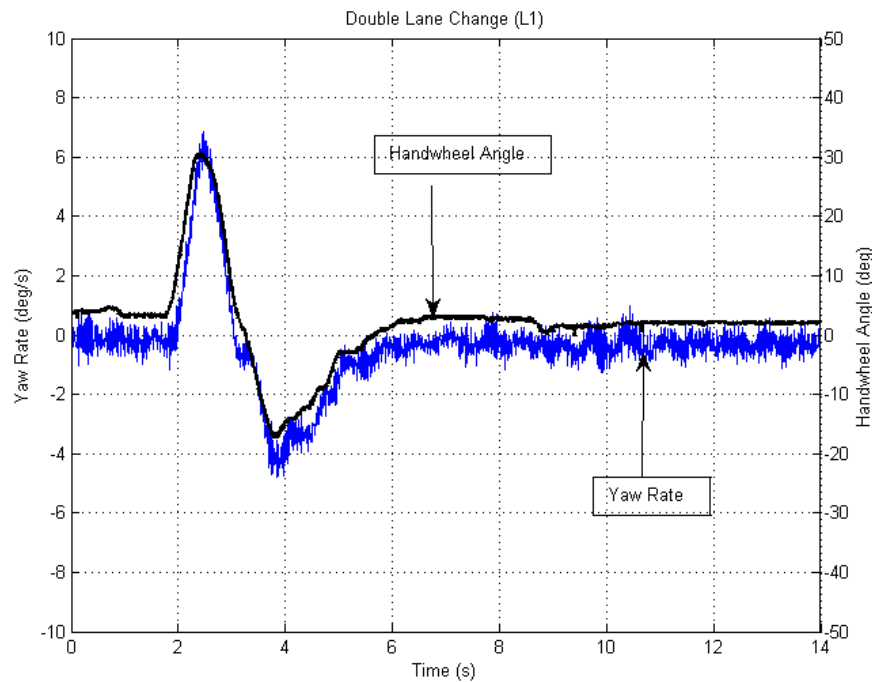
Figure 18: Double Lane Change – Yaw Rate & Handwheel Angle v Time

unabated afterwards. It could also have been generated by vibrations in the wheels themselves. It must also be recognized that some vehicle test manoeuvres were conducted on very rough and irregular ground surfaces and the effects of the perturbations experienced are present in the recorded data. What constitutes an intolerable level of noise depends on what is being sought. If only the low frequency general shape of a signal is required then quite a bit of high frequency noise can be accepted [Ramirez (1985), p.95]. Roll, pitch and yaw motions have typical frequencies well below 10Hz whereas the frequencies associated with noise are generally of a much higher value and appear superimposed on the fundamental signal.

51
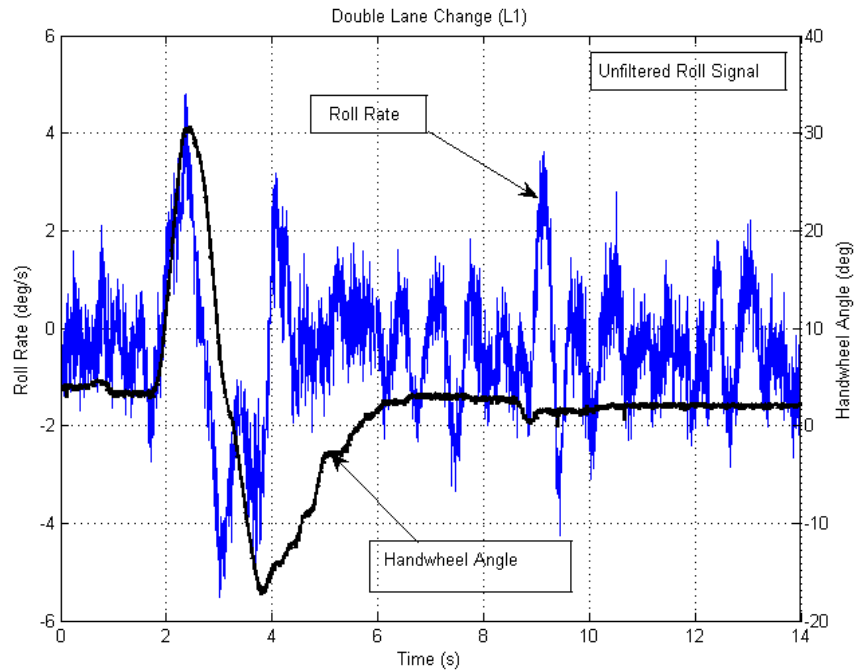
Figure 19: Double Lane Change – Roll Rate & Handwheel Angle v Time

In order to provide more easily readable results it was considered necessary to remove as much of this noise as possible without compromising genuine information related to the vehicle's dynamic behaviour. Hence, the data was filtered, as previously mentioned, using a cut-off or corner frequency of 40Hz.

Wheel hop frequency is the natural frequency or resonance mode of the unsprung mass of the tyre/wheel assembly. It is of an order of magnitude higher than the resonant frequency of the sprung mass which remains stationary during wheel hop. Previous research into this topic such as that conducted by Gillespie (1992) and Blundell & Harty (2004) invariably put wheel hop frequencies of road vehicles in the region of 10-15 Hz. The wheel hop frequencies of the test Mondeo were found to be about 11-12 Hz.

There is a commonly used formula [Gillespie, p.164 or Dixon (1999), p.124] for estimating wheel hop frequency which is valid when the sprung mass of the vehicle is much greater than the unsprung mass of the wheel assembly. In the case of the unladen Mondeo, whose kerb weight was 1312kg, the ratio of the vehicle's sprung to

unsprung mass was 8:1 at the front and 6.4:1 at the rear. When fully laden on the day of testing, the sprung mass was greatly increased and these ratios were even higher at 8.8 and 8.2 to 1 for the front and rear respectively.

The specifications for the test vehicle provided in <u>Table 5</u> were supplied by Ford UK:

Front Wheel:	Unsprung Mass (m)	48.955kg
	Wheel Rate (k_w)	32.56kN/m
	Tyre Rate (k_t)	201.73kN/m
Rear Wheel:	Unsprung Mass (m)	41.26kg
	Wheel Rate (k_w)	28.09kN/m
	Tyre Rate (k_t)	201.47kN/m

Table 5: Mondeo Suspension Rates and Masses

Using these values in conjunction with this formula in equations (4.1) and (4.2) the wheel hop frequencies of the Mondeo were determined as follows:

$$f_{front\_hop} = \frac{1}{2\pi}\sqrt{\frac{k_w + k_t}{m}} = \frac{1}{2\pi}\sqrt{\frac{32560 + 201730}{48.955}} = 11.01\text{Hz} \qquad (4.1)$$

$$f_{rear\_hop} = \frac{1}{2\pi}\sqrt{\frac{k_w + k_t}{m}} = \frac{1}{2\pi}\sqrt{\frac{28090 + 201470}{41.26}} = 11.87\text{Hz} \qquad (4.2)$$

In order to retain the wheel hop frequencies in the raw data, a second order Butterworth filter with a 40Hz corner or cut-off frequency was applied to smooth out the data and produce more readable results. Typical results of the filtered yaw data are shown in Figure 20 and those of the filtered roll data in Figure 21, each of which should be compared to Figures 18 and 19 respectively.
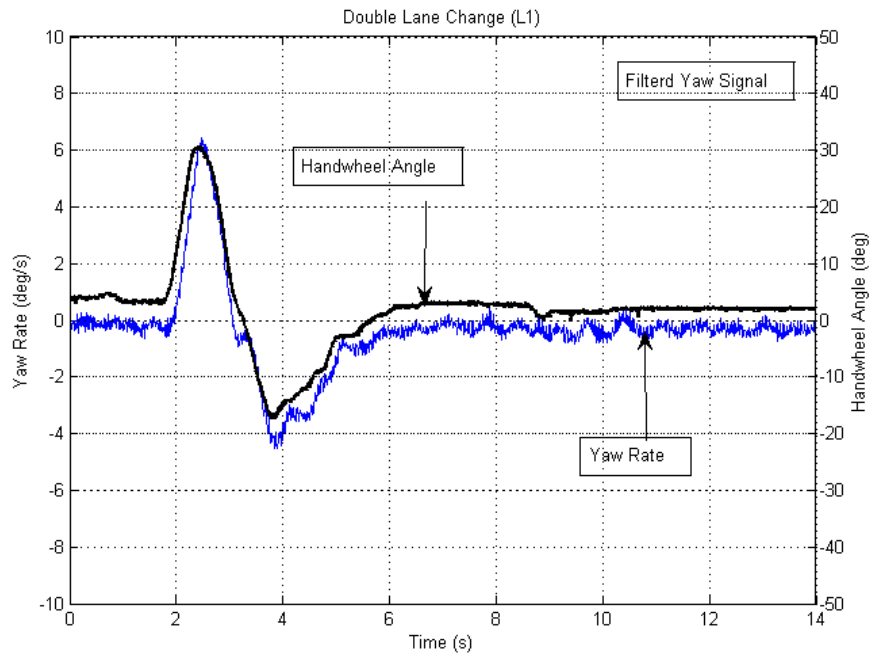
Figure 20: Filtered Yaw Data (40Hz Cut-off Frequency)
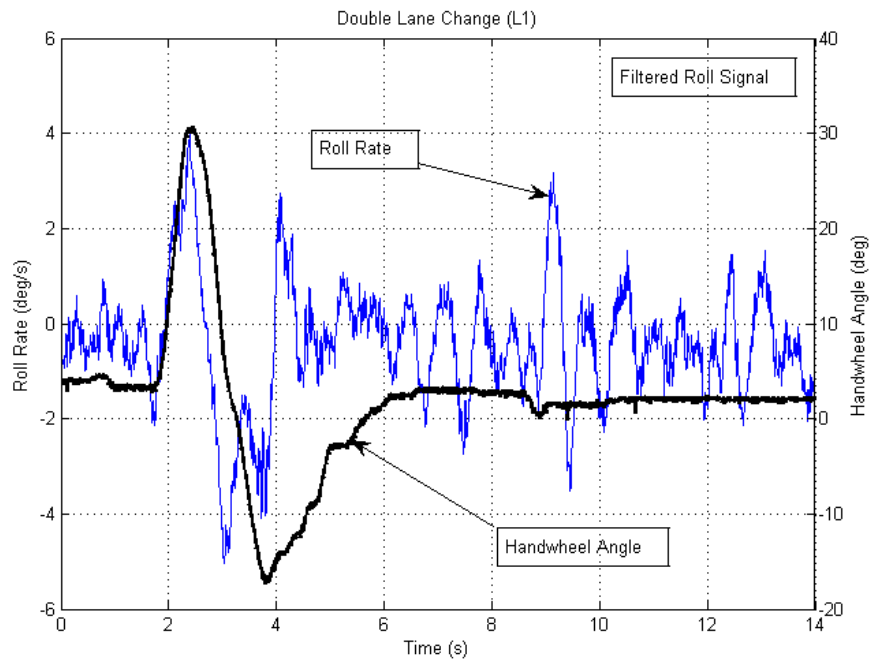
Figure 21: Filtered Roll Data (40Hz Cut-off Frequency)

Comparison of these results shows that the overall signature of the yaw and roll response remained unaffected and that filtering using a cut-off or corner frequency of 40Hz was a reasonable compromise between achieving a smooth output and retaining relevant underlying information.

The vehicle was fitted with linear transducers that recorded the vertical deflections (dZ) of each of the vehicle's road wheels. The output from these sensors is shown in Figure 22 where LF = Left Front wheel, RF = Right Front, LR = Left Rear, and RR = Right Rear. The left rear wheel sensor malfunctioned during testing. It is clear from this graph that the four wheel traces when superimposed give rise to confusion and required separation from each other in order to assist in unambiguous interpretation of the plot. Separation was achieved by adding bias values to the base or quiescent values and the result is shown in Figure 23.
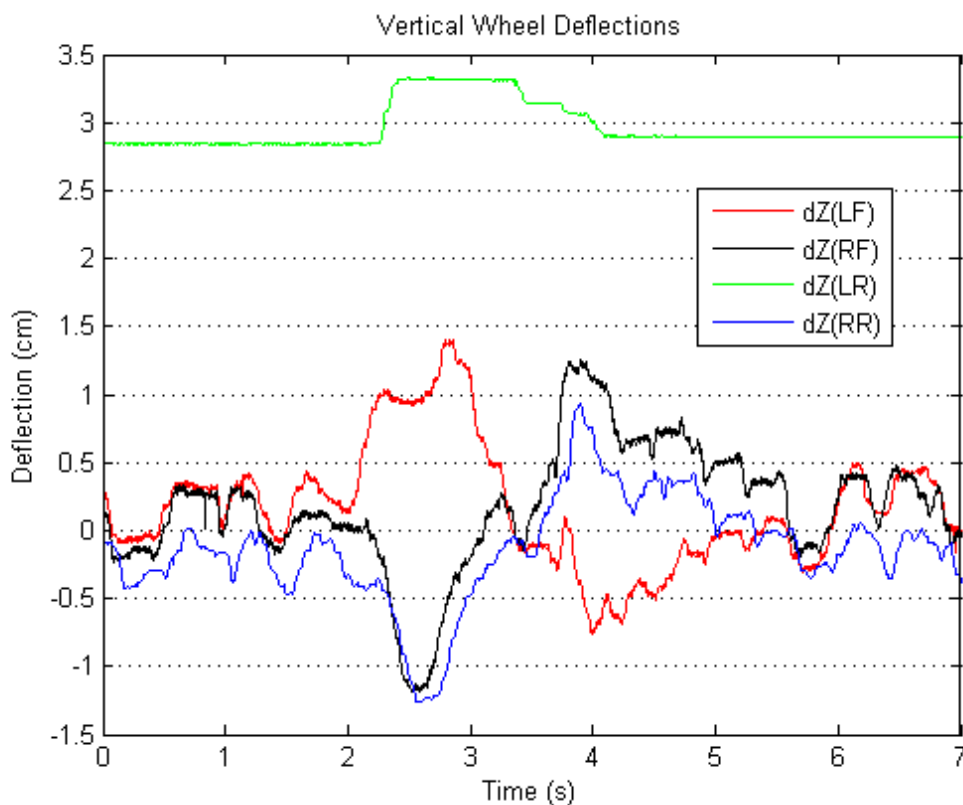
Figure 22: Double Lane Change – Wheel Deflections v Time

Figures 22 and 23 present unfiltered data. Figure 24 shows the wheel deflection data after it had been cleaned up using a Butterworth filter with a cut-off frequency of 40 Hz. Comparison with the unfiltered signal indicated that the difference was minimal. In this instance, the fluctuations in the vertical motion of the wheels were generated as the vehicle was driven at 103km/hr on the M1 motorway and had begun executing a lane change at the 1.5 second mark. The handwheel commands that controlled this manoeuvre were completed by the 6.5 second mark while data was being collected up to the 7 second mark and beyond.

It should be noted that the bias voltages added to the wheel deflection data in order to achieve separation of the these plots is only necessary for the purpose of their visual presentation together on a single graph, as depicted in Figure 23 and Figure 24.
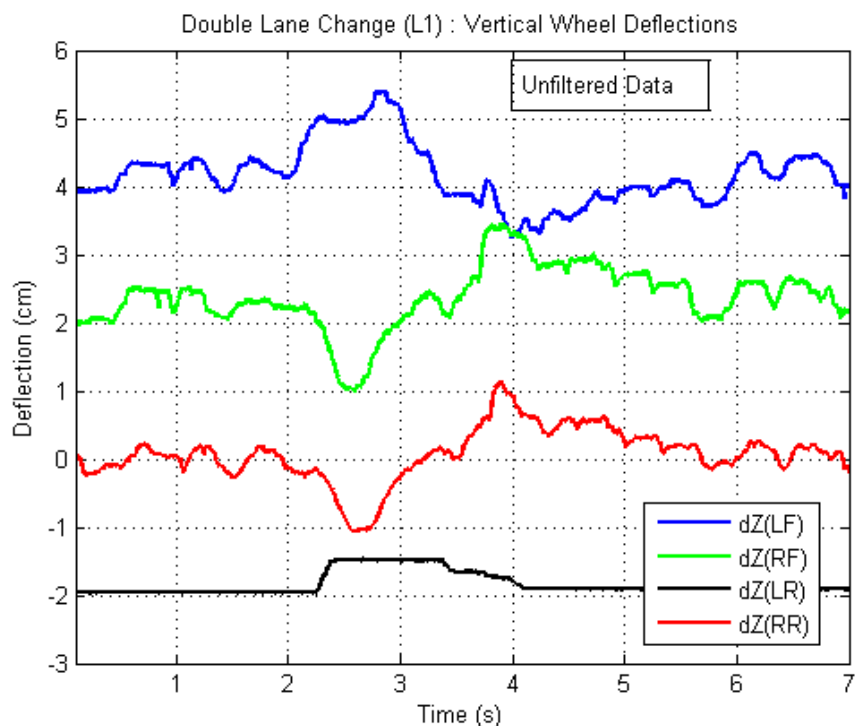
Figure 23: Vertical Wheel Deflections v Time (Unfiltered)
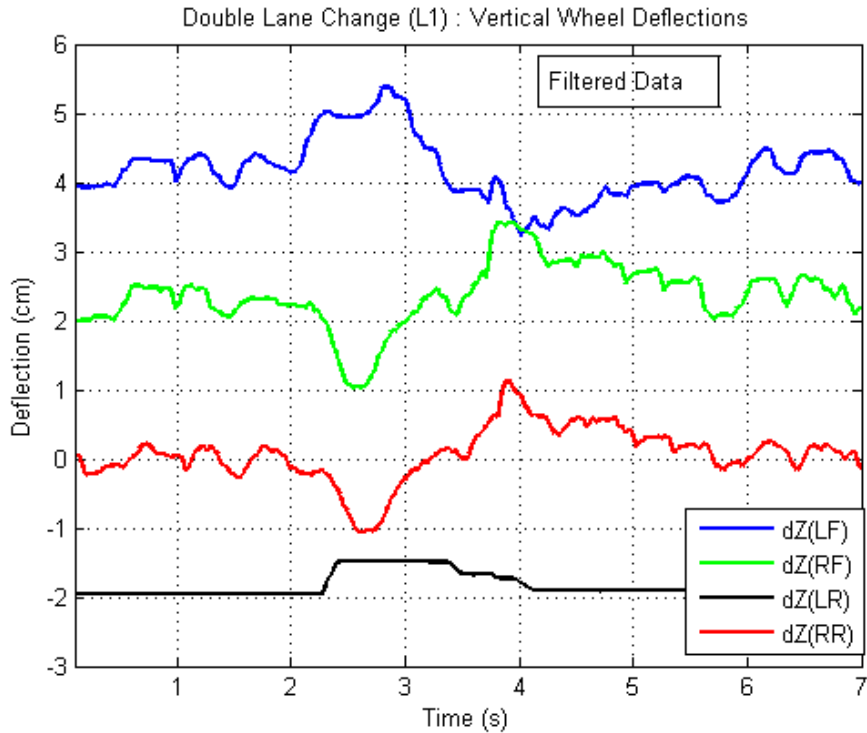
Figure 24: Double Lane Change – Vertical Wheel Deflections v Time
(Filtered: Corner Frequency = 40Hz)

4.3 Summary

This chapter has discussed issues regarding the preparation and post-processing of test data in order to make it useable for analysis. In its raw state data is merely a voltage that must be conditioned to render it into meaningful and readable information about the test vehicle's behaviour. Information has been provided on the bias voltages and calibration factors associated with the raw signals from each of the fifteen sensors with which the test vehicle was instrumented. In addition, the issue of noise was discussed and the problem it presented was highlighted, especially in relation to wheel hop which for this vehicle is in the region of 30Hz.

As a result, the third and part of the fourth objectives listed in Chapter 1 (p.10), requiring that a vehicle be instrumented and prepared for testing, and that the test data be readied for analysis, have been fulfilled.

Chapter 5: Analysis of Test Results

5.1   Introduction

Unfortunately, although data was recorded from all of these tests, that from the brake in a turn test not only failed to record the lateral acceleration and the sideslip angle but also the information regarding brakeline pressure and/or brake pedal force. For the purpose of vehicle characterization, the single and double lane change manoeuvres are of no real use and are essentially regarded as subjective tests because of the pronounced influence of the driver over the execution of the test. They also require a particular test lane set-up which was not possible to create and so these lane change manoeuvres were conducted during normal driving on the public motorway. Despite these drawbacks it is believed that some worthwhile data has been obtained which, though not of sufficient quality for standard vehicle characterisation purposes, was used for validation of a modal model (Chapter 6 and Appendix D). This body of data could be used also for validation of a handling model where the computer simulation involves a virtual test whose command inputs match the actual test that was conducted with the Mondeo and a comparison could then be made of the time histories from both the real test and the virtual test.

5.2   Steady State Cornering

A steady state constant radius cornering test was completed but it only involved a turn to the right because it was conducted on a public roundabout. The ISO standard requires that left- and right-hand versions of the test be performed and that in each case a steady state be achieved for a minimum period of three seconds at three different speeds on the same radius. Figure 25 shows one of the time plots from this test which lasted for approximately 25 seconds (from 17 seconds to 42 seconds on the plot) during which the vehicle made a number of circuits around the roundabout.

This manoeuvre was performed at an approximate turn radius of 10 metres and the speed was varied by the driver from approximately 21 km/hr to 24 km/hr as the

vehicle repeatedly negotiated the roundabout. At these speeds the vehicle experienced lateral accelerations in the range 3.4 to 4.5 m/s^2. The actual radius of turn was not measured but was estimated from the data recovered during the test. However, the ISO standard recommended a test radius of 100m but allows for a minimum radius of 30 metres to be used. The test may be conducted up to a maximum lateral acceleration of say 6m/s^2 or about 0.6g. Because of constraints associated with cost, shortness of time, lack of suitable facilities to set up a course and limited manpower, it was not possible to comply with these stipulations.
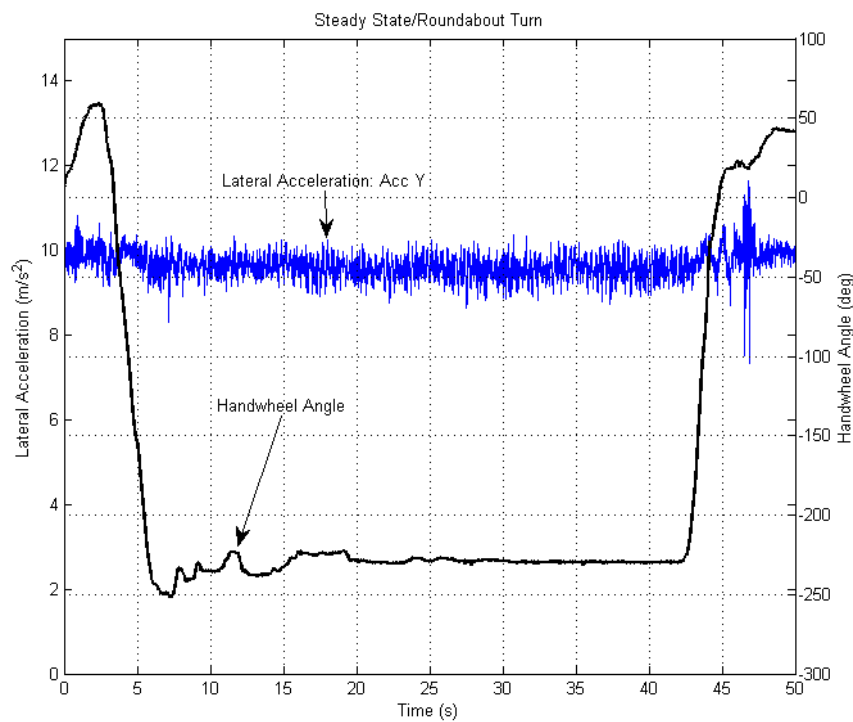
Figure 25: Steady State Turn – Lateral Acceleration & Handwheel Angle v Time

Unfortunately, also, the crucial information required from this manoeuvre – the lateral acceleration – was not recorded because of a sensor malfunction (Figure 25). It was disappointing to lose this signal but it was later thought possible, in accordance with ISO 4138, to make a fair estimate of lateral acceleration by substituting centripetal acceleration in its place. If this is done, a plot of handwheel angle versus lateral acceleration will allow an approximation of the understeer gradient to be determined and offer some indication of the steady state handling behaviour of the vehicle.

To be precise, however, it should be noted that lateral acceleration (a_Y) is not quite the same thing as centripetal acceleration (a_c). Centripetal acceleration (a_c) is the lateral acceleration (a_Y) after it has been adjusted for vehicle sideslip angle (β), which is itself due to the combined effect of the steering angles at the wheels and the elastic deformation of the tyres during cornering (Figure 26). The angle β is the angular difference between the longitudinal X-axis of the vehicle and its direction of local travel [Gillespie (1992) p. 206]. The ISO definition of the vehicle sideslip angle β is *'the angle from the X axis (of the vehicle) to the vertical projection of the velocity vector (v_h) on the ground plane about the Z axis'* [ISO 8855] . The ISO diagram, with additional vectors (in red) representing the centripetal and lateral acceleration of the vehicle, is reproduced in Figure 26.

Figure 26: ISO Bicycle Model of a Vehicle in a Turn

This substitution of centripetal acceleration for the lateral acceleration data means that the affect of the transient components that are present in any steering manoeuvre will be lost. The existence of these components was demonstrated in equation 2.6 (p.25).
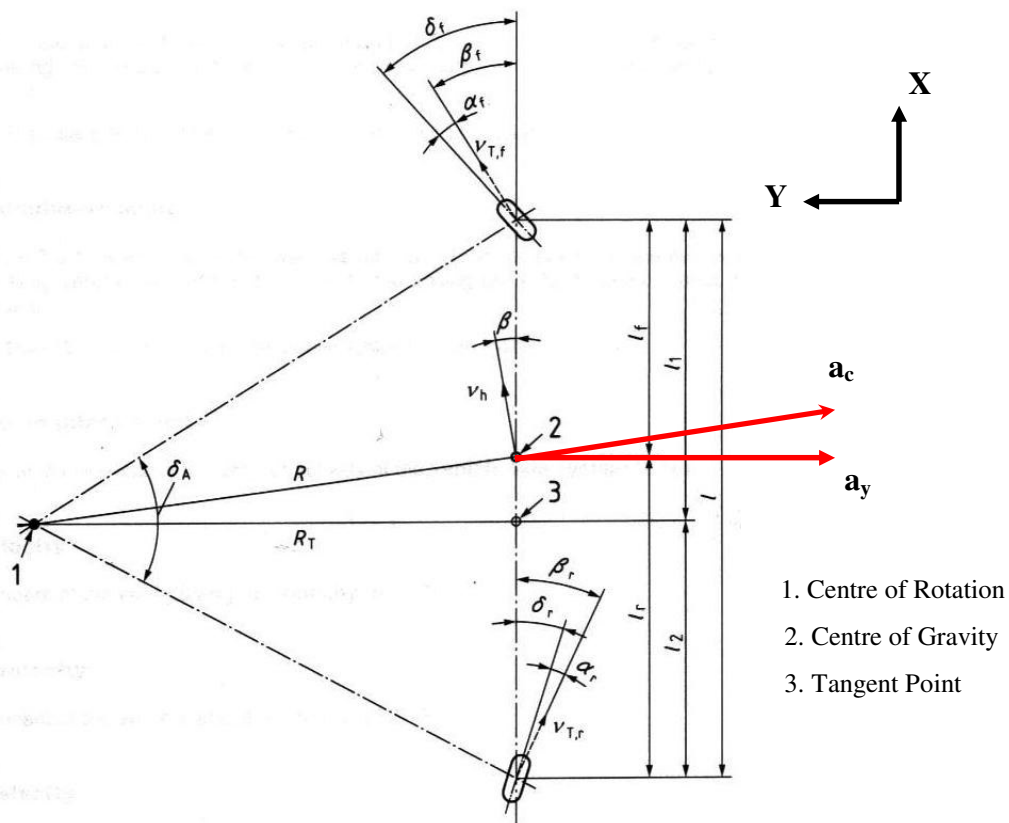
Dixon (1996, p275) defines the linear vehicle cornering behaviour, which he calls its primary handling regime, as anything up to about 0.3g of lateral acceleration. From that value up to 6m/s^2 is the secondary phase where the behaviour is becoming increasingly non-linear and the sideslip angle increases accordingly. However, Dixon qualifies this categorization by stating that modern high-performance cars can exhibit linear handling up to 0.45g. Rill (p.312) provides test data for a modern vehicle very similar to the Mondeo in terms of mass, wheelbase and position of centre of gravity which shows linearity up to a lateral acceleration of approximately 4m/s^2 and a maximum sideslip angle of 4°. The maximum lateral acceleration experienced by the Mondeo under test on the roundabout was 4.5m/s^2. Since lateral and centripetal acceleration differ only by the cosine of the vehicle sideslip angle, which would remain relatively small up to 4.5m/s^2, and since cosβ ≈ 1 for small values of β, using the centripetal acceleration as a substitute for lateral acceleration may be considered acceptable in the circumstances.

Figure 27 presents the ISO required information on the Mondeo's speed, handwheel angle and yaw rate plotted against time for the full duration of the roundabout manoeuvre. The Y-axis scale on this graph is generic and can be used to read values for each of these parameters in their appropriate units as specified in the legend. Negotiating a right-hand turn on a roundabout puts a vehicle into a negative yaw posture; in this case, averaging about 37 degrees per second in the steady state with the handwheel rotated 230 degrees clockwise from the neutral position.

The International Standard ISO 4138: 2004 states that the centripetal acceleration (a_c) may be calculated, equation (5.1), as the product of the vehicle horizontal velocity (v_h) and yaw rate (dψ/dt) as follows:

$$\text{Centripetal Acceleration, } a_c = \frac{d\psi}{dt} \times v_h \qquad (5.1)$$

ISO 8855: 2011 defines vehicle dynamics terms and describes the horizontal velocity (v_h) as the resultant of the vehicle's longitudinal velocity (v_X) and its lateral velocity

(v_Y). As the lateral velocity was unavailable it was necessary to substitute v_X for v_h and accept the introduction of another error at this point. The yaw rate (dψ/dt) is given in degrees per second and must be converted into radians per second (rad/s). The vehicle velocity must be quoted in metres per second (m/s), not kilometres per hour.
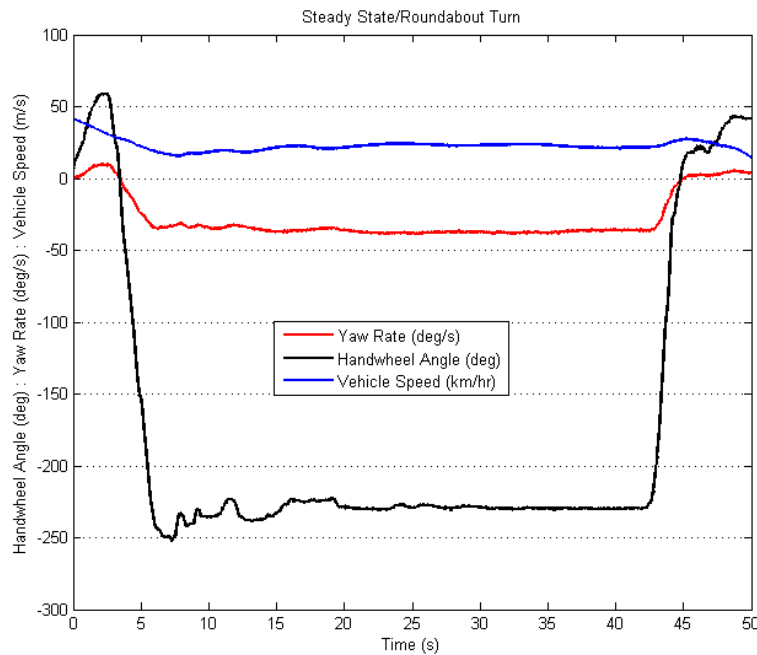
Figure 27: Roundabout Turn – Yaw Rate, Steer Angle & Vehicle Speed v Time

Using MATLAB's Data Cursor on Figure 27 it was possible to determine the vehicle velocity (v_X), yaw rate (dψ/dt) and handwheel angle ($δ_H$) at specific points in time during the steady state turn. The data values for these parameters at time t = 16s, that is, dψ/dt = -37.4 deg/s and v_X = 22.45 km/hr, were used in the following example of the calculation, Equation (5.2), for determining the centripetal acceleration at t = 16s:

$$a_c = \left[\frac{\pi(-37.4)}{180}\,\text{rad}\,/\,\text{s} \right]\left(\frac{22.45}{3.6}\,\text{m}\,/\,\text{s} \right) = -4.0706\,\text{m}\,/\,\text{s}^2 \qquad (5.2)$$

Figure 28 shows all of the time history data for the 25 second period of steady state behaviour during this test between t = 15s and t = 40s (see Figure 27). In MATLAB the column vectors containing the values of the yaw rate (dψ/dt) and the vehicle

velocity (v_X) for every data point in this interval were multiplied by each other to obtain an estimate of the centripetal acceleration of the test vehicle which was then used to determine the understeer gradient for the Mondeo as prescribed by ISO 4138.
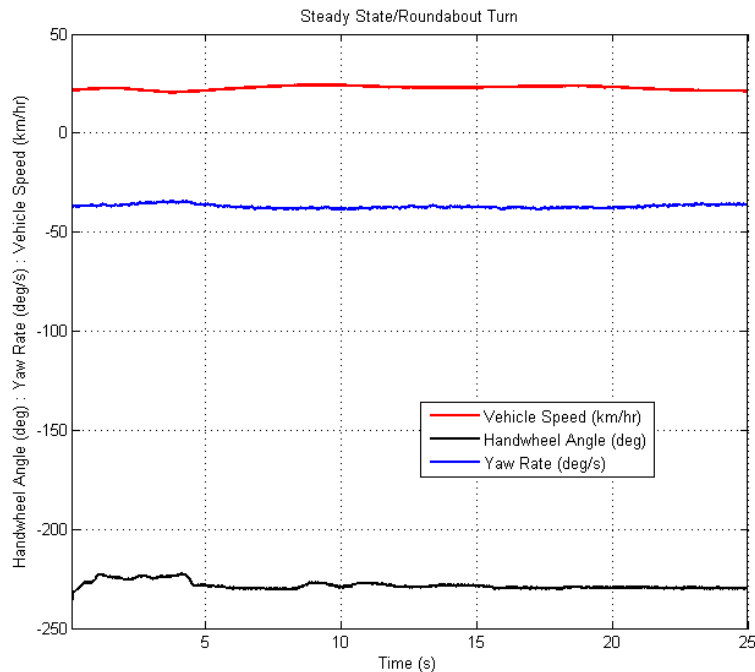
Figure 28: Steady State – Speed, Steer Angle & Yaw Rate v Time

Figure 29 illustrates the plotted results which appear as a cluster of scattered data points centred on a handwheel angle of -230° and a centripetal acceleration of approximately -4m/s². The understeer gradient K, as previously explained in Chapter 2 and presented in Figure 1 (p.28), is the slope of the steer angle curve (the dashed line, assuming linearity) and was calculated using Equation (5.3):

$$K = \frac{\partial \delta}{\partial a_Y} \qquad \text{where} \qquad \delta = \frac{L}{R} + Ka_Y \qquad (5.3)$$

The steer angle δ, in the case of a pair of steered wheels on the same axle, is the equivalent of the mean steer angle of the Mondeo's two steerable front road wheels.

The mean kinematic or Ackermann angle, $\delta_{m,kin}$, as defined by ISO 8855 *Vehicle Dynamics Vocabulary*, is the proportion of δ in Equation (5.3) arising solely from the kinematics of the steering system of the statically loaded vehicle in the absence of dynamic tyre forces and moments, and in the absence of dynamic vertical wheel displacements. The mean kinematic steer angle was calculated using Equation (5.4):

$$\delta_{m,kin} = \frac{L}{R} = \frac{2.745m}{10m} = 0.2745 rad = 15.7° \tag{5.4}$$

where R = 10m is the mean radius of turn on the roundabout and L = 2.745m is the vehicle's wheelbase. Later it will be seen that the units for understeer gradient are degrees per g (°/g) but it should be noted (Rill, 2012), that although the road wheel steer angle (δ) is used to characterise the understeer gradient, the value of that gradient is derived from measurements taken of the corresonding handwheel angle (δ_H). These two angles are related as follows, equation (5.5):

$$\delta_H = i_S \delta_{m,kin} \tag{5.5}$$

The steering ratio (i_S) is defined by ISO 8855 as the rate of change of the handwheel angle with respect to the *mean kinematic (Ackermann) angle* ($\delta_{m,kin}$) of a pair of steered road wheels. The steering ratio for the vehicle was not recorded at the time the vehicle was tested so the handwheel angle δ_H that corresponded to $\delta_{m,kin}$ had to be indirectly calculated based on the Mondeo's kerb-to-kerb turning circle, the full lock handwheel angle and the average Ackermann angle of its pair of front steerable wheels. The handwheel angle at full lock is 500° and was measured when the calibration of the steering pot (Figure 11, p.44) was being checked before taking the car out for testing. For a front wheel steering vehicle like the Mondeo, the diameter of the kerb-to-kerb turning circle is measured using the rolling arc of the outer steered wheel: this was 10.8m and therefore the radius is 5.4m. The inner steered wheel will roll on a smaller circle whose radius will be 5.4m less the front wheel track (T) (see Appendix A for *Ford Mondeo Vehicle Specifications*): that is, 5.4 - 1.522 = 3.878m.

Therefore, under full lock with the handwheel angle at 500°, the Ackermann angles for the front outer and the front inner steered wheels were, equations (5.6) and (5.7):

$$\delta_{A\_Outer} = \frac{L}{R} = \frac{2.745\text{m}}{5.4\text{m}} = 0.5083\text{rad} = 29.13° \qquad (5.6)$$

$$\delta_{A\_Inner} = \frac{L}{R-T} = \frac{2.745\text{m}}{3.878\text{m}} = 0.7078\text{rad} = 40.56° \qquad (5.7)$$

The average of these kinematic angles was 34.84°. With a 500° lock at the handwheel that represents a steering ratio (i_S) of $500 \div 34.84 = 14.35$ to 1. In reality, this may actually be too low because steering ratios in modern cars are variable and at full lock normally have a lower value than for handwheel angles at the central or mid range.

Returning to the roundabout manoeuvre, the handwheel angle corresponding to the mean kinematic angle ($\delta_{m,kin}$) of the Mondeo's pair of steered wheels, which was calculated using equation (5.4), was then estimated as follows, equation (5.8):

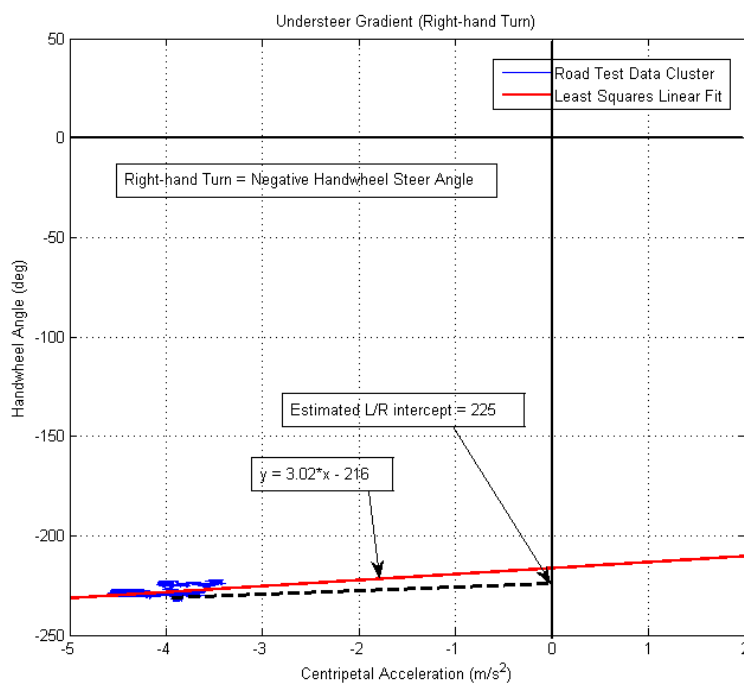$$\delta_H = i_S\delta_A = 14.35(15.7°) = 225° \qquad (5.8)$$

Figure 29: Steer Angle Curve – Handwheel Angle v Centripetal Acceleration

This value for the handwheel angle represents the 'L/R' intercept point on the understeer gradient plot shown in Figure 29. Based on the argument previously made, the assumption here is that the handling behaviour of the Mondeo is linear out to a lateral (≈ centripetal) acceleration of 0.4g (negative for a right-hand turn). This linearity is represented by the dashed line. At the intercept point there is zero lateral/centripetal acceleration and therefore no compliant slip angle effects on the steering. The understeer gradient K is the slope of the dashed line and a value for K can now be determined. Gillespie (p.228) states that a positive slope (upward to the right) is indicative of an understeer response. Evaluating the understeer gradient from the dashed line in Figure 29, the value of the gradient K, based on the handwheel angle, was determined to be about 12.3°/g using equation (5.9):

$$K = \frac{\Delta \delta_H}{\Delta a_Y} \approx \frac{-230° - (-225°)}{-4 m/s^2 - 0} \approx \frac{-5°}{-4 m/s^2} \approx 1.25° / m/s^2 \approx 12.3° / g \qquad (5.9)$$

This was adjusted by dividing by the estimated steering ratio (i_S = 14.35) in order to reference it, as is conventional, to the steer angle at the road wheels, thus giving:

$$K = \frac{12.3° / g}{14.35} = 0.86° / g \qquad (5.10)$$

However, a more accurate way of directly using the test data to determine the slope K and the intercept L/R is to perform a linearization process using the method of least squares. When the MATLAB curve-fitting tool is applied to the (blue) data cluster in Figure 29 the red line is generated. This has the generic straight line equation

$$y = 3.02x - 216$$

This analysis indicates an intercept value of L/R = -216° which is within 4% of the previously estimated value of 225°. The understeer gradient value obtained is 3.02°/m/s^2 or 29.63°/g at the handwheel. When this is divided by the estimated steering ratio of 14.35, as per Equation 5.10, in order to reference it to the road wheel, the result is 2°/g. Unlike the previous value of 0.86°/g which was based upon

estimates of extrinsic parameters this value, directly derived from the test data, must be considered more accurate and representative of the vehicle's characteristic behaviour. Moreover, the steering ratio of 14.35 is almost certainly an underestimate and therefore the understeer gradient of 2°/g may also be considered an upper bound of the true value.

However, it should also be noted that the cluster or cloud of data that was used to derive this linear fit is not uniform in nature but consists of two distinct 'linear' bands of data. Neither of these linear bands align very well with the least squares fit (red line) but seem to individually comply better with the original estimated (black dotted) line. These linear bands of data are due to the fact that the test vehicle driver did not negotiate the roundabout at the exact same radius and speed throughout the whole maneouvre. There were times when he drove very slightly faster at a slightly larger radius. The least squares linearization method, in having to accommodate both bands of data, is therefore skewed slightly and this would lead one to conclude that the actual understeer gradient of the Mondeo is closer to 0.86°/g than to 2°/g. A good estimate would be about 1°/g.

Different researchers quote different typical values for K which probably merely reflects the complex variety of vehicles that have been tested and their evolving designs over time. Based on the steer angle of the road wheel, Dixon (p.275) who published in 1991, gave typical values for K in the region of 1°/g to 3°/g depending on the magnitude of lateral acceleration. Dixon also observed that vehicles noteworthy for their good handling behaviour had understeer gradients closer to neutral steer. Published in 2008, Dukkipati et al (p.366) gave a typical K value for a car as 1.5°/g depending on lateral acceleration. Confusingly, they also state elsewhere that an average value for an American car is 0.45 deg/m/s^2 (4.4°/g) and for a European car 0.265 deg/m/s^2 (2.6°/g). The initial estimate of K = 0.86°/g and the more accurate value of 2°/g based upon numeric analysis appears to be reasonable bearing in mind the shortcomings in the testing and in the data obtained.

On the day of testing, the Mondeo had its centre of gravity shifted rearwards to a more central position between the front and rear axles. The change in load distribution on

the axles went from 60/40 (unladen) to 55/45 (laden). Unfortunately, as there is no information available concerning the cornering stiffness of the tyres no further analysis of the steer characteristics of the vehicle was possible. However, it may be noted that as the centre of gravity of a vehicle shifts to a more central position between the front and rear axles, the steer characteristic tends more towards neutral steer. In the case of a vehicle with equal loading on its front and rear wheels the only factor affecting the magnitude of the slip angles is the cornering stiffness of the front and rear tyres. It should also be noted that the estimated steering ratio of 14.35 is likely, in reality, to be greater and that would increase the neutral steer L/R value calculated using equation (5.8) which, in turn, would bring the understeer gradient calculated in equations (5.9) and (5.10) closer to zero, a neutral steer characteristic.

To summarise, the steady state cornering manoeuvre was not conducted properly as per the ISO standard and the limitations involved may be bulleted as follows:-

- Only one right-hand turn test was performed instead of a number of turns to both the left and right;
- The radius of turn was too small thus resulting in a large turn angle;
- The test was conducted at only one discreet speed instead of three;
- No lateral acceleration or sideslip angle data was recorded;
- The radius of turn and the steering ratio were not directly recorded.

The upshot of this lack of compliance was that the determination of the undeersteer gradient was based upon the use of centripetal acceleration as a substitute for lateral acceleration and the assumption of linear handling behaviour up to a lateral acceleration of 0.4g as depicted by the dashed line in Figure 29.

Finally, although not required by the ISO standard, plots of the vertical wheel deflections (cm) are presented in Figure 30. These deflections are positive when the wheel is in bump (suspension compressed) and negative when it is in rebound (suspension extended). In this plot, the four traces appear separated because bias deflection values have been deliberately added, otherwise all four traces would have overlapped and intertwined each other and been quite unreadable. The 25 seconds

between t = 17s and t = 42s represents the period of steady state cornering already analysed. Clearly, the left rear wheel deflection sensor malfunctioned during the test. The two lower plots show each of the front and rear right (offside) wheels to have been in a similar steady state rebound condition as the vehicle leaned out of its right-hand turn around the roundabout. The left front and right rear wheels (the two middle traces) seem almost mirror images of each other, reflecting the fact that the former was the most heavily loaded wheel during the manoeuvre while the latter was the most lightly loaded. For clarity the deflection data recorded from each of the three sensors that worked properly on the day of testing have each been presented on separate plots, Figures 31, 32 and 33.
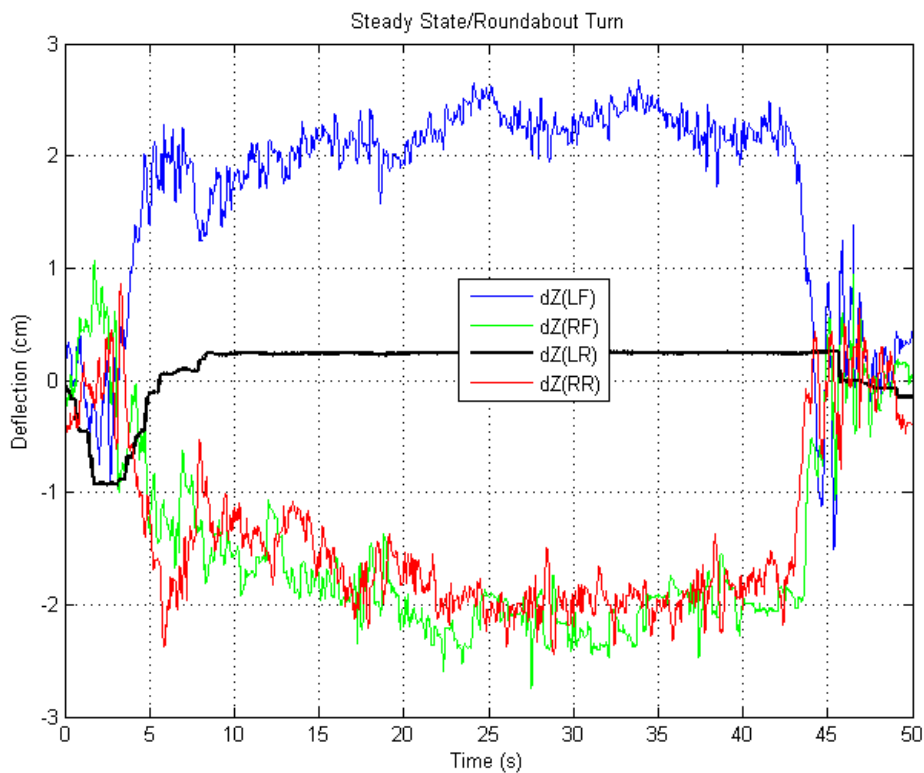
Figure 30: Steady State Turn – Vertical Wheel Deflections v Time
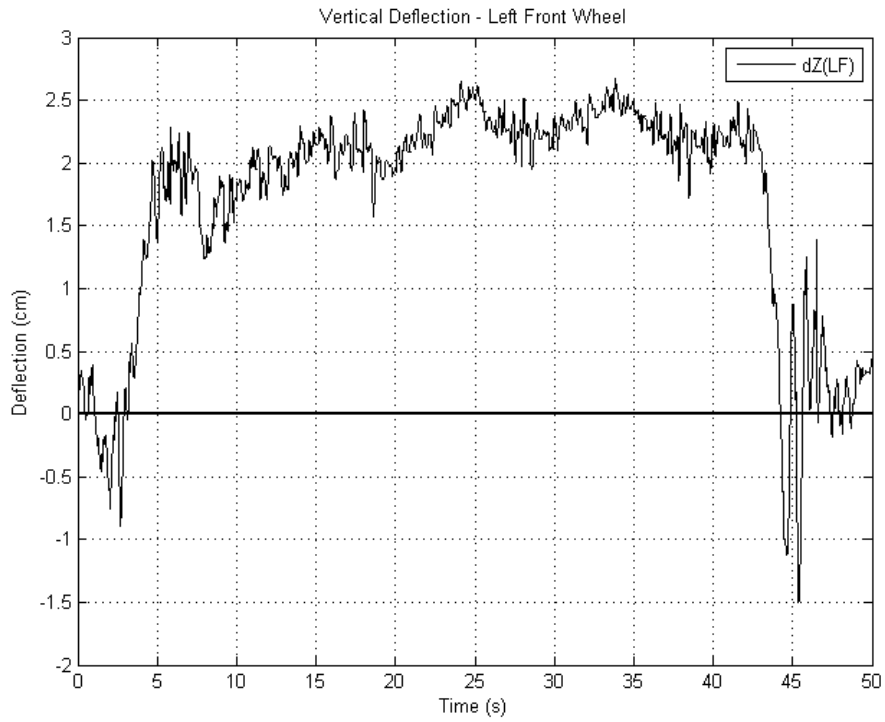
Figure 31: Left Front Wheel Vertical Deflections v Time
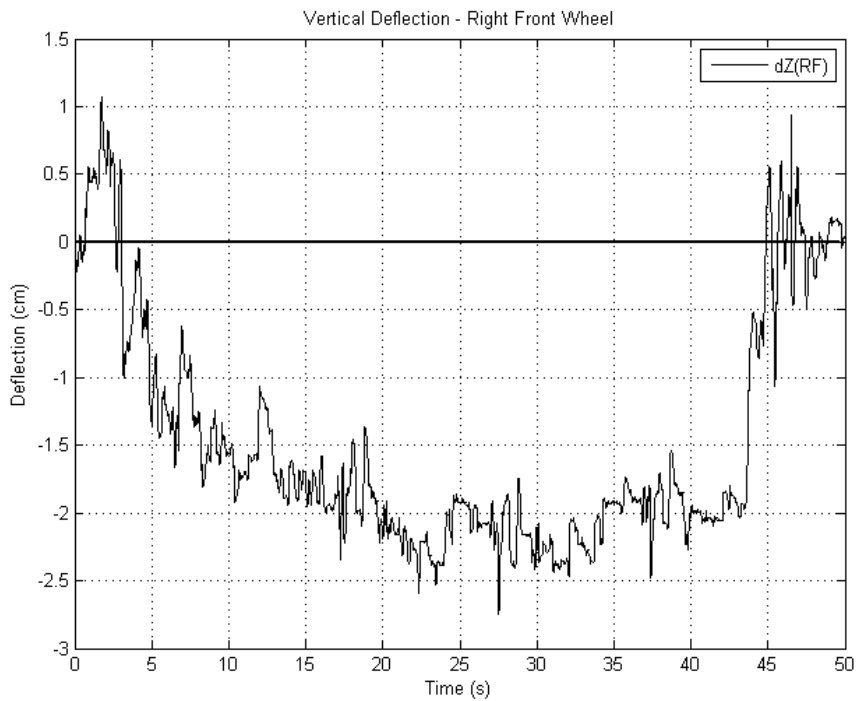
Figure 32: Right Front Wheel Vertical Deflections v Time
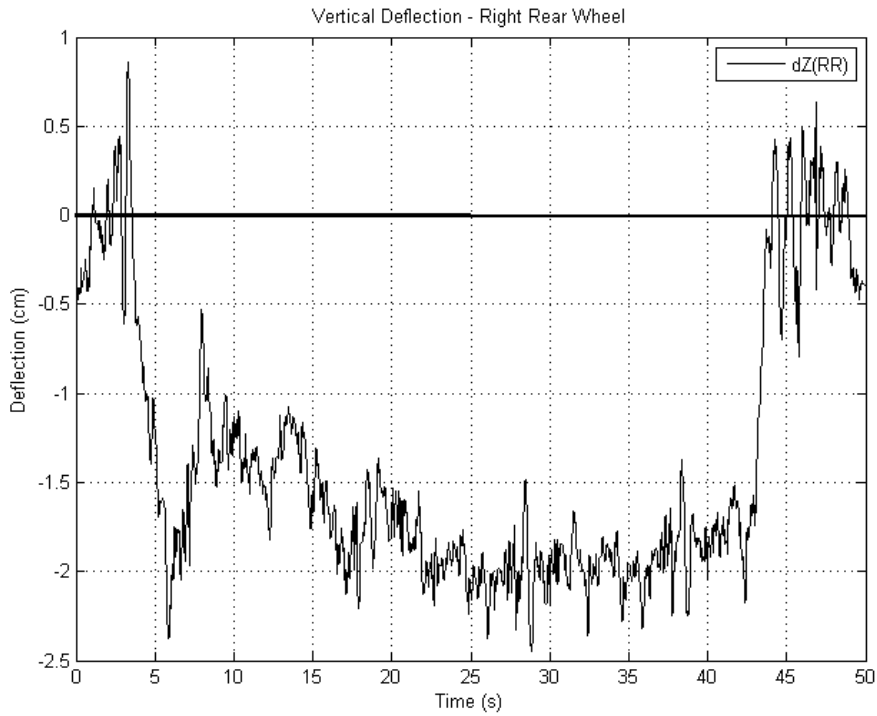
Figure 33: Right Rear Wheel Vertical Deflections v Time

5.3 Step Steer (J-turn)

Whereas the roundabout cornering manoeuvre previously analysed is used to characterise a vehicle's steady state steering behaviour, the step steer (J-turn) manoeuvre provides useful information about a vehicle's transient response to a handwheel steer angle (δ_H) input. The Mondeo performed four successful Step Steer or J-turn manoeuvres: two to the left and two to the right. The ISO 7401 standard recommends that at least three each be performed. The four successfully completed tests were all conducted at a nominal 32km/hr (20mph) on a very rough car park surface. A test speed of 100km/hr is recommended by the ISO standard but it also states that other test speeds may be used. The wheel speed sensors, from which the actual vehicle speed was taken, recorded a speed of 30 km/hr.

The results from one of the right-hand turn tests are presented in Figure 34 in the form of the required time history for handwheel angle (δ_H), lateral acceleration (a_Y) and yaw

velocity (dψ/dt). The Y-axis on this graph is generic and can be used to read off in the appropriate units the value of whatever parameter is being estimated.
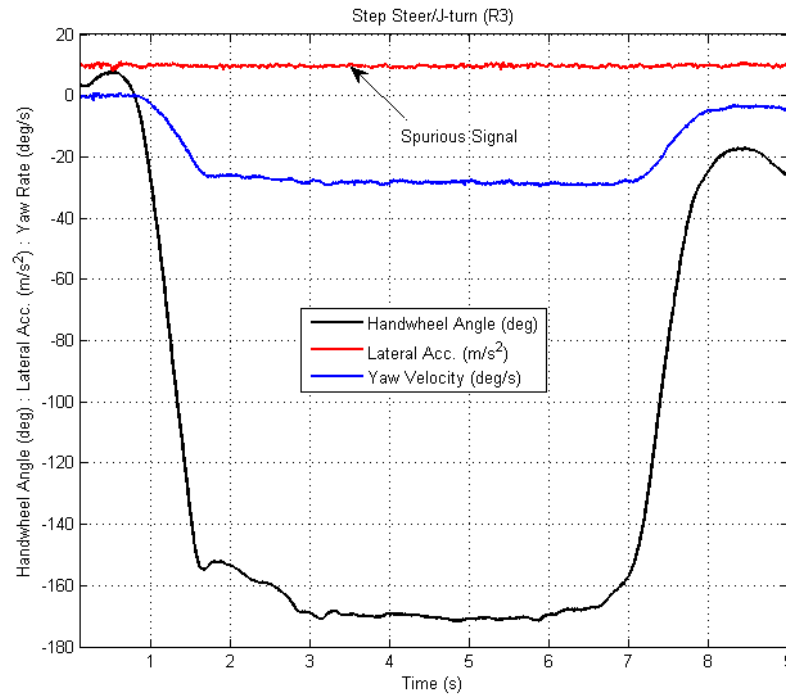
Figure 34: Handwheel Angle, Lateral Acceleration & Yaw (Rate) Velocity v Time

The top plot on this graph is that of the lateral acceleration. The faulty accelerometer recorded an average lateral acceleration value of approximately 10m/s² or 1g and malfunctioned just as it did during the steady state cornering test. Both of these tests, in fact, were performed during the same test session. Using the same arguments that were put forward previously it was decided to substitute centripetal acceleration – calculated as the product of yaw rate/velocity (dψ/dt) and longitudinal velocity (v_X) – for the unreliable lateral acceleration data. This calculation was performed using MATLAB and the result is presented in Figure 35.

Figure 36 shows a plot of the handwheel step steer command applied to the vehicle. Effectively, this is a ramp input. Based on the procedure prescribed in the ISO standard for analyzing this input and using MATLAB's Data Cursor on the plot in Figure 35, it was determined that the handwheel was rotated 170° clockwise in 0.78 seconds initiating a right-hand turn and creating a negative steady state yaw velocity

response of approximately 28°/s after a small time lag. (The yaw velocity plot can be seen on Figure 37). This turning manoeuvre was sustained for approximately 5.5 seconds. The plot of the handwheel angle input has been inverted here for the purpose of analysing it as a conventional step (or ramp) input as is demonstrated in ISO 7401.
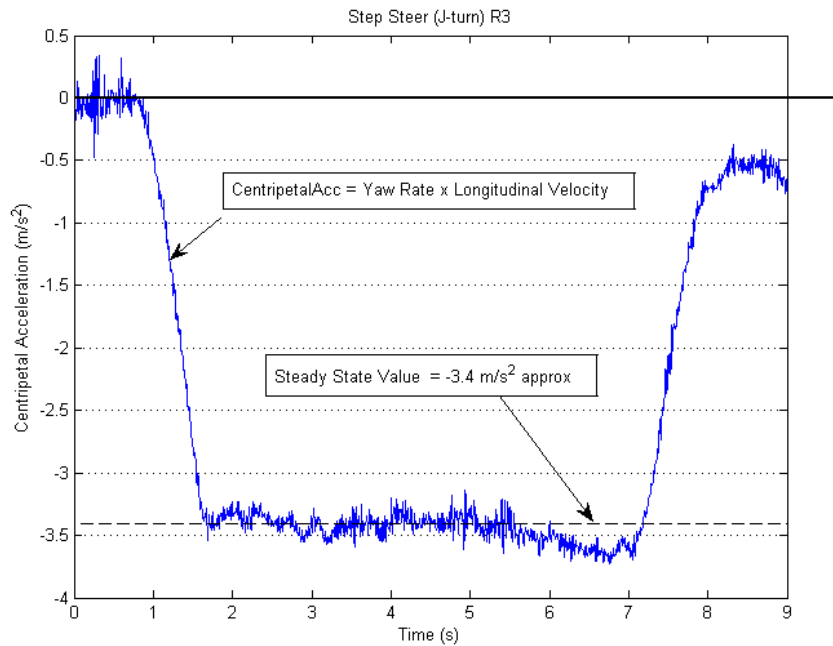
Figure 35: Step Steer – Centripetal Acceleration v Time

The step steer command achieved a steady state, δ_{SS}, at -170°. Using the MATLAB data cursor it was determined that the steer command was initiated at t = 0.87s and was nominally completed at t = 1.65s; that is, 1.65 – 0.87 = 0.78s. When analysing other response plots, the time at which 50% of the steady state steer input was completed was taken as the reference time (t_0) from which these other response times were measured. Again, by using the MATLAB data cursor on the handwheel angle plot in Figure 36 it was established that t_0 = 1.25s.

The ISO 7401 standard requires that the time histories of the yaw rate and lateral acceleration – now being replaced by the centripetal acceleration – be analysed in order to characterise the vehicle's transient behaviour. Figure 37 shows the plots of both the centripetal acceleration and the yaw velocity response.
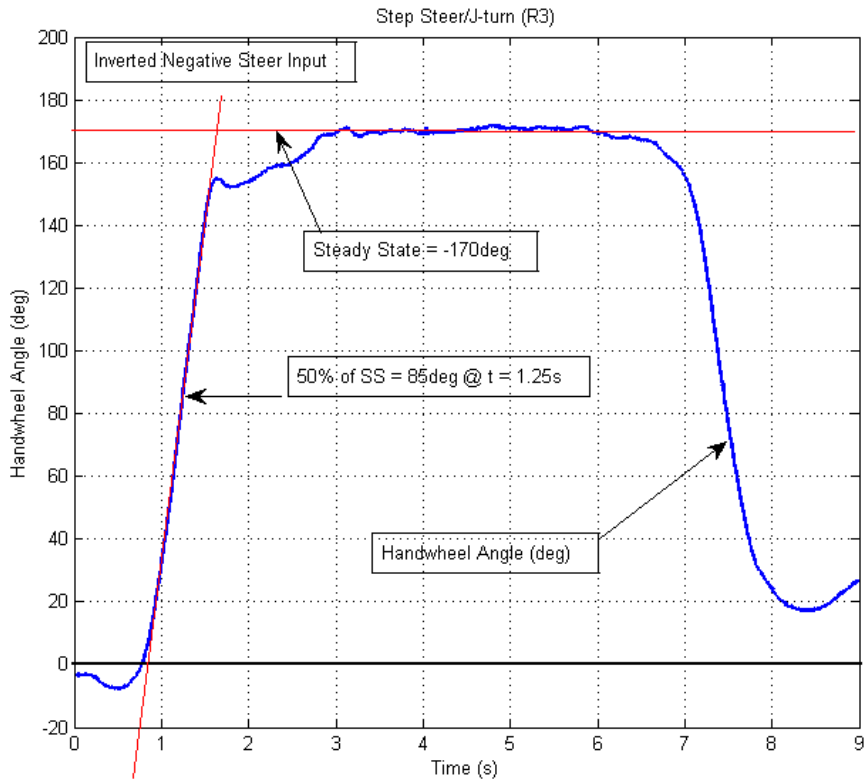
Figure 36: Analysis of the Handwheel Step Command Input
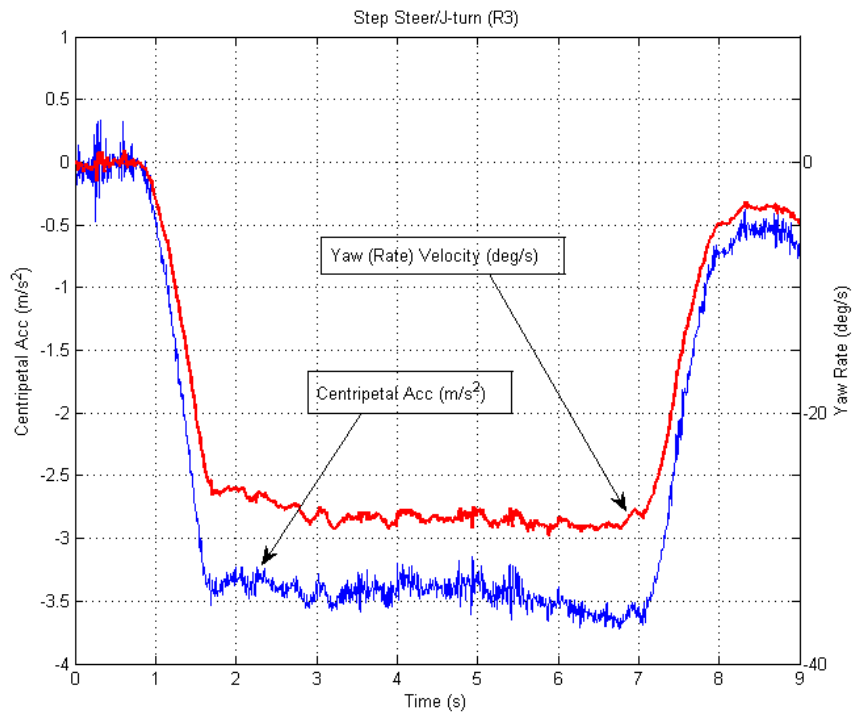
Figure 37: Step Steer Test – Centripetal Acceleration and Yaw Rate v Time

Again, using MATLAB's data cursor the steady state value for centripetal/lateral acceleration (a_{Y_SS}) was -3.4m/s^2 and for yaw rate (($\dot{\psi}_{SS}$) was 28°/s. With t_0 = 1.25s the response values provided in Table 6 were determined

Lateral Acceleration	Response Time	T_{aY}	0.31s
	Peak Response Time	T_{aYmax}	0.41s
	Overshoot	U_{aY}	0
Yaw (Rate) Velocity	Response Time	$T_{\dot{\psi}}$	0.39s
	Peak Response Time	$T_{\dot{\psi}\,max}$	1.57s
	Overshoot	$U_{\dot{\psi}}$	0

Table 6: Step Steer/J-turn Response Values

ISO 7401 defines the response time as the time taken to reach 90% of the steady state. For centripetal/lateral acceleration, 90% of -3.4m/s^2 is 3.06m/s^2 and this was reached at t = 1.56s. Therefore, T_{aY} = 1.56 – 1.25 = 0.31 seconds. Peak response time is the time to reach the maximum response value which for centripetal/lateral acceleration was 1.66s, so T_{aYmax} = 1.66 – 1.25 = 0.41s. The centripetal/lateral acceleration data was noisy and -3.4m/s^2 was the average steady state value. The fluctuations on the upper side of this mean value were not considered to represent an overshoot.

A similar analysis was conducted on the yaw velocity data which had a steady state value ($\dot{\psi}_{SS}$) of -28°/s. 90% of 28°/s is 25.2°/s and this value was reached at t = 1.64s so that the yaw velocity response time $T_{\dot{\psi}}$ = 1.64 – 1.25 = 0.39s. The peak yaw velocity response time $T_{\dot{\psi}\,max}$ = 2.82 – 1.25 = 1.57s. Dukkipati et al (2008) state that at a test speed of 31.3m/s (for this test it was 8.3m/s) and with a lateral acceleration of 0.4g (for this test it was 0.34g) a typical range for yaw velocity overshoot is 12% to 65%.

The final response value sought by the International Standard ISO 7401 (Par. 10.3.3) was the steady state yaw velocity gain, $(\dot{\psi} / \delta_H)_{ss}$, the rate of change of yaw velocity with respect to handwheel angle under steady state conditions. This measures the responsiveness or sensitivity of the vehicle to steering inputs at the handwheel and is based upon the relationship between the steady state yaw velocity ($\dot{\psi}_{ss}$) and the steer input that generated it. It was calculated as $\dot{\psi}_{ss} / \delta_{ss}$ = -28°/s ÷ -170° = 0.1647s^{-1}. Dixon, p.383, states that yaw velocity gains are referenced to the handwheel angle and that values in the range 0.2°/s per degree to 0.4°/s per degree are desirable and correspond to understeer gradients of 3.4°/g down to zero.

The procedures outlined here for analysing the 'Step Steer (R3)' manoeuvre were also performed for the other three successfully conducted J-turn tests, identified as L3, L4 and R4, where 'L' indicates a left-hand turn and 'R' a right-hand turn. The plots associated with these other tests, and upon which these analyses were made, are shown in Figure 38 and the results of the analyses have been entered into Table 7. For the purpose of comparison, the time history plots of the J-turn or Step Steer (R3) test have also been included in Figure 38.

It is clear from an inspection of the time histories in Figure 38 that the J-turns were not executed in the manner prescribed by the ISO standards. For example, these standards require that the handwheel step steer angle be executed in one clean action without hesitancy. Ideally, a physical stop or check should have been applied to the handwheel to facilitate better execution of the step steer.

The step steer tests should also have been conducted at a recommended test velocity of 100 km/hr and should have been performed separately on the vehicle when set up for minimum and maximum loading conditions as described in Chapter 2. None of these requirements were complied with.
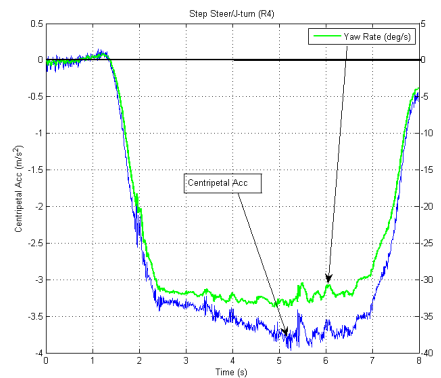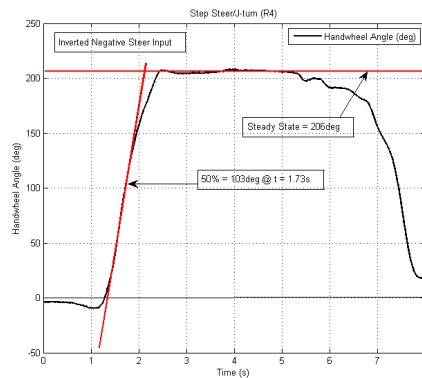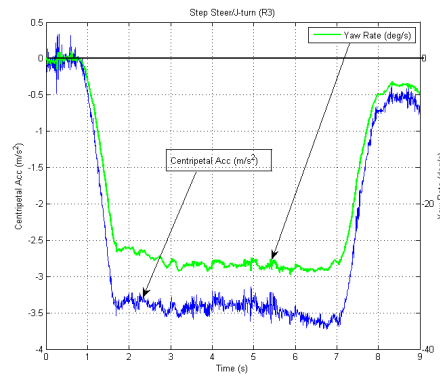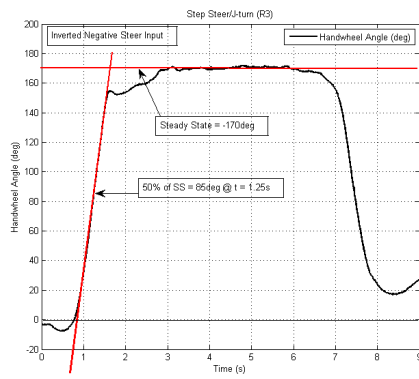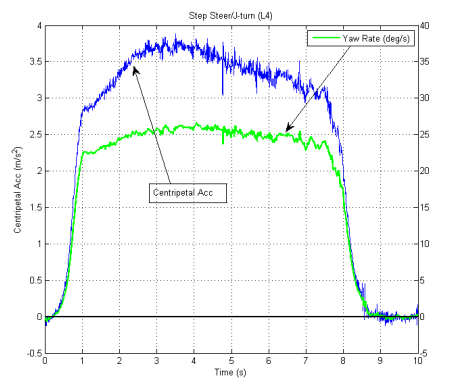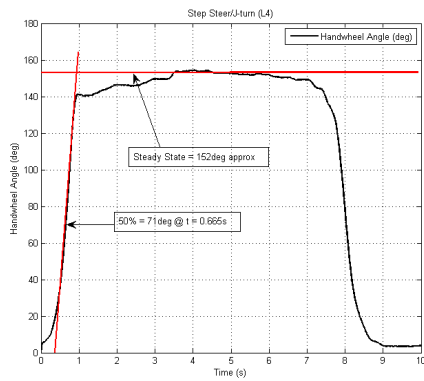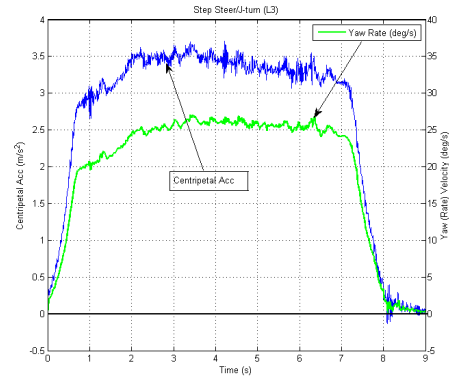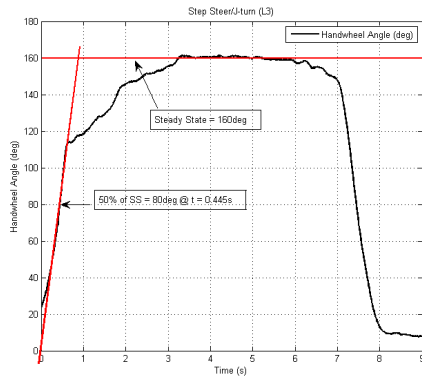
Figure 38: Time Histories for Step Steer Manoeuvres L3, L4, R3 and R4

77

Parameter	Symbol	Unit	Left Turns		Right Turns		Average
			(L3)	(L4)	(R3)	(R4)	
Steady State Yaw Vel. Gain	$(\dot{\psi}/\delta_H)_{SS}$	s^{-1}	0.1625	0.1645	0.1647	0.1602	0.1630
Lat Acc Response Time	T_{aY}	s	0.76	1.11	0.31	0.71	
Lat Acc Peak Response Time	T_{aYmax}	s	1.7	2.03	0.41	3.125	
Lat Acc Overshoot	U_{aY}	-	0	0.25	0	0.2	
Yaw Velocity Response Time	$T\dot{\psi}$	s	1.865	0.58	0.39	0.6	
Yaw Vel Peak Response Time	$T\dot{\psi}_{max}$	s	3.05	3.04	1.57	2.655	
Yaw Velocity Overshoot	$U\dot{\psi}$	-	0	0	0	0	

Table 7: Summary of the Step Steer/J-turn Response Data

In summary, the transient response values provided in Table 7 show that the results were not consistent, the large differences in the values obtained reflecting differences in the manner in which individual tests were carried out. However, despite the lack of absolute compliance with the ISO test standards, the yaw velocity gain ($\dot{\psi}_{SS}/\delta_{SS}$), was fairly consistent and provided an average value of 0.163°/s per degree which is less than the lower value in the range stated by Dixon. No overshoot in the yaw velocity response is indicative of a neutral steer condition according to Dixon (1996). This finding is reinforced by the steady state cornering analysis which previously showed a virtual neutral steer vehicle with a very small understeer characteristic. It will be recalled that a low steering ratio of 14.33, which is more likely to be higher, gave an understeer gradient of only 0.86°/g at the road wheel. If the steering ratio is actually higher the value of the understeer gradient would approach zero more closely or may even become consistent with an oversteer condition.

The wheel deflection sensor outputs for one manoeuvre is shown in Figure 39. LF = Left Front wheel, RF = Right Front, LR = Left Rear, and RR = Right Rear.
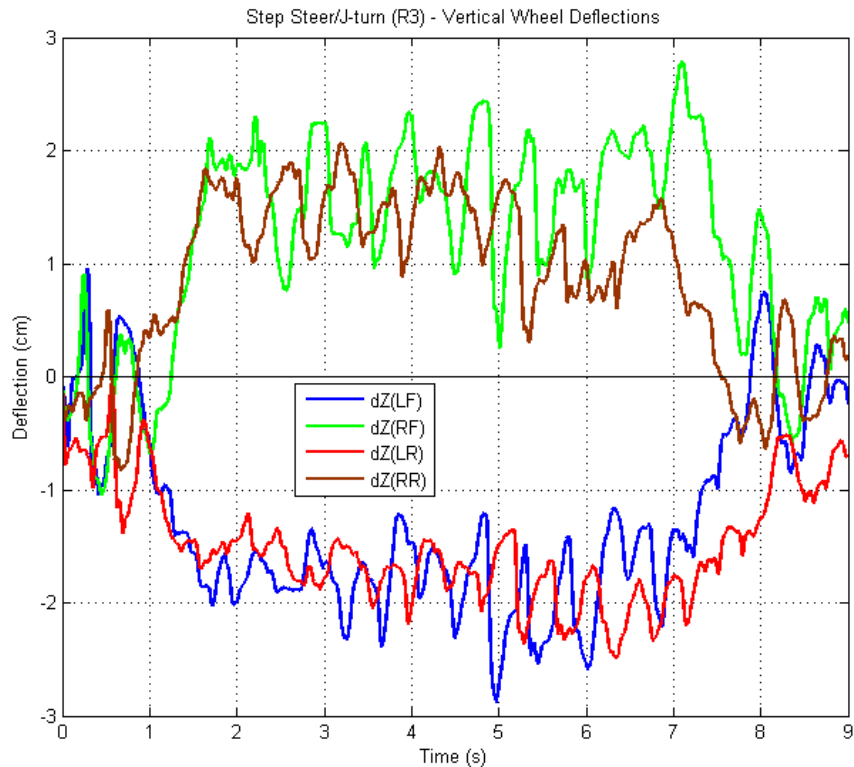
Figure 39: Step Steer/J-turn – Vertical Wheel Deflections v Time

5.4   Power-off in a Turn

This test should be performed in accordance with ISO 9816: 2006. The introduction to the ISO documentation says that 'insufficient knowledge is available concerning the relationship between accident avoidance and the dynamic characteristics evaluated in this test'. The purpose of this test is to investigate the power-off effect on the course holding and directional ability of a vehicle when operating in a steady state condition. The initial steady state conditions are defined by a constant longitudinal velocity and by a constant radius of turn. The power-off is introduced by a sudden release of the accelerator pedal after which the handwheel angle should be kept constant.

The constant radius test method involves initial conditions where the vehicle is being driven on a constant radius and the initial lateral acceleration is about $4m/s^2$. The lateral acceleration is incrementally increased by increasing the initial speed in each test run. The initial steering or handwheel (δ_H) angle will change as lateral

acceleration changes. This test demands a certain level of skill on the part of the driver who must achieve the initial steady state cornering conditions while following a circular path of fixed radius. It was not possible in the time available to facilitate the performance of practice runs as part of the current work and research. Four completed power-off tests were carried out on the Mondeo: two to the right (designated R1 and R3) and two to the left (L2 and L3).

ISO standards require the following information from the test: the moment of power off (t_0), the handwheel steer angle (δ_H), the yaw velocity ($d\psi/dt$), the longitudinal velocity (v_X) and the lateral acceleration (a_Y). Desirable parameters are the longitudinal acceleration (a_X), the lateral velocity (v_Y), and the pitch (θ) and roll (φ) angles.

Figure 40 shows the results obtained from one of the left-hand turn manoeuvres (L3). As with the previous two tests the lateral acceleration sensor malfunctioned for this test also and recorded a noisy acceleration signal centred on a value of 1g or 10m/s^2. Yet again, therefore, the calculated centripetal acceleration will be used as a substitute for the lateral acceleration.
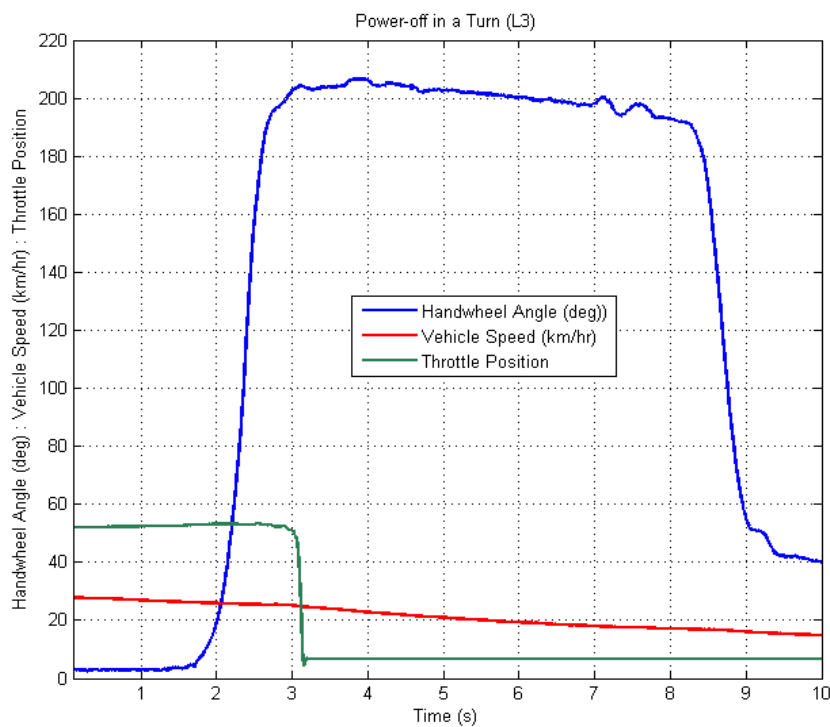
Figure 40: Power-off in a Turn – Throttle Opening & Handwheel Angle v Time

The Mondeo was put into the left-hand turn (L3) by rotating the handwheel anticlockwise by approximately 200° or so. The ISO standard for this manoeuvre stipulates that the steady state handwheel angle must remain within ±3% for the 2 seconds after the initiation of power-off. In this case the angle fluctuated between 207° and 202°, which is acceptable. Using the MATLAB Data Cursor on the throttle sensor plot it was determined that power-off was initiated at approximately 3 seconds into the recorded data, i.e. $t_0 = 3s$.

The ISO standards state that there is insufficient knowledge regarding which test variables best represent the subjective feeling of the driver and which vehicle characteristic values best describe the dynamic reaction of the vehicle. It therefore suggests that twelve separate characteristic values (f_1, f_2, ... f_{12}), representing the vehicle's response, should be determined based upon the time histories of the forward velocity, centripetal acceleration, yaw velocity and radius of turn recorded from the test. Four of these characteristic values (f_8, f_9, f_{10} and f_{11}) require direct knowledge of the sideslip angle (β) which was not measured in any of the tests and so were not determined. The procedures involved in determining the other eight of the Mondeo's characteristic values derived from the 'L3' turn are presented in detail here and the values from the other turns – L4, R1 and R3 – are all presented in Table 8.

The characteristic values are all evaluated from the data recorded between time t_0 and time $t_n = t_0 + 2s$. The ISO standard states that most modern cars when powered-off in a turn while maintaining a constant handwheel angle will follow a curvature with a slightly decreased radius. So, the first calculation is to determine a reference yaw velocity ($\dot{\psi}_{Ref}$) and lateral acceleration ($a_{Y,Ref}$) for the particular test undertaken. ISO defines these reference values as those values that would have occurred at time t_n had the initial turn radius been maintained. These are calculated from the following formulae, equation (5.11), based upon equations (2.2) and (2.3):

$$\dot{\psi}_{Ref,t_n} = \frac{v_{X,t_n}}{R_0} \quad \text{and} \quad a_{Y,Ref,t_n} = \frac{v_{X,t_n}^2}{R_0} \qquad (5.11)$$

where R_0 is the initial radius of the turn. This, unfortunately, was not recorded so it had to be estimated from the initial centripetal acceleration and the initial forward velocity at time t_0. Using the Matlab Data Cursor these were read off Figure 40 and Figure 41 at $t_0 = 3$s and found to be 3.75m/s^2 and 25km/hr respectively. The forward velocity at $t_n = t_0 + 2$s $= 5$s was 21km/hr.

The subsequent calculations prescribed by the ISO standard were then performed:

$$a_{Y,t_0} = \frac{v_{X,t_0}^2}{R_0} \qquad \Rightarrow \qquad R_0 = \frac{v_{X,t_0}^2}{a_{Y,t_0}} = \frac{\left(\frac{25}{3.6}\right)^2}{3.75} = 12.86\,\text{m} \qquad (5.12)$$

$$\dot{\psi}_{Ref,t_n} = \frac{v_{X,t_n}}{R_0} = \frac{\frac{21}{3.6}}{12.86} = 0.4536\,\text{rad}/\text{s} = 26\,^\circ/\text{s} \qquad (5.13)$$

$$a_{Y,Ref,t_n} = \frac{v_{X,t_n}^2}{R_0} = \frac{\left(\frac{21}{3.6}\right)^2}{12.86} = 2.646\,\text{m/s}^2 \qquad (5.14)$$
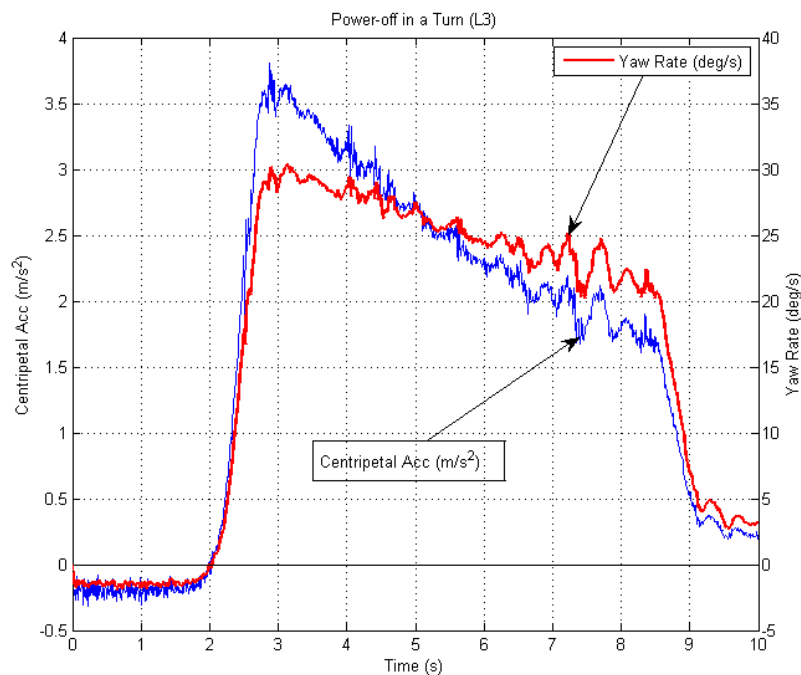
Figure 41: Power-off in a Turn – Yaw Rate & Centripetal Acceleration v Time

The reference values given by equations (5.13) and (5.14) were used in conjunction with other values read directly from the time history plots in Figure 40 and Figure 41 to determine the remaining characteristic values required by ISO 9816. These were:-

(1) The mean longitudinal acceleration $(-\bar{a}_{X,t_n})$ during the time interval $t_n - t_0$:-

$$f_1 = -\bar{a}_{X,t_n} = \frac{v_{X,t_0} - v_{X,t_n}}{t_n - t_0} = \frac{\left(\frac{25}{3.6}\right) - \left(\frac{21}{3.6}\right)}{5 - 3} = \frac{6.9\dot{4} - 5.8\dot{3}}{2} = -0.\dot{5}\,\text{m/s}^2 \quad (5.15)$$

(2) The ratio of the yaw velocity at t_n to that at t_0:

$$f_2 = \frac{\dot{\psi}_{t_n}}{\dot{\psi}_{Ref,t_n}} = \frac{27.46°/s}{26°/s} = 1.0566 \quad (5.16)$$

(3) The ratio of the maximum yaw velocity ($\dot{\psi}_{max}$) with respect to the *corresponding* reference yaw velocity ($\dot{\psi}_{Ref,t_{max}}$). In this case $\dot{\psi}_{max} = 30.37°/s$ at $t_{max} = 3.135s$. At t_{max} the corresponding reference yaw velocity using equation (5.14) is 30.48°.

$$f_3 = \frac{\dot{\psi}_{max}}{\dot{\psi}_{Ref,t_{max}}} = \frac{30.37°/s}{30.48°/s} = 0.996 \quad (5.17)$$

(4) The difference between the instantaneous yaw velocity at time t_n and the reference yaw velocity at time t_n:

$$f_4 = \Delta\dot{\psi}_{t_n} = \dot{\psi}_{t_n} - \dot{\psi}_{Ref,t_n} = 27.46°/s - 26°/s = 1.46°/s \quad (5.18)$$

(5) The maximum value of the difference between the yaw velocity during power-off and the affiliated reference yaw velocity:

$$f_5 = \Delta\dot{\psi}_{t_{max}} = \left(\dot{\psi}_t - \dot{\psi}_{Ref,t}\right)_{max} = 30.37°/s - 30.48°/s = -0.11°/s \quad (5.19)$$

(6) The instantaneous value of yaw acceleration evaluated at time t_n:

$$f_6 = d\ddot{\psi}_{t_n} = (d\dot{\psi}/dt)_{t_n} \approx -2 \ °/s^2 \tag{5.20}$$

The data for yaw velocity ($\dot{\psi}$) showed a great deal of local fluctuation in the period immediately before and after time t_n, although the general trend was quite linear over the whole period of the power-off manoeuvre. The instantaneous yaw acceleration at time t_n was therefore estimated based upon the average of the yaw acceleration over the whole period of the manoeuvre

(7) The ratio of the lateral acceleration at time t_n to the reference value of the lateral acceleration at time t_n. However, here the centripetal acceleration was used.

$$f_7 = \frac{a_{Y,t_n}}{a_{Y,Ref,t_n}} = \frac{2.75m/s^2}{2.646m/s_2} = 1.042 \tag{5.21}$$

(8) The path deviation at time t_n defined as the radial distance of the vehicle reference point (centre of gravity) and its initial circular path (which was approximated in this case by the difference between R_0 and R_{tn} the radius length at t_n). The latter was estimated using equation (5.12) with $v_{Xtn} = 21km/hr$ and after having read the value of the centripetal acceleration at time $t = 5s$ as $2.74m/s^2$:

$$a_{Y,t_n} = \frac{v_{X,t_n}^2}{R_{t_n}} \quad \Rightarrow \quad R_{t_n} = \frac{v_{X,t_n}^2}{a_{Y,t_n}} = \frac{(21/3.6)^2}{2.74} = 12.42\,m \tag{5.22}$$

$$f_{12} = \Delta s_{Y,t_n} = R_{t_0} - R_{t_n} = 12.86 - 12.42 = 0.44\,m \tag{5.23}$$

A similar set of time history plots for the other left- and right-hand power-off in a turn manoeuvres are provided in Figure 42. The same calculations and analysis that was performed above in the case of the 'L3' manoeuvre was also carried out on these time histories. The results obtained from all of these analyses are presented in Table 8.
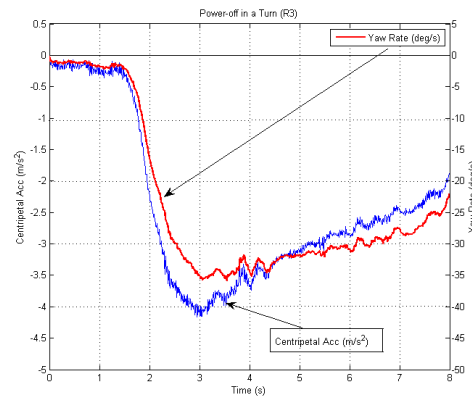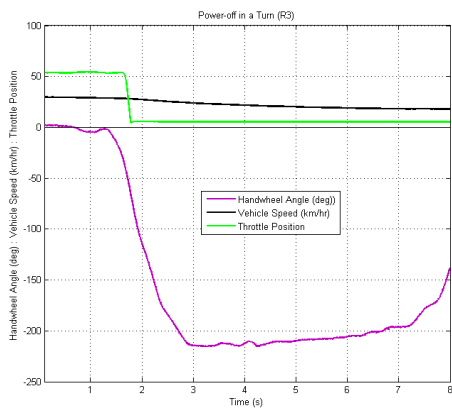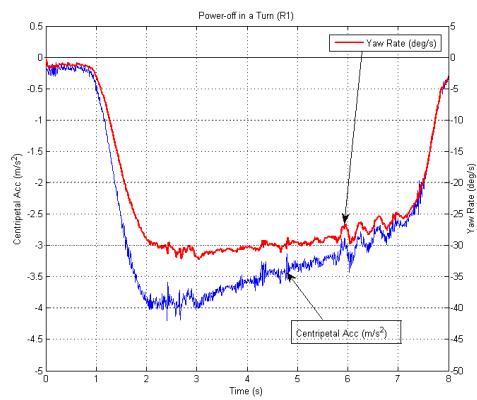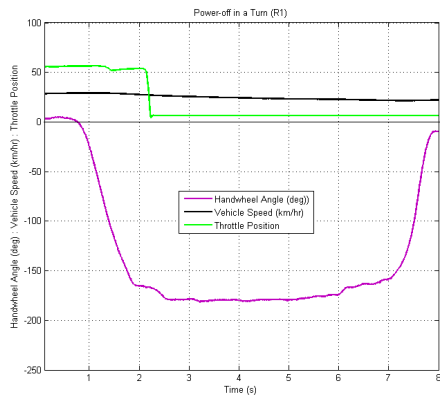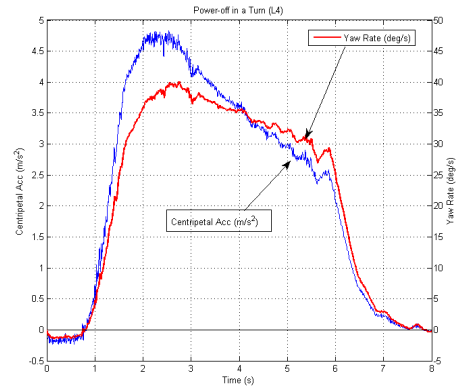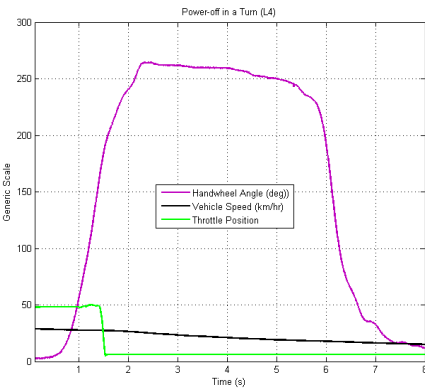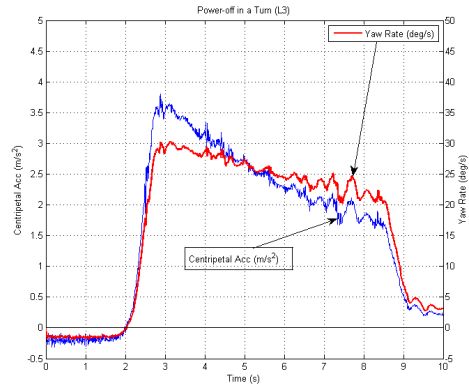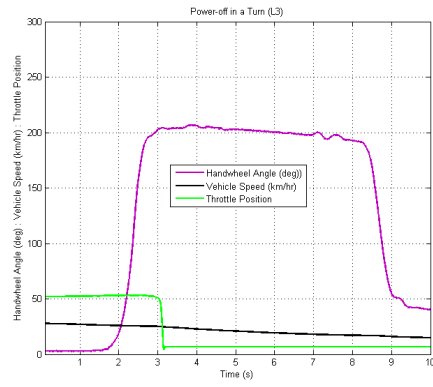
Figure 42: Time Histories of the Power-off Manoeuvres L3, L4, R1 and R3

The time histories shown in Figure 42 graphically demonstrate that the power-off tests were not conducted properly or consistently in accordance with the recommendations of the ISO standard. Before power-off occurs, the vehicle should have already been in a steady state turn condition for at least 1.5 seconds. This plainly was not the case. In addition, the lateral acceleration and the sideslip angle were not recorded properly and so the centripetal acceleration was again substituted for the former.

In summary, the characteristic values of the vehicle presented in Table 8 show a large degree of variance from each other and little evidence of any underlying consistency. This reflects the lack of repeatability in the actual tests conducted. These tests were all conducted at different velocities at different turning radii using different handwheel commands. Here, however, all of the values obtained are dependent upon the initial conditions of each test run and are characteristic of the vehicle's transient response to a power-off. Unlike the step steer results, none of these values are intrinsic to the vehicle in a steady state condition.

Characteristic Values		Power-off in a Turn Test Manoeuvres			
		L4	L3	R1	R3
f_1	$-\overline{a}_{X,t_n}$	-0.72 m/s^2	-0.5 m/s^2	-0.42 m/s^2	-0.814 m/s^2
f_2	$\dot{\psi}_{t_n} / \dot{\psi}_{Ref,t_n}$	1.323	1.0566	1.145	1.52
f_3	$\dot{\psi}_{max} / \dot{\psi}_{Ref,t_{max}}$	1.33	0.996	1.141	1.46
f_4	$\dot{\psi}_{t_n} - \dot{\psi}_{Ref,t_n}$	9 °/s	1.46 °/s	-3.85 °/s	-12 °/s
f_5	$\left(\dot{\psi}_t - \dot{\psi}_{Ref,t}\right)_{max}$	10 °/s	-0.11 °/s	-3.98 °/s	-13 °/s
f_6	$d\ddot{\psi}_{t_n}$	-3.3°/s^2	-2°/s^2	0.625°/s^2	1.875°/s^2
f_7	$a_{Y,t_n} / a_{Y,Ref,t_n}$	1.3	1.042	1.14	1.496
f_{12}	$R_{t_0} - R_{t_n}$	3.04 m	0.44 m	1.75 m	5.1 m

Table 8: Summary of Power-off Test Response Values

However, concerning these characteristic values and their evaluation, the ISO (2006) standard for this test states:

'*At the present level of knowledge, it is not yet known which variables best represent the subjective feeling of the driver and which variables (i.e. which characteristic values) best describe the dynamic reaction of vehicles.*' (Par. 9.1, p.5)

It then goes on to say that the set of specified variables, itemised f_1 to f_{12} on Table 8, represent only suggested examples for the evaluation of any test results. This qualification implies that these values may not be the best means of characterising the vehicle either for comparison with other vehicles performing the same manoeuvre or for validating a computer model of the vehicle. Be that as it may, some of the results obtained from this test (f_{12}, for example) seem dubious, to say the least, and cannot be accepted with any great confidence. It can be argued, therefore, that the raw time history data which cannot be gainsaid is a fundamentally more reliable data set upon which to validate any virtual model undergoing a simulation of the original test conditions.
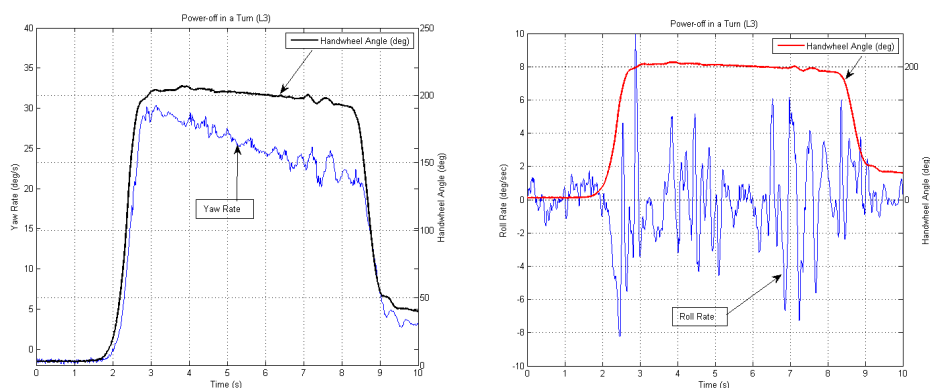
Figure 43: Power-off in a Turn – Yaw Rate, Roll Rate & Handwheel Angle v Time

With reference to other aspects of the manoeuvre, Figure 43 shows a clear correspondence between handwheel steering angle and the rate of yaw which initially lagged by approximately 0.15 second. Once the handwheel was held at about 205° the vehicle was in a steady turn manoeuvre but the yaw rate was consistently decreasing. Just after the 7 second mark there was some disturbance of the handwheel position which clearly appeared as an increase in amplitude of oscillation in the yaw response. The vehicle's yaw, roll and pitch behaviour can be seen in Figures 43 and Figure 44.

These are affected to some arbitrary extent by the roughness of the ground upon which the manoeuvre was carried out. Figure 45 shows the wheel deflections and clearly demonstrates the bumpy nature of the surface that was negotiated.
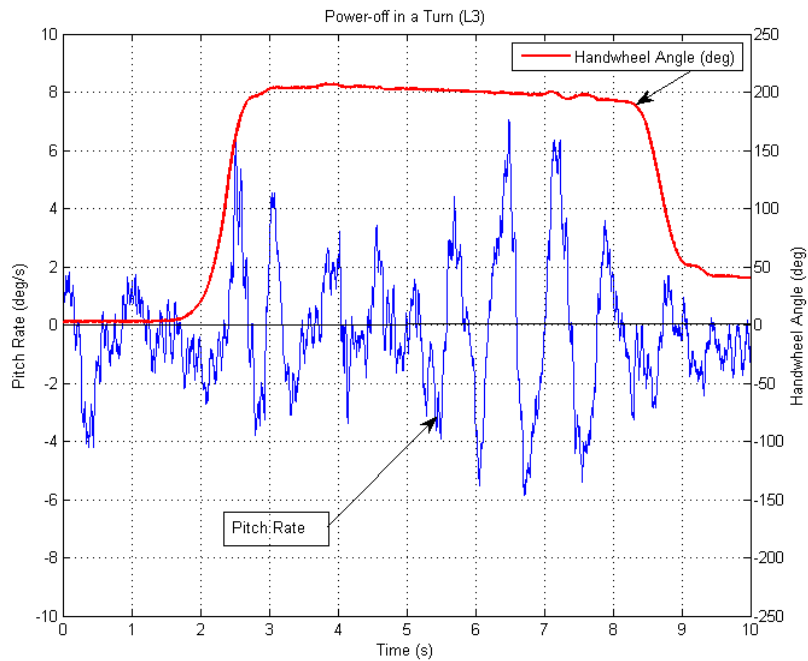
Figure 44: Power-off in a Turn – Pitch Rate & Handwheel Angle v Time
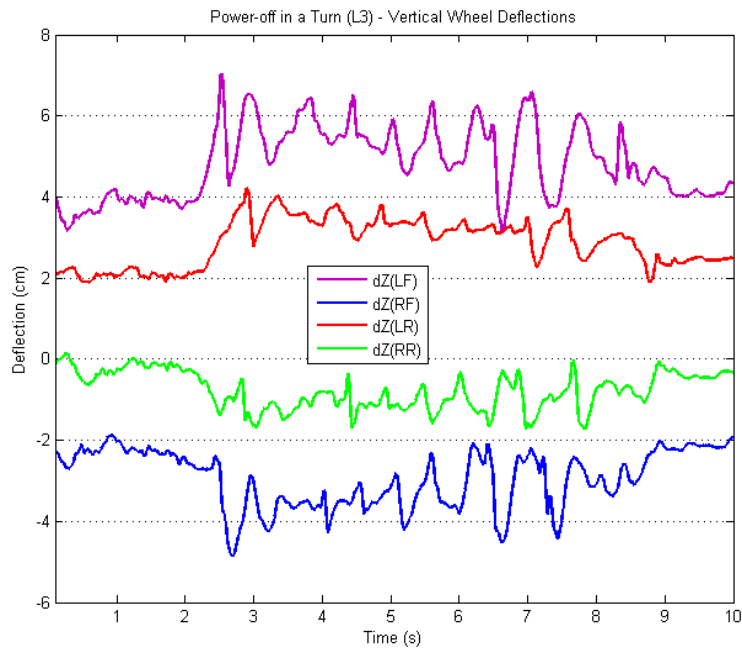
Figure 45: Power-off in a Turn – Vertical Wheel Deflections v Time

5.5 Summary of the Test Data Obtained

This chapter has provided an analysis of the data recorded from three types of test to which the test vehicle was subjected: steady state cornering, step steer (J-turn) and power-off in a turn. Generally, there was no attempt at full compliance with regard to either the test procedures or the test conditions recommended by the ISO standards. Despite this, two steady state results have been obtained from the test data: an understeer gradient, $K = 0.86°/g$ and a yaw rate gain, $\dot{\psi}_{SS}/\delta_{SS} = 0.163/s$. A third set of values derived from an analysis of the data associated with the transient behaviour of the vehicle in response to a power-off in a turn has also been obtained. Unlike the steady state characteristic values, these latter exhibited little consistency from test to test but may be of use if the particular conditions of each test can be recreated in a future virtual simulation.

Table 9 summarises the status of all of the data recorded from all of the tests performed on the test vehicle, not just those whose data was analysed for this work. This table is comparable to Table 1 but also shows, using a colour coding system, the type and quality of the data obtained from all of the tests performed on the test vehicle. The ISO test standards stipulate the information that it is necessary (**N**) to record from each test and that which is desirable (**D**). These are indicated accordingly on this table. Data that was considered to be reliable has been colour coded green whereas data that has been colour coded red was not properly recorded, usually due to a sensor failure. Yellow colour coding indicates information that can be derived from other good (green) data. The table also shows the symbol used for each parameter as designated by the International Standard ISO 8855: 2011 *Road Vehicles – Vehicle Dynamics and Road-holding Ability – Vocabulary*, Second Edition (2011).

In summary, this chapter has addressed the fourth, fifth, sixth and seventh objectives stated in Chapter 1; that is, that data be plotted, analysed in accordance with ISO procedures to determine the relevant characteristic values, and assessed in the light of its possible use for the validation of computer models of the test vehicle. It also fulfils the fifth objective concerning the comparison of these tests to the standard test procedures recommended by the ISO.

Vehicle Parameter, ISO Symbol	Steady State Corner-ing ISO 4138	Pulse Steer Input ISO 7401	Step Steer or J-Turn ISO 7401	Power-off in a Turn ISO 9816	Brake In a Turn ISO 7975	Double Lane Change ISO 3888
Test Initiation Time, t_0	—	N	N	N	N	—
Steering/Handwheel angle, δ_H	N	N	N	N	N	—
Longitudinal Velocity, v_X	N	N	N	N	N	N
Lateral Velocity, v_Y	D	D	D	N	N	—
Longitudinal Acc., a_X	D	—	—	D	N	
Lateral Acc., a_Y	N	N	N	N	N	
Vertical Acc., a_Z	—	—	—	—	—	
Roll Angle, φ	D	D	D	D	D	—
Pitch Angle, θ	—	—	—	D	D	—
Yaw Angle, ψ	—	—	—	—	—	—
Roll (Velocity) Rate,	—	—	—	—	—	
Pitch (Velocity) Rate	—	—	—	—	—	
Yaw (Velocity) Rate	D	N	N	N	N	—
Sideslip Angle, β	—	D	D	N	N	—
Radius of Turn, r	—	—	—	—	—	
Moment of Power-off	—	—	—	N	N	—
Handwheel Torque, M_H	D	D	D	—	—	—
Brakeline Pressure, pB	—	—	—	—	N	—
Brake Pedal Force, Fp	—	—	—	—	N	—
Brake Pedal Travel, sp	—	—	—	—	N	—
Stopping Distance,	—	—	—	—	D	—
Throttle Opening (deg)	—	—	—	—	—	
Engine Speed (RPM)	—	—	—	—	—	
Drive Wheel Speed (km/hr)	—	—	—	—	—	
Front Left Wheel Deflections (dZ)	—	—	—	—	—	
Front Right Wheel Deflection (dZ)	—	—	—	—	—	
Rear Left Wheel Deflections (dZ)	—	—	—	—	—	
Rear Right Wheel Deflections (dZ)	—	—	—	—	—	—

Legend: **N** = Necessary Test Parameter   **D** = Desirable Test Parameter

🟩 Good Data   🟥 Poor/No Data   🟨 Derivable Data

Table 9: Summary of All Test Data Recorded

Chapter 6: Computer Modelling & Validation

6.1   Introduction

Some of the major drivers of research in vehicle dynamics in recent decades have been the growing need for improved vehicle safety and the competitive nature of the global marketplace. One important development has been the power of computing and the application to automotive engineering research of newly developed multi-body system codes (Segel, 1993). Nowadays, improved efficiency in developing an engineering product relies heavily on predictive methods. These in turn are dependent on computer models that facilitate rapid experimentation, improved comprehension, and better ranking and optimization of design variables (Blundell & Harty, p.10). Two broad approaches to computer modelling are generally employed: the multi-body formulation (MBF) method and the lumped parameter mass (LPM) method. With the MBF method, the user creates the discretised rigid bodies that make up the model, together with specifying their connecting joints and internal forces. The computer assumes six degrees of freedom for each body and automatically generates the governing and constraint equations in the background. The LPM approach involves the derivation and solution of a set of simultaneous differential equations that are directly formulated by the analyst who can decide how many degrees of freedom (DOFs) to include in a model, which of them are important for a given investigation, and whether or not to insert forcing functions if required. Unlike complex MBF modelling platforms such as ADAMS (Automatic Dynamic Analysis of Mechanical Systems) and LMS *Virtual.Lab Motion*, this advantage of the simpler LPM models ensures that the user is engaged directly with the mathematical structure of the model which is not obscured behind an elaborate user interface. This advantage must be balanced by the recognition that too simple a model will limit the scope of the analysis and prevent a satisfactory comprehensive analysis.

For the purpose of completing the aims of this research an LPM modal or 'ride model' was created in MATLAB and validated by comparison to a Fast Fourier Transform

(FFT) analysis of the vehicle test data. Such models can be used for fundamental studies of ride comfort and safety. Time response plots cannot convey any sense of the 'feel' of a vehicle. Modal modelling can reveal the possible presence of important vibrations that may significantly impact the occupants' subjective experience of the vehicle's ride character. The stages in its creation involved the formulation of the model, derivation of the governing equations, scripting and verification of the computer coding and comparison of the vehicle test results with the modal model outputs. This was a seven degree of freedom model incorporating body bounce, pitch and roll, and the vertical deflections of the four wheels (Figure 46). For each of these DOFs the governing differential equation was written based upon the Lagrange energy method. The specifications for the MATLAB model are those of the Ford Mondeo test vehicle and are provided in Appendix A. The system governing equations and the MATLAB m-file code required to carry out the eigen analysis needed to determine the eigenvalues and mode shapes are all provided in Appendix C.
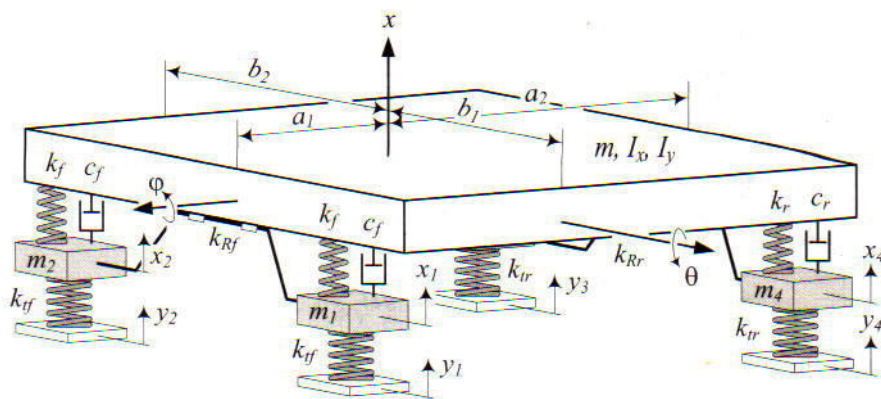
[Ref.: Jazar, Reza N., *Vehicle Dynamics: theory and application* (Springer, 2008)]

Figure 46: Full Vehicle Model with two rollbars

All free systems vibrate harmonically at their own intrinsic natural frequency when disturbed. Free systems are so-called because they are free of any damping or imposed excitation by external forces. As such they are governed by the set of differential equations expressed by Equation 6.1:

$$[M]\{\ddot{x}\} + [k]\{\dot{x}\} = \{0\} \qquad\qquad (6.1)$$

where [M] and [k] are matrices incorporating the system's mass and stiffness properties, and $\{\ddot{x}\}$ and $\{\dot{x}\}$ are the acceleration and velocity vectors of its DOFs respectively. A system with n DOFs has n natural frequencies. These natural frequencies ($\omega_1, \omega_2, \dots \omega_n$) are solutions of the characteristic equation, Equation 6.2:

$$\det\left[[k] - \omega^2[M]\right] = 0 \qquad\qquad (6.2)$$

Each natural frequency has an associated mode shape ($u_1, u_2, \dots u_n$, etc.) relating to the manner in which the entire system moves in response to any particular frequency of excitation. These mode shapes are described by eigenvectors having as many elements as the system has DOFs. The magnitude of the elements of an eigenvector, when expressed in normal form, gives an indication of the relative motion of each DOF at a given frequency. The element of an eigenvector whose absolute magnitude is greatest indicates which DOF is resonating in response to a given excitation frequency. Further explanation of the process involved in this analysis and the identification of the vehicle's natural frequencies is provided in Appendix C.

To facilitate validation and comparison of the vehicle test results with the modal model outputs, Fast Fourier Transform (FFT) analysis was applied to the test data and some of the results are presented in Appendix D.

6.2   MATLAB Modal or Ride Model

The ride model of the Ford Mondeo (Figure 46) was created in MATLAB based upon the relevant geometry, stiffness and mass properties of the vehicle (Table 10 and Appendix A). When analysed this model is capable of giving the natural frequency of vibration associated with each degree of freedom in the model. As stated, the road test data already presented here was subjected to FFT analysis and comparison with the MATLAB results enabled the important natural frequencies of the vehicle to be identified and confirmed. This identification process is partly based upon manual

calculations of the wheel hop, bounce, pitch and roll frequency which has been confirmed by MATLAB modelling calculations.

As indicated in Table 10, the test vehicle was heavier at 1535kg than the standard Ford Mondeo whose nominal unladen mass ('kerb weight') is 1492kg. This is made up of the four unsprung wheel masses and the vehicle sprung mass as follows:

Kerb 'Weight' (Mass) = 2(48.995kg) + 2(41.26kg) + 1311.57kg = 1492kg

On the day of testing the car contained three occupants – two in the front and one on the middle of the back seat – plus the test equipment which was situated in the boot. This additional mass was estimated at 223kg (see Appendix B for further details as to how this extra mass was distributed on the wheels). This additional mass brought the sprung mass of the test vehicle up to 1534.6kg and its overall mass to 1715kg. The unsprung masses of the vehicle remained unchanged.

FORD MONDEO	Standard Unladen Mass or 'kerb weight' (kg)	Laden Test Vehicle (3 occupants)
Sprung Mass	1312	1535
Front Unsprung Mass	97.9	97.9
Rear Unsprung Mass	82.5	82.5
TOTAL MASS	1492.0	1715.0

Table 10: Ford Mondeo – Mass Properties

The natural frequencies of vibration of a body are affected by changes in the mass of the body. Any alteration in the sprung mass of a vehicle will cause a change in both the roll and the pitch moments. The roll and pitch moments of inertia of the lighter 1492kg car were 396.7kgm^2 and 2240kgm^2 respectively. This information was supplied by Ford and was used by their researchers in constructing an ADAMS model of the Mondeo. It is not known whether Ford measured these values experimentally or derived them from their ADAMS model, or some other model. As stated, the additional three occupants in the test car added 223kg to its sprung mass changing it

from 1311.6kg to 1534.6kg. The new roll and pitch inertias of this heavier vehicle were unknown and it was not possible to measure them directly at the time. It was decided, therefore, to assume linearity and scale up the original values to match the greater sprung mass of the test vehicle. The relevant calculations are provided in equations (6.3) and (6.4).

$$\text{Roll Moment of Inertia:} \qquad \frac{396.7(1534.6)}{1311.6} = 464\text{kgm}^2 \qquad (6.3)$$

$$\text{Pitch Moment of Inertia:} \qquad \frac{2240(1534.6)}{1311.6} = 2621\text{kgm}^2 \qquad (6.4)$$

These estimated values were used in creating the MATLAB model of the test vehicle. The MATLAB model was constructed by applying the Lagrange method to generate the differential equation of motion for each degree of freedom (Appendix C) and writing these in matrix form for analysis by MATLAB. In each case, the natural frequencies result from the eigenvalues of the relevant system of matrix equations.

Wheel Hop Frequency (Hz)		Bounce (Hz)	Roll (Hz)	Pitch (Hz)
Front	Rear			
11.024	11.886	1.354	3.096	1.57
11.023	11.883	(1.31)	(2.869)	(1.39)

Table 11: MATLAB Full Vehicle Model – Modal Frequencies

The results obtained are presented in Table 11. There were two versions of the model: one based on the unladen kerb weight of the Mondeo and another on the greater weight of the laden test vehicle. The effect of the additional mass of the occupants, etc, was factored into the latter and the results for it are given in brackets in Table 11. As expected, the wheel hop frequencies of the laden test vehicle were unchanged because the unsprung masses remain unchanged, but the bounce, roll and pitch frequencies were all somewhat lower.

The bounce frequency of the heavier vehicle was predictably lower due to the increased inertia of the greater unsprung mass. The roll frequency was similarly affected although the additional inboard mass of the occupants was roughly spread symmetrically (50%/50%) about the car's longitudinal X axis. Again, for details of how the added mass was distributed see Appendix B. The pitch frequency of the heavier vehicle was affected by the non-symmetric distribution (25%/75%) of the mass of the three occupants about the lateral axis of the car. It would also have been affected by the small mass of the data recording instrumentation which was located in the boot.

6.3   The Wheel Hop Frequencies

Wheel hop is the name given to the natural frequency of the wheel assembly of a car which can obviously vibrate independently when excited. Because wheel hop is independent of the sprung mass, a quarter-car model (Figure 47) of the wheel assembly can be used to determine the wheel hop frequency. Wheel hop is a function of three parameters: the unsprung mass (m_u), which is the mass of all of the components in the wheel assembly not supported by the suspension itself; the stiffness or rate of the suspension spring (k_s); and the stiffness or rate of the tyre (k_u) which is considered to be a rubber spring.

The values of these parameters were different for the front and rear wheel assemblies of the Mondeo so the front and rear wheel hops were consequently different. However, because the unsprung mass (m_u), the suspension spring stiffness (k_s) and the tyre stiffness (k_u) were all relatively unchanged by the increase in the sprung mass of the tested vehicle, the wheel hops of the tested vehicle remained unchanged.

Manual calculation of the wheel hop frequencies using the standard formulae given by Equations (6.5) and (6.6) agree with the values from MATLAB presented in Table 11. The wheel hop frequencies were calculated using equations (6.5) and (6.6):

$$f_{front\_hop} = \frac{1}{2\pi}\sqrt{\frac{k_w + k_t}{m}} = \frac{1}{2\pi}\sqrt{\frac{32560 + 201730}{48.955}} = 11.01\text{Hz} \qquad (6.5)$$

$$f_{rear\_hop} = \frac{1}{2\pi}\sqrt{\frac{k_w + k_t}{m}} = \frac{1}{2\pi}\sqrt{\frac{28090 + 201470}{41.26}} = 11.87\text{Hz} \qquad (6.6)$$
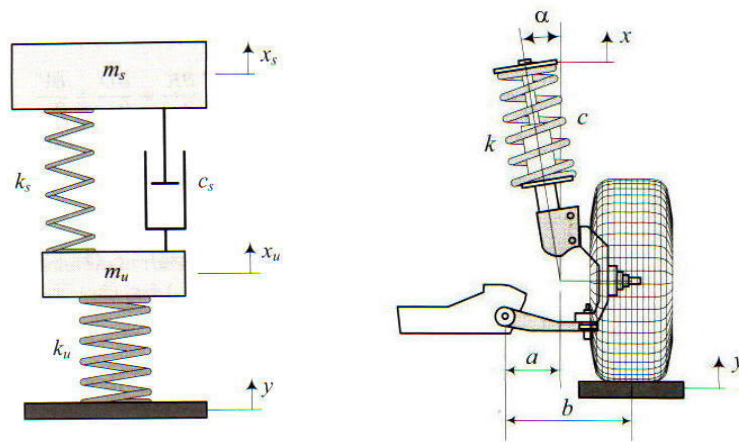
[Ref.: Jazar, Reza N., *Vehicle Dynamics: theory and application* (Springer, 2008)]

Figure 47: Quarter Car Model

The results of the FFT analysis were examined to identify the Mondeo's wheel hop frequencies as well as its natural frequency of vibration in bounce, roll and pitch modes. The expected wheel hop frequencies were sought in the road test data but were not found in many cases. Figure 48 shows the time history data from the vertical displacement of the front driver's side wheel in a J-turn together with the FFT analysis of the same data. There is some evidence of wheel hop frequency there.

Elsewhere, a fairly consistent wheel hop frequency component of 11-12Hz was evident in the data recovered from many of the tests. This is especially true of the *Step Steer or J-turn* test, the *Power-off in a Turn* test, the *Pulse Steer* test and the *Braking in a Turn* manoeuvre (see Appendix D, Figure D.1, D.2, D.3, D.4 and D.5). It would be expected that wheel hop would be excited by any suddenly introduced disturbing

force impacting the wheel and this appears to have been the case with the test data analysed using FFT. However, wheel hop would not normally be found in the signals from body mounted gyros and accelerometers except that in this case the ground upon which these tests were conducted was extremely rough in nature.
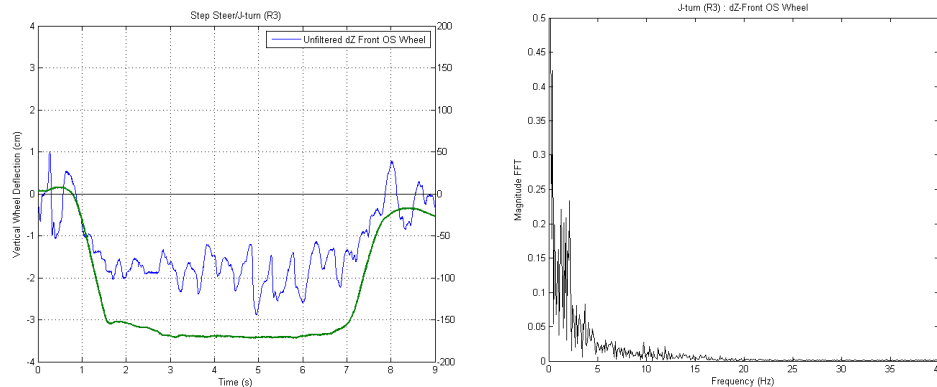
Figure 48: Vertical Displacement Front Driver's Side Wheel

6.4   Body (Sprung Mass) Frequencies

Part of the modelling process in MATLAB involved the creation of quarter- and half-car models. The quarter-car model has already been introduced. Half-car models of the front and rear end lateral roll were created as well as a 'bicycle' model for vehicle pitch motion. Although not fully presented here these half-car models gave agreement with the results obtained from the full-car model given in Table 11. The results from all of the MATLAB models are presented in Table 12 where the values in brackets indicated by an asterisk are those that relate to the more heavily laden test vehicle.

Using the vehicle specifications provided in Table 10 and Appendix A the natural frequency in bounce of the front and rear sprung mass of the vehicle may be calculated in the following manner, where k_w is the relevant wheel rate, k_t is the relevant tyre rate, k_{comb_Fr} and k_{comb_Rr} are the front and rear combined (or overall) suspension rates respectively, and m_{spr_Fr} and m_{spr_Rr} are the front and rear sprung masses per wheel respectively:

98

$$\text{Front:} \qquad k_{\text{comb\_Fr}} = \frac{k_w k_t}{k_w + k_t} = \frac{32560(201730)}{32560 + 201730} = 28035.037\,\text{N/m} \qquad (6.7)$$

$$f_{\text{front\_bounce}} = \frac{1}{2\pi}\sqrt{\frac{k_{\text{comb\_Fr}}}{m_{\text{spr\_Fr}}}} = \frac{1}{2\pi}\sqrt{\frac{28035.037}{394.2}} = 1.34\,\text{Hz} \qquad (6.8)$$

$$\text{Rear:} \qquad k_{\text{comb\_Rr}} = \frac{k_w k_t}{k_w + k_t} = \frac{28090(201470)}{28090 + 201470} = 24652.78\,\text{N/m} \qquad (6.9)$$

$$f_{\text{rear\_bounce}} = \frac{1}{2\pi}\sqrt{\frac{k_{\text{comb\_Rr}}}{m_{\text{spr\_Rr}}}} = \frac{1}{2\pi}\sqrt{\frac{24652.78}{261.6}} = 1.545\,\text{Hz} \qquad (6.10)$$

MODEL	Wheel Hop Frequency (Hz)		Bounce (Hz)	Roll (Hz)	Pitch (Hz)
	Front	Rear			
¼ Car Front Wheel	11.024 (11.023)*	-	1.341 (1.295)*	-	-
¼ Car Rear Wheel	-	11.886	1.543 (1.344)*		
½ Car Pitch Model	11.024	11.886	1.354 (1.309)*		1.571 (1.390)*
½ Car Front End Roll	11.024 11.039	- -	1.341 (1.295)*	3.600 (3.481)*	
½ Car Rear End Roll		11.886 11.902	1.543 (1.344)*	3.994 (3.480)*	
Full Car Model	11.024	11.886	1.354 (1.309)*	3.096 (2.869)*	1.571 (1.39)*

Table 12: All MATLAB Models – Natural Frequencies

These results give the ride natural frequencies in bounce to be: 1.34Hz (front) and 1.54Hz (rear). These values are in line with the observation by Dixon (1999) and others that, for good ride behaviour, the rear frequency in bounce is generally higher

than the front, possibly even by as much as 20%. This ensures that when the vehicle encounters an isolated disturbance the higher rear frequency will catch up with the front and the overall motion of the vehicle is biased towards bounce rather than pitch, the latter motion being considered the much more objectionable.

All of these values were derived using the kerb weight of the Mondeo whereas the test vehicle, as has been noted, had a heavier sprung mass due to its occupants. When the same calculations were performed using the new load distribution of the heavier vehicle the revised values for bounce were 1.295Hz at the front and 1.344Hz at the rear. As might be expected the bounce natural frequency obtained from the full car model was 1.31 Hz, a value also very close to the front end natural bounce frequency. Again, the laden test vehicle with its three occupants and data acquisition equipment had increased the sprung mass and thus reduced the overall bounce frequency from 1.35 Hz to 1.31 Hz.

Regarding the vehicle's natural roll dynamics there were two quite different roll rates owing to the different stiffness and mass characteristics in the front and rear of the vehicle. Both the front and rear half car models incorporated their respective roll bars and these were also inserted into the full-car model. An inspection of the FFT results in Appendix D and Table 13 shows a possible roll frequency of the laden Mondeo at about 3Hz or less. This range accurately captures the computer value of 3Hz for the *unladen* roll frequency. MATLAB calculated the laden roll frequency at 2.87Hz which is within the range shown by the FFT results for roll frequency. Consideration must be given to the fact that the MATLAB model is using estimates for the roll inertia and for the distribution of the sprung mass about its centre of gravity.

The pitch frequency given by the half car pitch model was 1.57Hz. Again because of symmetry, it would be expected that both the 'bicycle' and the full car model would give a similar result, and they do. For the heavier test vehicle the pitch inertia was estimated assuming linearity. Here too, as anticipated, the greater mass of the occupied test vehicle had a reduced pitch frequency at 1.39 Hz but it must be noted that the vehicle's centre of gravity is shifted and its k^2/ab value is thereby altered.

Any of the vehicle's natural frequencies may be excited by disturbance inputs to the vehicle of a random or cyclic nature. Dixon (1999) gives the formula shown in equation (6.11) relating vehicle speed (v) to the wavelength (λ_R) of a cyclic input disturbance at which resonance (f_N) is excited:

$$v = \lambda_R f_N \qquad (6.11)$$

Based on this formula estimates can be made of particular combinations of vehicle speed and road surface disturbance inputs that would give rise to resonant responses in the vehicle. For example, the Mondeo's wheel hop frequencies would be excited by 10cm (4 inch) cobblestones driven over at speeds between 4 and 5 km/hr. However, given the nature of the surfaces the Mondeo was tested on, a more likely source to excite a resonant response would be a single side pothole or bump strike where the wheels on one side of the vehicle only would encounter the disturbance but with a delay depending on the speed of the vehicle. If taken at about 28-30 km/hr this would excite resonance in roll. Bounce would be most pronounced over a ramp taken at about 13-14 km/hr or pitch over a ramp at 14-16 km/hr.

6.5   MATLAB Full Car Model Results

The natural frequencies of vibration of the 7 DOF full vehicle model are presented in Table 13 together with the tentative identifications of these frequencies from the FFT analysis whose results are presented in Appendix D.

Modes	Mode Frequency (Hz)	
	MATLAB	FFT
Wheel Hop	11.0 – 13.4	11 - 12
Bounce	1.35 (1.31)	1.2 – 1.3
Roll	3.10 (2.89)	2.4 – 3.1
Pitch	1.57 (1.39)	1.3 – 1.6

Table 13: Comparative Summary of Mondeo's Natural Frequencies

The unbracketted results relate to the standard unladen Mondeo having a kerb weight of 1492kg: the bracketed results to the laden vehicle of 1715kg as used in the tests.

Obviously, Ford did not provide figures for the test vehicle as it was set up while undergoing tests. The occupants of the vehicle during testing increased its sprung mass only and would have had no effect on the unsprung mass associated with the wheel assemblies. The results shown for this heavier vehicle – the reduced natural frequencies in bounce, roll and pitch – were all consistent with the increased inertia of the sprung mass and these frequencies have been identified using FFT analysis in the time history data recorded from the field testing. In this manner it has been demonstrated that the data obtained from those tests that did not comply in all aspects with the ISO standards, while being generally unacceptable for the purpose of vehicle characterization and for comparison with other vehicles undergoing the same tests, remains viable for computer model validation.

6.6   Model Validation

The ISO tests conducted on the Mondeo were handling tests and the information that ISO requires is used to characterise the steady state and/or transient handling response of the test vehicle. These tests were not performed with sufficient rigour to obtain good quality characterization values that could be used to compare the Mondeo's performance to that of other vehicles.

The validation process outlined here involved a modal ride model and not a handling model. Such models give information concerning a vehicle's natural frequencies of vibration. Although the ISO tests that the Mondeo underwent were poorly executed and some of the recorded data was compromised, they do appear to have excited the various natural frequencies of the vehicle and an FFT analysis has tentatively identified these frequencies in the test data and thereby corroborated the modal model (Appendix D). This analysis recovered the frequency content of the original sensor signal data and their magnitude. Nearly all of the frequencies identified by this FFT analysis, including those of most interest to the current work, were consistently

evident in the data recorded by the various onboard sensors for the different test manoeuvres, although they were not always the dominant frequency found in the data and their magnitudes varied. The ubiquitous nature of these frequencies is strong evidence that they were not spurious or noise related but genuine signatures of the vehicle's own response to test command inputs. Irrespective, then, of how compromised the ISO vehicle characterisation process might have been, the time history results from these inadequate tests were useable as a basis for a FFT analysis that identified certain attributes of the test vehicle and confirmed the ride model of the vehicle.

This confirmation, however, is somewhat qualified and does not rest on a perfect correlation between the FFT results and the MATLAB computer models (Table 13). There are discrepancies and some questions remain unanswered. Some frequencies were not found at all; for example, the wheel hops were not evident in the vertical displacement sensor data (Figure 48). It may be argued that the wheel hop was not excited to any measurable extent but then it is hard to explain the 11-12Hz frequency in the other sensor data which was identified as the probable wheel hop frequency. Other natural frequencies, such as the roll, are not found exactly at the frequency value expected but are still close. These discrepancies may be explained away by reference to other factors such as the increased sprung mass of the test car and the estimate made of the pitch and roll inertia values but nonetheless they generally remain within acceptable limits of the expected value.

At this point it should be pointed out that it would not be possible to obtain a perfect correlation between the natural frequencies of the MATLAB modal model and the frequencies visible in the FFT graphs of the test data. There are a number of reasons why this must be so.

Firstly, MATLAB models the vehicle systems and component parts as though they are rigid bodies connected by elastic elements (lumped parameter model). Aside from the tyre and suspension spring rates, the elastic properties of the metal components and the bushings of the wheel assembly were not taken into account in the rigid body model and therefore the overall stiffness of the suspension system was greater and

consequently computed higher values of natural frequency than were naturally inherent in the system. This factor was exacerbated by the fact that the 7 DOF MATLAB model did not incorporate the complexity of the real vehicle and, in particular, that it was some ten years old and all of the bushings and many of the parts were worn.

Secondly, the MATLAB model incorporated a lot of estimated values because the actuall values were unknown. Changes to the sprung and unsprung masses will result in changes to the natural frequencies. During road testing each of the Mondeo's wheels had their unsprung mass slightly increased by the mass of the displacement sensors attached to them, although admittedly the affect of this would be quite small. On the other hand, the sprung mass was increased by a considerable amount. The magnitude of this increase could only be estimated. So, too, was the manner in which this extra mass was distributed and the position of the new centre of gravity. Furthermore, the relationship between system stiffness and mass is not usually linear and therefore as the suspension of the test vehicle was more heavily loaded this may not have had the effect of proportionally increasing the stiffness of the tyres, the suspension springs and the suspension components.

Thirdly, with respect to the wheel hop, the MATLAB modelling only included the reciprocating inertia of the wheels and their rotational inertias were not incorporated into the model. Equation (6.7) is used to calculate the equivalent mass (m_{eq}) which was a combination of the wheels gravitational and rotational inertias:

$$m_{eq} = m_{unsprung}\left[1 + \left(\frac{r_{gyration}}{r_{wheel}}\right)^2\right] \qquad (6.7)$$

Rotational inertia increases the equivalent mass of each wheel and that would effectively result in a lower wheel hop frequency. The additional equivalent mass represented by the squared term in this equation would be relatively small.

Fourthly, damping, which is always present, slightly reduces vibration frequency but its effect was not incorporated into the MATLAB model. The relationship between natural (f_n) and damped (f_d) frequency of vibration is given by the standard formula (6.6):

$$f_d = \frac{\omega_d}{2\pi} \qquad \text{where} \quad \omega_d = \omega_n \sqrt{1 - \zeta^2} \qquad\qquad (6.6)$$

In this calculation ω_n and ω_d are the natural and the damped circular frequencies respectively and ζ is the damping ratio. When damping is included, as it would be in the response of the real vehicle, the natural frequencies are slightly lower than those found for the undamped case.

Finally, the MATLAB model of the laden test vehicle includes estimated values for the roll and pitch inertias. These have been based upon a linear extrapolation of the values of the unladen vehicle as described earlier in this chapter.

These shortcomings certainly introduce a margin of error that goes some way towards undermining confidence in the validation of the computer model. This might be enough to negate any claim that the MATLAB model of the test vehicle, and of the natural frequencies it has produced, has not been validated by the FFT results. There are many frequencies evident in the FFT analysis of the test data that are unexplained or that are being ignored. This failure can be accounted for in a number of ways:

1. the degree of estimation needed to create the MATLAB modal models was insufficiently accurate to produce a faithful model of the actual test vehicle;
2. the vehicle specifications used as the basis for estimating the values required to create the MATLAB models were not actually those of the test vehicle;
3. the model itself was too simple and lacked the complexity to properly represent the test vehicle;
4. the data derived from the vehicle testing was unreliable.

That the data was unreliable, is unlikely because, even though some sensors failed and the data from others may have been poor, all of it cannot be discounted. Moreover, the natural frequencies that were identified in the data were shown in <u>Appendix D</u> to be consistently evident across all of the sensors and all of the tests. This would seem to suggest, therefore, that the vehicle specifications used to create the model in MATLAB were either not the correct ones for the vehicle tested or there was too much estimating needed to produce a model.

6.7   Summary

In general, it can be tentatively claimed that the data obtained from the vehicle tests validate the modal model of the test vehicle and therefore, despite some anomalies and a certain degree of inaccuracy, confirm the contention that vehicle testing in full compliance with the procedures and conditions stipulated by the ISO is not necessary for validation of computer models. Perfectly viable data from non-standard versions of the ISO tests can be used for this purpose.

This chapter has addressed the last objective stated in Chapter 1 (p.10) – that a representative rigid-body ride or modal model of the test vehicle would be created and validated by reference to the test data collected from the various tests to which the vehicle was subjected.

Chapter 7: Conclusions & Recommendations

7.1   Summary of the Vehicle Testing Programme

The main shortcomings of the vehicle testing that was conducted using the Ford Mondeo have already been identified and itemised previously in some detail. Generally these were mainly the lack of compliance with the recommended ISO test procedures, the failure to record some essential data due to equipment malfunction and the estimates that were made in order to determine vehicle characteristic values based on the subsequent analysis of the test data that was available.

A number of factors conspired to compromise the work that was planned and the tests that were undertaken, and although these were not conducted in full compliance with the standards for such tests, it is argued that the results obtained were of sufficient quality to add to knowledge in the discipline of vehicle dynamics. An instrumented Ford Mondeo test vehicle was available for use but there was only a relatively small budget to cover costs and for any additional expenses. Also, the vehicle was only available for a period of one week. The time available for testing was further reduced because of calibration and other setting-up problems and the vehicle had also to be shared by other researchers during that time.

The test vehicle had already been extensively used by other researchers and many of the eleven sensors with which it was already equipped needed servicing and recalibration and four new wheel deflection sensors were installed on it and calibrated within the one week window. However, it transpired that two of the existing eleven sensors and one of the newly installed sensors proved faulty and failed to operate correctly during testing. Fortunately, a means of overcoming the problems presented by these failures was found.

Testing was conducted in car parks and other public places because state-of-the-art test sites and facilities were unavailable or could not be laid out due to a lack of space, funding, time or manpower. As the vehicle was driven and tested in public places, issues of insurance and cost meant that the vehicle was not driven by a professional vehicle test-driver and proper control of the test environment was not possible. The effect of these restrictions was that the tests were not conducted in full compliance with the ISO standards, the benchmark against which the test programme was measured. Nevertheless, a sufficient amount of reliable data was collected, post-processed and made available for follow-up validation purposes.

7.2   Model Validation

Values for the natural frequency of the vibration modes of the Ford Mondeo test car were determined by two independent means: MATLAB modelling of the vehicle and FFT analysis of the road test data. In addition, a third independent source of information was Ford UK who supplied general information regarding the test vehicle in the form of text files (see Appendix E) used in the modelling of the vehicle in ADAMS (an acronym for Automatic Dynamic Analysis of Mechanical Systems) software. Table 13 summarises the various natural frequency values obtained to date.

Ford UK supplied technical information about the Mondeo that was used for testing purposes but no value for the vehicle's natural roll frequency was given. In regard to the wheel hop, bounce and pitch natural frequencies there was no agreement between the Ford UK values and those obtained from the MATLAB modal model of the test vehicle. This was due to the evident use of an incorrect tyre stiffness value in the calculations that underlie some of the derived values provided in Appendix E.

As has been dealt with previously, the lower values given in brackets in Table 13 are for the heavier vehicle that was actually used during testing. As might be expected, its increased sprung mass has resulted in a lowering of the bounce, roll and pitch natural frequencies. Because the unsprung mass of the wheel assemblies remained unchanged at all times, the MATLAB wheel hop frequencies remain unchanged.

108

Allowing for the fact that the test vehicle was heavier and had a greater inertia, comparison of the MATLAB results with those of the FFT analysis resulted in a tentative correlation being achieved regarding the primary frequencies of interest. However, the FFT analysis produced many other frequencies that are unaccounted for and cannot be matched with any of those derived from the computer modelling in MATLAB. One can only speculate as to the origin of these vibrations although, undoubtedly, some are attributable in many cases to the rough ground over which some of the tests were conducted, some to coupling effects, and some also to other elastically excitable vehicle components not specifically investigated whose signature is evident in the data.

As there is some concern regarding the issue of aliasing, it should be noted here that the data acquisition system used on the test vehicle included an analogue filter. Unfortunately, no information is currently available regarding this filter but it is presumed, on the basis that the vehicle was regularly used for research purposes in an academic environment, that the hardware filter used was fitted in accordance with standard practice. In this case, as the sampling rate was 200Hz, that would require a low pass filter of 100Hz.

The most important observation to be made regarding the identification of the natural frequencies in the FFT results is that these frequencies must be there. When any vehicle is put through a series of tests such as those to which the Mondeo was subjected, its natural frequencies must be excited to some degree. Certain tests may excite some natural frequencies more than others and certain sensors may register these effects with greater sensitivity than others, but the natural vibrations of the vehicle will be evident in its response to the manoeuvres it performs. The actual measured responses may vary from test to test and from sensor to sensor but some trace evidence, at least, should be there. It is therefore quite reasonable to expect that the natural frequencies identified by the analysis of the MATLAB vehicle model (Appendix C) can be found in the FFT results (Appendix D).

7.3   General Conclusions

The main conclusion that can be drawn from this work is that it is not necessary to conduct vehicle tests in strict compliance with ISO standards if the purpose of the testing is to gather data which will be used to validate computer models of the vehicle. The basis for this conclusion is the fact that ISO standard tests are designed to ensure repeatability in order that valid comparisons can be made between different vehicles undergoing the same test. A quite different philosophy underlies the process of validation of a vehicle computer model. In this case the objective is to build as economic a numeric model as possible that will output the same or similar results as those obtained from the real vehicle under test. Although the actual tests were not performed in full compliance with the ISO standards, the data obtained was useable for validation of a modal ride model and this was demonstrated to an acceptable degree of accuracy in Chapter 6.

It was also possible to extract from the test data two significantly important vehicle characteristic values which will prove essential in any validation process of a handling model of the vehicle. These were the understeer gradient and the yaw velocity gain. The value of the understeer gradient was shown, by reference to the literature, to be consistent with similar vehicles to the Mondeo that was tested. A similar claim can be made for the yaw velocity gain, the same value for which was consistently derived from disparate inconsistent versions of the same test. This is indicative of its being a true characteristic value, intrinsic to the dynamic response of the vehicle.

The set of derived values, f_1 to f_{12}, obtained from the *Power-off in a Turn* tests were very inconsistent in character and, being dependent on the particular nature of an individual test run, clearly reflect the differences between test runs and their non-compliance with ISO recommended procedures. Nevertheless, it should be possible using the time histories of the parameters obtained from these tests to recreate the same conditions in a computer simulation of the virtual vehicle. By applying the same command input history to the virtual handling model, iterating through each time step, it should output similar or comparable results, all else being equal. Ideally, however, conducting such tests in strict compliance with the ISO standards ensures greater

viability and versatility of the data, not just for validation of computer models but also for orthodox vehicle characterisation and for purposes of comparison between different vehicles undergoing the same type of test.

Although vehicle characterisation values derived from standard ISO tests seem rather precise, they are nevertheless determined using test variables that may already have inbuilt error. Paragraph 9.1 of ISO 4138 – *Steady State Cornering*, for example, allows that average values of measured variables be used in calculation and that a standard deviation for lateral acceleration shall not exceed 5% of its mean value. In addition, it is recommended that tests be repeated a number of times so that average values may be computed. Essentially this implies that vehicle characterisation values are estimates that incorporate an acceptable level of inaccuracy and recognises that there are limits to the degree of precision that can be obtained. This would be true of any data that is obtained from physical testing.

Nevertheless, within the confines of the tests that were conducted certain characteristic values were determined for the vehicle and if it were to undergo a similar test procedure with the same test parameters it would, it is argued, produce a similar result. This is what would be expected of a computer model of the vehicle that is subjected to a simulation that matched the original test procedure and conditions.

The use of centripetal acceleration as a substitute for the missing lateral acceleration is not acceptable for orthodox vehicle characterisation purposes but may be used for validation of a computer model of the Mondeo in which centripetal acceleration is made the relevant parameter. The time history results from the actual tests could be directly compared to the outputs from computer model simulations designed to mimic them.

Not all of the vehicle characteristic values were too flawed to be of use. The yaw rate (velocity) gain of 0.163 deg/s per degree must be characteristic of the Mondeo despite the suboptimal test procedure from which it was obtained. Irrespective of the precise nature of a test that involves a handling response, and irrespective of the way in which such a test is carried out, it is reasonable to expect that the vehicle will respond in its

own characteristic manner. In other words, the yaw velocity gain is an intrinsic characteristic of the vehicle whose value cannot be dependent on extrinsic factors and despite the diverse nature of the step steer tests that were performed, the values obtained for it were all within 2% of the average value of 0.163 deg/s per degree.

The initial understeer gradient value of K = 0.85°/g that was derived from the steady state cornering test was lower than anticipated but remains plausible. However, its veracity can still be questioned because this value is based not only upon one single right-hand turning manoeuvre about a roundabout but also upon too much estimation. The radius of turn was not directly measured but was estimated from the test data recorded and the vehicle's steering ratio was estimated based upon the extreme kerb-to-kerb steering circle. The assumption was made that the steering ratio was a constant value over the whole steering range. Often, as is shown by Reimpell & Stoll (p.196), it reduces with increased handwheel angle and is at its lowest value at full lock, which was where it was estimated in this work. However, when a linearization process was performed on the cluster of data taken directly from the roundabout test the understeer gradient was shown to have an upper bound value of 2°/g.

7.4   Recommendations

Ideally, it would be best to adhere to the ISO standard test procedures if any future field tests were to be contemplated. This, of course, is not possible with the Ford Mondeo that was used for the purpose of this research. All that physically remains from the original test programme is the data that was recorded.

Only a modal model of the Mondeo was created and arguably validated. The road test data was in the time domain; the MATLAB and FFT results were in the frequency domain. The road test data was rendered into the frequency domain using the FFT and although the MATLAB model of the vehicle was also a frequency (or modal) model it cannot be subjected to simulated driver inputs. To do so would require the use of SIMULINK, ADAMS or LMS Virtual.Lab Motion to create MBF handling models that can be subjected to simulated handling tests and to which handling commands

may be applied. A model created using one of these platforms would allow driver inputs to be made and the time domain results to be directly compared with the road test data for correlation and validation. Moreover, the understeer gradient and the yaw velocity gain that was derived from the actual Mondeo test data could then be directly compared with the value obtained from such a handling model.

In order for the results of any MBF handling model to be comparable on a like with like basis to the results obtained from the original tests it would be necessary for the computer simulation to match those tests as closely as possible. That would require simulation of the bumpy ground that the Mondeo was tested upon. Most computer models are designed to represent vehicle manoeuvres on smooth road surfaces. The wheel deflection data could be used as an input to such a model. This is especially relevant to computer simulations that are intended to investigate transient behaviour.

Dixon (1996, p.379) states that transient disturbance may be caused by road roughness but that theoretical investigation of this area has been hampered by a lack of information about tyre characteristics. To some extent this problem has been given recent attention by researchers although they have concentrated on small fluctuations in tyre normal force. Vehicle handling stability depends on the generation of quite large sideforces by the tyres and these in turn are directly dependent on the tyre normal forces. The ability of a vehicle to corner effectively is dependent upon the loading on the wheels which, in turn, are affected by wheel vertical travel. For large fluctuations, if the normal force is greatly reduced, or goes to zero, vehicle handling is compromised. Wheel deflections are important also in analysing roll steer effects (Dukipati et al, p.395). Handling is critically dependent on the tyres on the vehicle. Any model would require information on the vehicle tyres of sufficient quality to replicate their effect (Blundell & Harty, p248) but applying the actual wheel deflection data experienced by the test vehicle used in this study would be necessary, not only to simulate the rough ground on which the vehicle was tested, but to ensure the model received the same stimulus that generated its vibrations and produced the particular time history data that was recorded.

The same tests that the Mondeo was subjected to should be virtually recreated with any further computer model simulation of the vehicle using the time history data of the handwheel and other command disturbances as the inputs. In some cases, because of the variability in the command disturbances delivered by the driver, the mean of a set of input values could be used to actuate the model. Alternatively, the actual time history of a command input applied to initiate a particular test run may be applied to a model simulation whose output can then be compared to the output data recorded for that test run. For this reason, the data from some subjective vehicle tests that were not analysed could be used for validation purposes.

7.5   General Summary

The central question at the heart of this research was posed in Chapter 1 (p.10). It asked whether it was necessary to test a vehicle in accordance with ISO testing standards in order to acquire data that would be used as the basis for the validation of computer models of the test vehicle. Arising from that question, the main aim was to test a vehicle and assess the quality of the characteristic values obtained from the test and, as part of the strategy needed to achieve that main aim, a series of nine objectives were outlined. It is now proposed to restate those objectives and explain where each was addressed in this thesis:-

(1) The first two objectives were to complete a Literature Survey in order to identify and study the work of relevant researchers in the field of vehicle dynamics and vehicle testing, and to decide upon a programme of tests. The first of these, to complete a literature review, was provided in Chapter 2, where the general theory of vehicle dynamics was presented and, in the course of which, the second objective, the choice of tests, was made and the relevant theory that applied was also discussed.

(2) The third objective, to prepare and instrument a test vehicle (a Ford Mondeo), was described in Chapter 3.

(3) The fourth objective, to post-process and plot the test data, was described in Chapter 4 and was further evidenced in later chapters and appendices.

(4) Chapter 5 has dealt with the fifth, sixth and seventh objectives; that is, to assess the quality of the tests conducted, analyse the time history data recorded, and assess the characteristic values obtained in light of their use for the purpose of validating a computer model of the test vehicle.

(5) Chapter 6, in conjunction with Appendices C and D, has demonstrated the successful achievement of the ninth objective, the creation of a modal model of the test vehicle and its validation using an FFT analysis of the test data obtained.

(6) the eight objective, the determination of how rigorously vehicle tests have to be conducted for the purpose of obtaining characteristic values for use in validation of computer models, has been addressed in general throughout the thesis but particularly in Chapter 2, Chapter 5 and Chapter 6 where it has been argued that standard ISO testing is unnecessary for this purpose.

Having met the objectives set out at the beginning of this thesis there remains only one outstanding issue – the answer to the question posed by the title of this work – *is vehicle characterization in accordance with standard ISO test procedures a necessary prerequisite for validating computer models of a test vehicle?*

This thesis has presented evidence that vehicle characterization based upon non-standard test procedures is a sufficient means of typifying a vehicle's dynamic response and that standard ISO testing is not a necessary prerequisite for validation purposes.

Bibliography

[1]   Bastow, D., Howard , G. & Whitehead, J.P., "Car Suspension and Handling", 4th Edition, SAE Intenational, Warrendale, Pa., USA, 2004.

[2]   Blundell, M. & Harty, D., "The Multibody Systems Approach to Vehicle Dynamics", Elsevier/Butterworth Heinemann, Oxford, 2004.

[3]   Campbell, Colin, "Automobile Suspensions", Chapman & Hall, London, 1981.

[4]   Dixon, John C., "Tires, Suspension and Handling", 2nd Edtion, Society of Automotive Engineers, Inc., Warrendale, Pa., © 1996.

[5]   Dixon, John C., "The Shock Absorber Handbook", Society of Automotive Engineers, Inc., Warrendale, Pa.,© 1999.

[6]   Dukkipati, Rao V., Pang, Jian, Qatu, Mohamad S., Sheng, Gang, Shuguang, Zuo, "Road Vehicle Dynamics", SAE International (2008).

[7]   Ellis, J.R., "Vehicle Handling Dynamics", Mechanical Engineering Publications Ltd., Bury St. Edmunds, 1994.

[8]   Fenton, John, "Handbook of Automotive Powertrain and Chassis Design", Professional Engineering Publishing Ltd., London & Bury St. Edmunds, 1998.

[9]   Genta, Giancarlo, "Motor Vehicle Dynamics: Modelling and Simulation", Series on advances in mathematics for applied sciences, Vol. 43, World Scientific CO. Pte. Ltd., 1997.

[10]   Gillespie, Thomas D., "Fundamentals of Vehicle Dynamics", Society of Automotive Engineers, Inc., ©1992.

[11]   Happian-Smith, Julian (ed.), "An Introduction to Modern Vehicle Design", Butterworth-Heinemann, Oxford, 2001.

[12]   International Standard ISO 2631: 1997 *Mechanical Vibration and Shock Evaluation of Human Exposure to Whole-body Vibration* (1997).

[13]   International Standard ISO 7401: 2011 *Road Vehicles – Lateral Transient Response Test Methods – Open-loop Test Methods*, Third Edition (2011).

[14] International Standard ISO 8855: 2011 *Road Vehicles – Vehicle Dynamics and Road-holding Ability – Vocabulary*, Second Edition (2011)

[15] International Standard ISO 9816: 2006 *Passenger Cars – Power-off Reaction of a Vehicle in a Turn – Open-loop Test Method*, Second Edition (2006)

[16] Jazar, Reza N., "Vehicle Dynamics : Theory and Application", Springer Science & Business Media, New York, 2008.

[17] Liu, C.Q. & Huston, Ronald L., "Principles of Vibration Analysis with Applications in Automotive Engineering", SAE International (2011).

[18] Matschinsky, Wolfgang, "Road Vehicle Suspensions", (translated by Alan Baker), Professional Engineering Pub. Ltd., London & Bury St Edmunds, 2000.

[19] Milliken, W.F. & Milliken, D.L., "Race Car Vehicle Dynamics", Society of Automotive Engineers, Inc., Warrendale, PA, © 1995.

[20] Milliken, W.F. & Milliken, D.L., "Chassis Design: Principles and Analysis [Based on previously unpublished technical notes by Maurice Olley]", Professional Engineering Publishing Ltd., London & Bury St Edmunds, 2002.

[21] Pacejka, Hans B., "Tyre and Vehicle Dynamics", Butterworth-Heinemann, Oxford, 2002.

[22] Radt, H.S., & Pacejka, H.B., "Analysis of the Steady State Turning Behaviour of an Automobile", Proceedings, Symposium on Control of Vehicles during Braking and Cornering, IMechE, London 1963.

[23] Rahnejat, H., "Multi-Body Dynamics: Vehicles, Machines and Mechanisms", Professional Engineering Publishing Ltd., London, 1998.

[24] Rahnejat, H., "Multi-body dynamics: historical evolution and application", Procs. Instn. Mech. Engrs. Vol 214 Part C, CO2999, IMechE, 2000.

[25] Rahnejat, H. & Whalley, R. (eds.), "Multi-body Dynamics: Monitoring and Simulation Techniques", Mechanical Engineering Publications Ltd., London & Bury St Edmunds, 1997. [Collected refereed papers of the First International Symposium on Multi-body Dynamics held at University of Bradford, 1997].

[26] Ramirez, Robert W., "The FFT: Fundamentals and Concepts", Prentice-Hall Inc., New Jersey, 1985.

[27]   Rill, Georg, *"Road Vehicle Dynamics: Fundamentals and Modelling"*, CRC Press, Boca Raton, Florida (2012)

[28]   Segel, L., *"An Overview of Developments in Road-vehicle Dynamics: Past, Present and Future"*, Procs. IMechE International Conference on Vehicle Ride & Handling, C466/052/93, 1993.

[29]   Wade-Allen, R., Christos, J.P., Howe, G., Klyde, D.H., & Rosenthal, T.J., *Validation of a Non-linear Vehicle Dynamics Simulation for Limit Handling*, IMechE Paper D04301 (2002).

[30]   Watanabe, Y. & Sayer, M.W., *The Effect of Non-linear Suspension Kinematics on the Simulated Pitching and Rolling Dynamic Behaviour of Cars* (2004).

[31]   Willumeit, H-P., Neculau, M., Vikas, A., & Wohler, A., "Mathematical models for the computation of vehicle dynamic behaviour during development", IMechE, C389/318, No. 925046, 1992.

[32]   Wong, J.Y., "Theory of Ground Vehicles", 2nd Edition, John Wiley & Sons, Inc., New York, 1993.

Appendix A: Ford Mondeo Vehicle Specifications

Specification	MATLAB Symbol	VALUE	
Unladen Mass (kerb 'weight')		1492 kg	(1715 kg)*
Sprung Mass (Total)	m	1311.6 kg	(1534.6 kg)*
Sprung Mass (Front Axle)		788.3754 kg	(844.3754 kg)*
Sprung Mass (Rear Axle)		523.1946 kg	(690.1946 kg)*
Unsprung Mass (Front Wheel)	mf	48.995 kg	
Unsprung Mass (Rear Wheel)	mr	41.260 kg	
Wheelbase	B	2.745 m	
Front Wheel Track	Wf	1.522 m	
Rear Wheel Track	Wr	1.528 m	
Front Wheel Rate	kf	32560 N/m	
Rear Wheel Rate	kr	28090 N/m	
Front Tyre Rate	ktf	201730 N/m	
Rear Tyre Rate	ktr	201470 N/m	
Front Roll Bar Rate	kRf	90183.56 N/rad	
Rear Roll Bar Rate	kRr	71390.54 N/rad	
Roll Moment of Inertia	I_x	396.7 kgm^2	(464 kgm^2)*
Pitch Moment of Inertia	I_y	2240 kgm^2	(2621 kgm^2)*
Distance of CG to Front Axle	a1	1.097m	
Distance of CG to Rear Axle	a2	1.648m	
Distance of CG to Nearside	b1	0.76166m	
Distance of CG to Offside	b2	0.7616m	

[*The bracketed values refer to the vehicle as laden on the day of testing.]

<u>Appendix B:</u>   **Weight Distribution in the Test Vehicle**

1. Unladen Vehicle

Kerb 'weight' is defined as the weight (mass) of the vehicle ready to drive with all operational consumables at serviceable levels; that is, a full tank of fuel with oil and water topped up but without driver, passengers or cargo. The nominal kerb weight of the Mondeo is 1492kg – of this 1312kg is sprung and 180kg is unsprung mass.

The wheelbase of the vehicle is 2745mm and its centre of gravity (CG) is positioned 1095mm from the front axle line. This puts the CG in the vehicle's YZ plane at or forward of the handbrake pivot point.
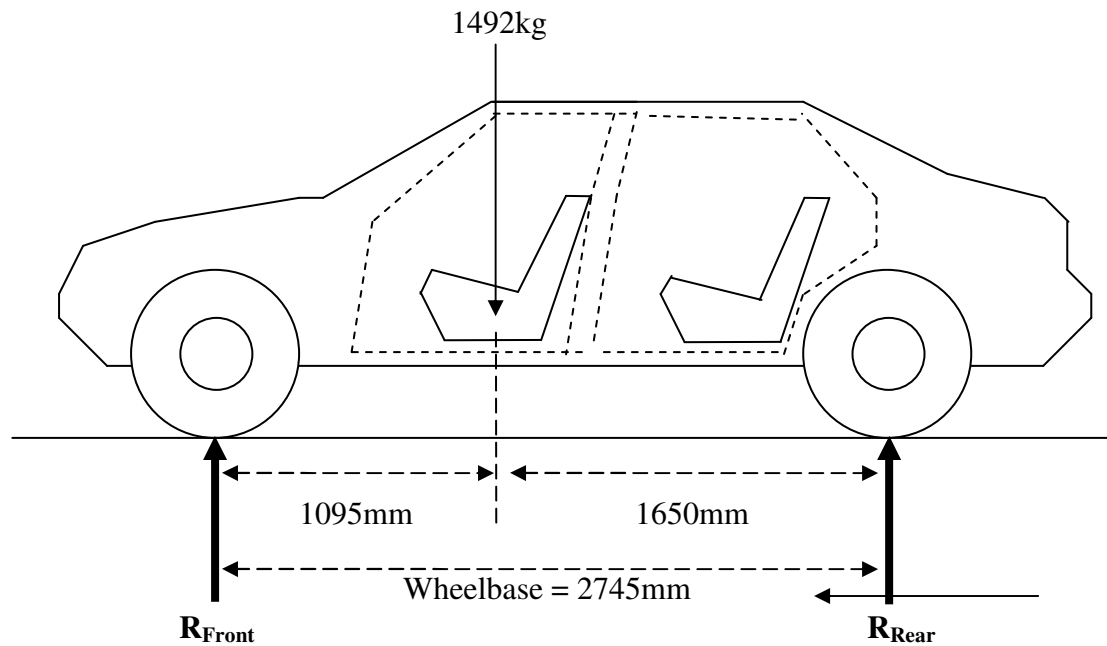
1492kg

1095mm   1650mm

Wheelbase = 2745mm

R_{Front}   **R_{Rear}**

Figure A1: Ford Mondeo – Mass, Wheelbase & Centre of Gravity

Ford state that the front unsprung mass is 97.91kg and the rear unsprung mass is 82.52kg thus making the total sprung mass of the vehicle:

$$1492 - (97.91 + 82.52) \ = \ 1492 - 180.43 \ = \ \underline{1311.57kg}$$

Further calculation gives the manner in which this load is distributed on the wheels:

Front Sprung Mass: $\quad m_{Fr\_spr} = \dfrac{1.650m(1311.6kg)}{2.745m} = 788.4kg$

Rear Sprung Mass: $\quad m_{Rr\_spr} = \dfrac{1.095m(1311.6kg)}{2.745m} = 523.2kg$

Front Ground Reaction:	=	Front Sprung Mass + Front Unsprung Mass
	$\Rightarrow$	788.3754 + 97.91 = 886.2854 kg
	$\Rightarrow$	886.2854(9.81) = <u>8694.46 N</u>

Rear Ground Reaction:	=	Rear Sprung Mass + Rear Unsprung Mass
	$\Rightarrow$	523.1946 + 82.52 = 605.7146 kg
	$\Rightarrow$	605.7146(9.81) = <u>5942.06 N</u>

2. Laden Test Vehicle

While the Mondeo underwent its road test manoeuvres it contained three occupants: a driver and passenger in the front seats, and another passenger who sat in the middle of the back seat. It also had extra mass associated with the test equipment, most of which was in the boot compartment. These additions to the vehicle constituted an estimated increase in its total sprung mass of 223kg.

The resulting changes to the mass (weight) distribution on the vehicle's wheels had a direct influence on the natural frequency of the vibration modes of the vehicle and therefore needed to be determined. It was not possible to measure the altered wheel loads directly so an estimate had to be made regarding the distribution, front and rear, of the additional 223kg of mass.

Information from Ford and inspection of Figure A1 indicates that the centre of gravity of the unoccupied Mondeo is at or near the handbrake pivot point so that most of the added 223kg would be carried through the rear wheels. The estimate made was that this would amount to about 56kg (25% of the added mass) on the front and 167kg (75%) to the rear. The new sprung masses are then

Front Unsprung Mass:	788.3754kg + 56kg	=	<u>844.3754kg</u>

Rear Unsprung Mass:	523.1946kg + 167kg	=	<u>690.1946kg</u>

Front Ground Reaction:	=	Front Sprung Mass + Front Unsprung Mass
	$\Rightarrow$	844.3754 + 97.91 = 942.2854 kg
	$\Rightarrow$	942.2854(9.81) = <u>9243.82 N</u>

Rear Ground Reaction:	=	Rear Sprung Mass + Rear Unsprung Mass
	$\Rightarrow$	690.1946 + 82.52 = 772.7146 kg
	$\Rightarrow$	772.71(9.81) = <u>7580.33 N</u>

Total Ground Reaction	=	9243.82 + 7580.33 = <u>16824.15 N</u>

Total Mass (Weight)	=	1492 + 223 = 1715kg
	=	1715(9.81) = <u>16824.15N</u>

Appendix C: Mondeo Full Vehicle Model

1. Governing Equations

The full vehicle ride model has 7 degrees of freedom: body bounce (x), body roll (φ), body pitch (θ) and the four wheel vertical displacements (wheel hops). Using the notation and vehicle specifications given in Appendix A and referring to Figure 46 (p.92) the following equations of motion for each degree of freedom of the full car model are derived:

(1)
$$m\ddot{x} + k_f(x - x_1 + b_1\varphi - a_1\theta) + k_f(x - x_2 - b_2\varphi - a_1\theta) + ...$$
$$....k_r(x - x_3 - b_1\varphi + a_2\theta) + k_r(x - x_4 + b_2\varphi + a_2\theta) = 0$$

$\Rightarrow$
$$m\ddot{x} + 2(k_f + k_r)x + (b_1 k_f - b_2 k_f - b_1 k_r + b_2 k_r)\varphi + ...$$
$$....2(a_2 k_r - a_1 k_f)\theta - k_f x_1 - k_f x_2 - k_r x_3 - k_r x_4 = 0 \qquad \underline{\text{Eqn. 1}}$$

(2)
$$I_x\ddot{\varphi} + b_1 k_f(x - x_1 + b_1\varphi - a_1\theta) - b_2 k_f(x - x_2 - b_2\varphi - a_1\theta) - ...$$
$$b_1 k_r(x - x_3 - b_1\varphi + a_2\theta) + b_2 k_r(x - x_4 + b_{2\varphi} + a_2\theta) + ...$$
$$..kR_f\left(\varphi - \frac{x_1 - x_2}{W_f}\right) + hR_f\left(\frac{x_4 - x_3}{W_r}\right) = 0$$

$$I_x\ddot{\varphi} + (b_1 k_f - b_1 k_r + b_2 k_r - b_2 k_f)x + (b_1^2 k_f + b_2^2 k_f + b_1^2 k_r + b_2^2 k_r + ...$$
$$..kR_f + kR_r)\varphi + (a_1 b_2 k_f - a_1 b_1 k_f - a_2 b_1 k_r + a_2 b_2 k_r)\theta + ...$$

$\Rightarrow$
$$..\left(-b_1 k_f - \frac{kR_f}{W_f}\right)x_1 + \left(b_2 k_f + \frac{kR_f}{W_f}\right)x_2 + ... \qquad \underline{\text{Eqn. 2}}$$

$$..\left(b_1 k_r - \frac{kR_r}{W_r}\right)x_3 + \left(-b_2 k_r - \frac{kR_r}{W_r}\right)x_4 = 0$$

(3)
$$I_y\ddot{\theta} - a_1 k_f(x - x_1 + b_1\varphi - a_1\theta) - a_1 k_f(x - x_2 - b_2\varphi - a_1\theta) + ...$$
$$...a_2 k_r(x - x_3 - b_1\varphi + a_2\theta) + ...$$
$$...a_2 k_r(x - x_4 + b_2\varphi + a_2\theta) = 0$$

$$\Rightarrow \quad \begin{aligned} &I_y \ddot{\theta} + 2(a_2 k_r - a_1 k_f)x + (a_1 b_2 k_f - a_1 b_1 k_f - a_2 b_1 k_r + a_2 b_2 k_r)... \\ &\quad\quad + 2(a_1{}^2 k_f + a_2{}^2 k_r)\theta + (a_1 k_f)x_1 + ... \\ &\quad\quad ...(a_1 k_f)x_2 + (-a_2 k_r)x_3 + (-a_2 k_r)x_4 = 0 \end{aligned} \quad \underline{\text{Eqn. 3}}$$

(4)
$$m_f \ddot{x}_1 - k_f(x - x_1 + b_1\varphi - a_1\theta) - \frac{kR_f}{W_f}\left(\varphi - \frac{x_1 - x_2}{W_f}\right) + k_{tf}(x_1 - y_1) = 0$$

$$\Rightarrow \quad \begin{aligned} &m_f \ddot{x}_1 - k_f x + \left(-b_1 k_f - \frac{kR_f}{W_f}\right)\varphi + (a_1 k_f)\theta + ... \\ &\quad\quad ...\left(k_f + k_{tf} + \frac{kR_f}{W_f{}^2}\right)x_1 + \left(-\frac{kR_f}{W_f{}^2}\right)x_2 = k_{tf} y_1 \end{aligned} \quad \underline{\text{Eqn. 4}}$$

(5)
$$m_f \ddot{x}_2 - k_f(x - x_2 - b_2\varphi - a_1\theta) + \frac{kR_f}{W_f}\left(\varphi - \frac{x_1 - x_2}{W_f}\right) + k_{tf}(x_2 - y_2) = 0$$

$$\Rightarrow \quad \begin{aligned} &m_f \ddot{x}_2 - k_f x + \left(b_2 k_f + \frac{kR_f}{W_f}\right)\varphi + (a_1 k_f)\theta + ... \\ &\quad\quad ...\left(-\frac{kR_f}{W_f{}^2}\right)x_1 + \left(k_f + k_{tf} + \frac{kR_f}{W_f{}^2}\right)x_2 = k_{tf} y_2 \end{aligned} \quad \underline{\text{Eqn. 5}}$$

(6)
$$m_r \ddot{x}_3 - k_r(x - x_3 - b_1\varphi + a_2\theta) + \frac{kR_f}{W_f}\left(\varphi - \frac{x_4 - x_3}{W_r}\right) + k_{tr}(x_3 - y_3) = 0$$

$$\Rightarrow \quad \begin{aligned} &m_r \ddot{x}_3 + (-k_r)x + \left(b_1 k_r + \frac{kR_r}{W_r}\right)\varphi + (-a_1 k_r)\theta + ... \\ &\quad\quad ...\left(k_r + k_{tr} + \frac{kR_r}{W_r{}^2}\right)x_3 + \left(-\frac{kR_r}{W_r{}^2}\right)x_4 = k_{tr} y_3 \end{aligned} \quad \underline{\text{Eqn. 6}}$$

(7)
$$m_r \ddot{x}_4 - k_r(x - x_4 + b_2\varphi + a_2\theta) - \frac{kR_r}{W_r}\left(\varphi - \frac{x_4 - x_3}{W_r}\right) + k_{tr}(x_4 - y_4) = 0$$

$$m_r \ddot{x}_4 + (-k_r)x + \left(-b_2 k_r - \frac{kR_r}{W_r}\right)\varphi + (-a_2 k_r)\theta + \dots$$

$$\Rightarrow \qquad \dots\left(-\frac{kR_r}{W_r^2}\right)x_3 + \left(k_r + k_{tr} + \frac{kR_r}{W_r^2}\right)x_4 = k_{tr} y_4 \qquad \text{Eqn. 7}$$

Ignoring the forcing functions associated with y_1, y_2, y_3 and y_4 these equations were then written in matrix form:

$$[m]\{\ddot{x}\} + [k]\{x\} = \{0\}$$

2. MATLAB m-file code

A reproduction of the MATLAB m-file for solving this system of equations of motion follows.

```
% **************************************** %
% FORD MONDEO WITH FRONT AND REAR ROLLBARS %
% **************************************** %

% The following determination of the natural frequencies of vibration
% of a 7DOF full vehicle model of a Ford Mondeo test vehicle is based
% upon the formulation presented in Reza N. Jazar, 'Vehicle Dynamics:
% Theory & Application' (pp. 864-870). The Lagrange method is applied
% to the model in order to derive the governing equations of motion
% that are then written in matrix form and solved for the eigenvalues
% and eigenvectors in order to determine the natural frequencies and
% the mode shapes.

% The 7 DOFs are:    (1) Body Bounce
%                    (2) Body Roll
%                    (3) Body Pitch
% and (4), (5), (6), (7) Wheel Hop for each of the four wheels


m = 1312;         % Sprung Mass (kg) (1535kg for laden test car)
mf = 48.955;      % Front wheel unsprung mass (kg)
mr = 41.26;       % Rear wheel unsprung mass (kg)
a1 = 1.095;       % Distance CG to front axle (m) (1.237 laden car)
a2 = 1.65;        % Distance CG to rear axle (m)  (1.508 laden car)
B = 2.74527;      % Wheelbase (m) = a1 + a2
b1 = 0.76166;     % Distance CG to Nearside (m)
b2 = 0.76166;     % Distance CG to Offside (m)
Wf = 1.5422;      % Front Track (m)
Wr = 1.528;       % Rear Track (m)
kf = 32560;       % Front Wheel Rate (N/m)
kr = 28090;       % Rear Wheel Rate (N/m)
ktf = 201730;     % Front Tyre Rate (N/m)
ktr = 201470;     % Rear Tyre Rate (N/m)
```

```
kRf = 90183.56;    % Front Roll Bar Rate (Nm/rad)
kRr = 71390.54;    % Rear Roll Bar Rate (Nm/rad
Ix = 396.7;        % Roll Inertia (kg.m^2) (464 for laden test car)
Iy = 2240;         % Pitch Inertia (kg.m^2)(2621 for laden test car)


% Note: The front and rear wheel tracks are different to each other
% and, therefore, b1 and b2 had to be calculated from other data.


M = [m 0 0 0 0 0 0;            % Sprung mass - Bounce
     0 Ix 0 0 0 0 0;          % Roll Inertia
     0 0 Iy 0 0 0 0;          % Pitch Inertia
     0 0 0 mf 0 0 0;          % Unsprung Mass Front Nearside Wheel
     0 0 0 0 mf 0 0;          % Unsprung Mass Front Offside Wheel
     0 0 0 0 0 mr 0;          % Unsprung Mass Rear Nearside Wheel
     0 0 0 0 0 0 mr];         % Unsprung Mass Rear Offside Wheel


k11 = 2*(kf + kr);
k12 = b1*kf - b2*kf - b1*kr + b2*kr;
k13 = 2*(a2*kr - a1*kf);
k14 = -kf;
k15 = k14;
k16 = -kr;
k17 = k16;
k21 = k12;
k22 = kRf + kRr + kf*(b1^2 + b2^2) + kr*(b1^2 + b2^2);
k23 = a1*b2*kf - a1*b1*kf - a2*b1*kr + a2*b2*kr;
k24 = -b1*kf - kRf/Wf;
k25 = b2*kf + kRf/Wf;
k26 = b1*kr + kRr/Wr;
k27 = -b2*kr - kRr/Wr;
k31 = k13;
k32 = k23;
k33 = 2*(kf*a1^2 + kr*a2^2);
k34 = a1*kf;
k35 = k34;
k36 = -a2*kr;
k37 = k36;
k41 = k14;
k42 = k24;
k43 = k34;
k44 = kf + ktf + kRf/Wf^2;
k45 = -kRf/Wf^2;
k46 = 0;
k47 = k46;
k51 = k15;
k52 = k25;
k53 = k35;
k54 = k45;
k55 = kf + ktf + kRf/Wf^2;
k56 = 0;
k57 = k56;
k61 = k16;
k62 = k26;
k63 = k36;
k64 = k46;
k65 = k56;
k66 = kr + ktr + kRr/Wr^2;
k67 = -kRr/Wr^2;
k71 = k17;
k72 = k27;
k73 = k37;
k74 = k47;
k75 = k57;
```

```
k76 = k67;
k77 = kr + ktr + kRr/Wr^2;


K = [k11 k12 k13 k14 k15 k16 k17;
     k21 k22 k23 k24 k25 k26 k27;
     k31 k32 k33 k34 k35 k36 k37;
     k41 k42 k43 k44 k45 k46 k47;
     k51 k52 k53 k54 k55 k56 k57;
     k61 k62 k63 k64 k65 k66 k67;
     k71 k72 k73 k74 k75 k76 k77];


A = inv(M)*K;

eig(A);

sqrt(eig(A));

[V,D] = eig(A);

(sqrt(eig(A)))/(2*pi);  % outputs the natural frequencies .....


ans =

     11.8862          % but 11.8827 Hz     for Laden Test Vehicle
     11.0240          % but 11.0233 Hz     for Laden Test Vehicle
      1.3538          % but  1.3094 Hz     for Laden Test Vehicle
      1.5714          % but  1.3890 Hz     for Laden Test Vehicle
      3.0955          % but  2.8688 Hz     for Laden Test Vehicle
     13.4553          % but 12.8007 Hz     for Laden Test Vehicle
     12.8146          % but 13.4389 Hz     for Laden Test Vehicle


V =

      0.0047   -0.0064    0.9354    0.3723    0.0000   -0.0000   -0.0000
     -0.0000   -0.0000   -0.0000   -0.0000    0.8833    0.0372   -0.0355
      0.0042    0.0046   -0.2346    0.8687    0.0000   -0.0000   -0.0000
      0.0004    0.7071    0.1727   -0.0992    0.2506   -0.6986    0.0811
      0.0004    0.7071    0.1727   -0.0992   -0.2506    0.6986   -0.0811
     -0.7071    0.0005    0.0720    0.2087   -0.2170   -0.1063   -0.7020
     -0.7071    0.0005    0.0720    0.2087    0.2170    0.1063    0.7020


% Four Wheel Hops - 11.8827, 11.0233, 12.8007 & 13.4389 which are
% almost the same for both the unladen and the laden test vehicle
%
% Bounce - 1.354 (unladen vehicle) and 1.309 (laden test vehicle)
%
% Pitch - 1.571 (unladen vehicle) and 1.389 (laden test vehicle)
%
% Roll - 3.095 (unladen vehicle) and 2.869 (laden test vehicle)
```

Identification of Vehicle Natural Frequencies

The MATLAB model has 7 DOFs and outputs seven natural frequencies in the order shown. It also produces a 7×7 matrix, V, of the eigenvectors that relate to the model's seven mode shapes. Each column in this matrix corresponds to a particular natural frequency; the vector represented by Column 1 of the matrix V corresponds to the mode shape associated with the first natural frequency, 11.8862 Hz, and so on. The elements in each column, in descending order, correspond to the model DOFs; the first element to body bounce (x), the second to body roll (ψ), the third to pitch (θ), the fourth and fifth to the front wheel hops (x_1 and x_2), and the sixth and seventh to the rear wheel hops (x_3 and x_4).

The elements of greatest magnitude in each column (eigenvector) are coloured red for ease of identification. Inspection of the columns of this matrix leads to the following conclusions:

(1) the first column relates to the frequency of 11.8862 Hz and its largest element is associated with resonance of the rear wheel hops, x_3 and x_4;
(2) the second column relates to the frequency of 11.0240 Hz and its largest element is associated with resonance of the front wheel hops, x_1 and x_2;
(3) the third column relates to the frequency of 1.3538 Hz and its largest element is associated with resonance of the body bounce, x;
(4) the fourth column relates to the frequency of 1.5714 Hz and its largest element is associated with resonance of the body pitch, θ;
(5) the fifth column relates to the frequency of 3.0955 Hz and its largest element is associated with resonance of the body roll, φ.

It is thus possible to make the following identifications between the seven natural frequencies obtained from this eigen-analysis and the seven modes of vibration of the model's seven DOFs:-

Mode		Natural Frequency (Hz)	
		Unladen Vehicle	Laden Vehicle
Bounce	x	1.3538	1.3094
Roll	ψ	3.094	2.8688
Pitch	θ	1.5714	1.3890
Front Wheel Hop	x_1, x_2	11.0240*	
Rear Wheel Hop	x_3, x_4	11.8862*	

*These frequency values substantially agree with those that were manually calculated in Chapter 6, Equation 6.5 and Equation 6.6.

Appendix D: Fast Fourier Transform (FFT) of Test Data

1. Introduction

Fast Fourier Transform (FFT) analysis was applied to the experimental road test data in order to identify those frequencies associated with the vehicle's natural vibration responses to road load disturbances. Most ride and handling vibrations involve frequencies well below a range of 40-50 Hz, and with the exception of wheel hop, the most important are below 10 Hz or even 5 Hz. Depending on amplitude, it is generally true that frequencies below 40-50 Hz are felt whereas those above that frequency range are heard. The FFT was applied to the time domain test data in order to identify the frequency components contained within it. When filtering the test signal data a second order Butterworth filter with a cut-off frequency of 40 Hz was employed. The MATLAB frequencies that were sought in the FFT plots were those of the heavier vehicle (bracketed values in Table 10 or Table 11).

When comparing the MATLAB results to the FFT of the experimental road test data it was considered that many other frequencies besides wheel hop, bounce, pitch and roll might be present. A cursory inspection of most of the FFT plots show a multiplicity of frequencies most of which have not been accounted for. It is possible to speculate about the origin of these other frequencies. The Ford Mondeo test vehicle was quite old with a high mileage and generally well-worn parts. Any static or dynamic imbalance associated with any of the 29cm radius road wheels would generate a detectable vibration frequency at less than 40Hz depending on the vehicle's speed. Some other possible sources might be undulations in the road surface, joints in the road surface, worn bearings and bushings and aerodynamic ('booming') effects. A consistent frequency at about 28-30 Hz was evident in most of the data. This could have been a natural flexing frequency associated with the vehicle body. Furthermore, the only tests that were conducted on public roads were the steady state cornering test and the single and double lane change. All of the other tests – the steer tests, and braking and power-off in a turn tests - were performed on a very bumpy and uneven

car-park surface. This undoubtedly contributed to the noisy signals and the plethora of low frequencies evident in some of the FFT plots.

An analogue hardware filter was used in the data collection process – it is assumed with a cut-off frequency of 100Hz, at least – and the data itself was subsequently filtered using a software filter with a cut-off frequency of 40Hz. None of the low frequency components in the FFT results are believed to be attributable to noise. It is also unlikely that a spurious frequency would be detected across many sensors and test manoeuvres. However, some do not appear in the data recorded by the wheel vertical deflection sensors. This is to be expected with regard to the body motions, bounce, pitch and roll, and the wheel hop frequencies should not appear strongly, if at all, in the data recorded by the gyros and accelerometers located at or near the centre of gravity of the sprung mass. The example of the bogus lateral acceleration signal associated with the steady state turn and the step steer was easily identified as such and has been ignored for FFT purposes.

In order to identify the vehicle's natural frequencies scrutiny of the FFT results was guided solely by the eigenanalysis conducted in Appendix C. Perfectly matching frequencies were sought but not always found although the correspondences were close. There are many frequencies in the FFT results, so many that there is always one sufficiently close in value to be regarded as a suitably matching candidate. It cannot be argued that all of the values picked up by the sensors are spurious or are due to noise because, although some of them undoubtedly may be, many of them appear in much of the data across most or all of the tests. This is especially true of those that are being tentatively identified as the wheel hop (11 and 12Hz), bounce (1.3Hz), pitch (1.4Hz) and roll (3Hz) frequencies. The correspondence is not always exact for the reasons outlined in Chapter 6 and Chapter 7. However, we can be quite confident that the vehicle's natural frequencies were actually recorded in the data and do appear in the FFT results.

Correlations between the MATLAB results and the FFT results remain reasonably accurate. However, if this identification process is considered to be faulty or unsafe

then the only other possible explanation is that the data used to create the MATLAB model is itself incorrect and does not belong or refer to the vehicle tested.

2. Wheel Hop Natural Frequency

The results of the FFT analysis were examined to identify the Mondeo's wheel hop frequencies and its natural frequency of vibration in bounce, roll and pitch modes. The expected wheel hop frequencies of 11Hz (front) and 12Hz (rear) were sought in the road test data and are somewhat in evidence in the pitch signal from the *J-Turn or Step Steer* (Figures D.1), the *Braking in a Turn* (Figure D.2), the *Pulse Steer* (Figure D.3), and the *Power-off in a Turn* (Figure D.4) manoeuvre. They may also possibly be apparent in the *Power-off in a Turn* (Figure D.5) and the *Braking in a Turn* (Figure D.7). It would be expected that wheel hop would be excited by any suddenly introduced disturbing force impacting the wheel and this appears to have been the case with the test data analysed using FFT. Much of the ground over which these tests were conducted was very rough and bumpy and there can be no doubt that the wheel assemblies were excited in their region of resonance. The magnitude of their signature in the FFT results is small because their contribution to the motions recorded at the gyros and accelerometers is small.

Happian-Smith (2001), pp.323-326, discusses the effect of suspension stiffness ratio (r_s) – the ratio of tyre stiffness (k_t) to suspension stiffness (k_s) – on the input-to-output displacement transmissibility between the road and the sprung mass. A high ratio ($r_s \geq$ 8) offers low transmissibility and corresponds to a soft suspension and good ride quality whereas a low ratio ($r_s \leq 5$) corresponds to a hard suspension and high transmissibility. The Mondeo has ratios of 6.2 at the front and 7.2 at the rear which puts it in the mid-range where the transmissibility of road inputs relative to the sprung mass is of the order of 1.5 to 2.5 at low frequencies (f < 5Hz) and, relative to the unsprung mass, of the order of 1.5 at the wheel hop frequency (10-12Hz). The Mondeo's transmissibility relative to the sprung mass at the wheel hop frequency is in the region of 0.1-0.2, showing a high level of attenuation. However, some transmission does occur and, as the vehicle was tested on very rough ground, it is no surprise that the signature of the wheel hop frequencies is present in the FFT results.
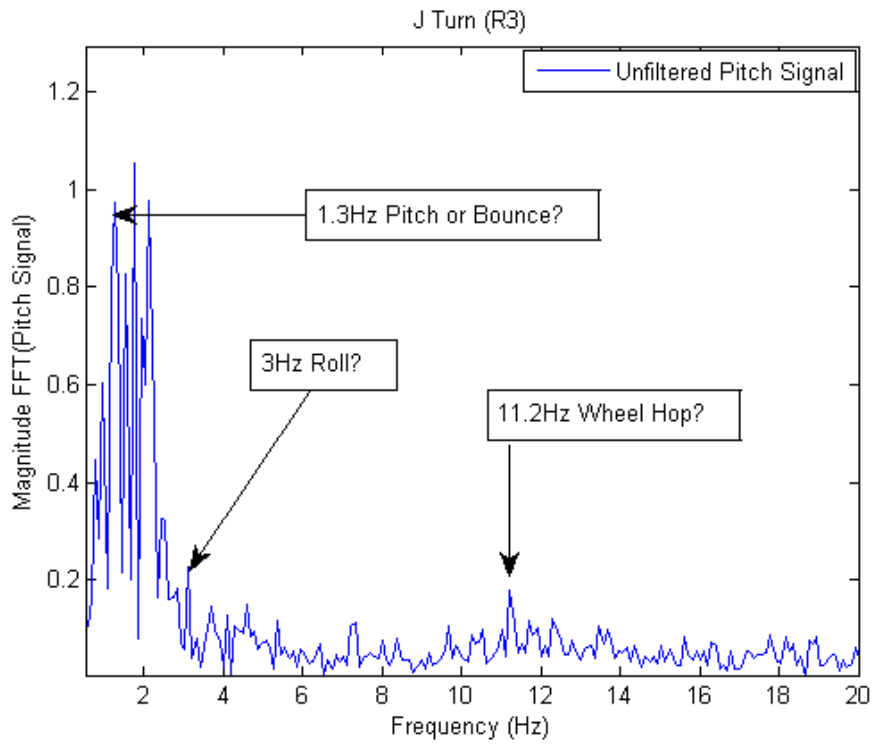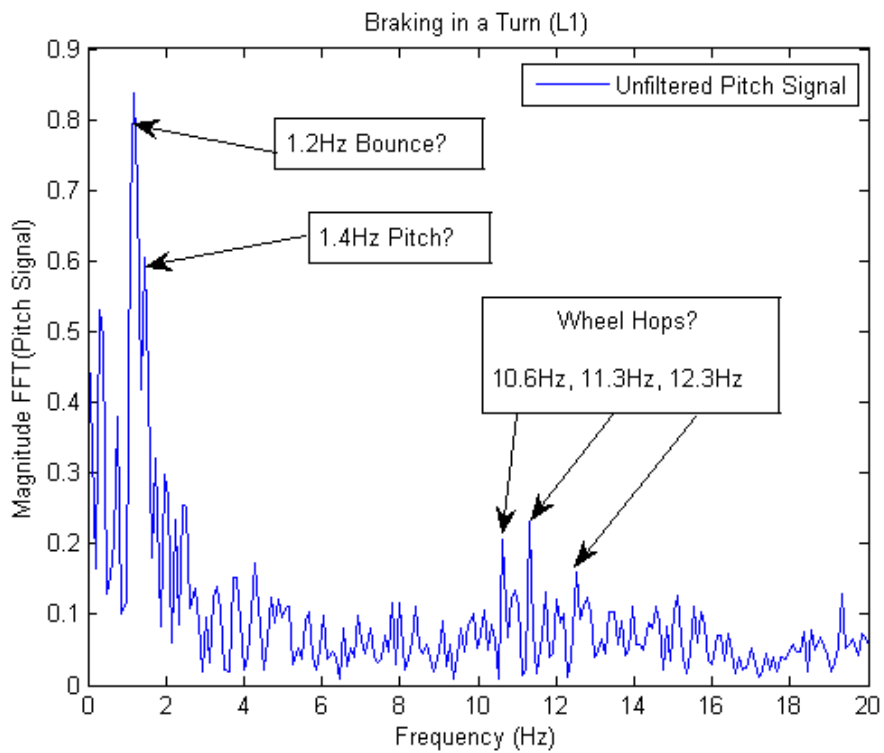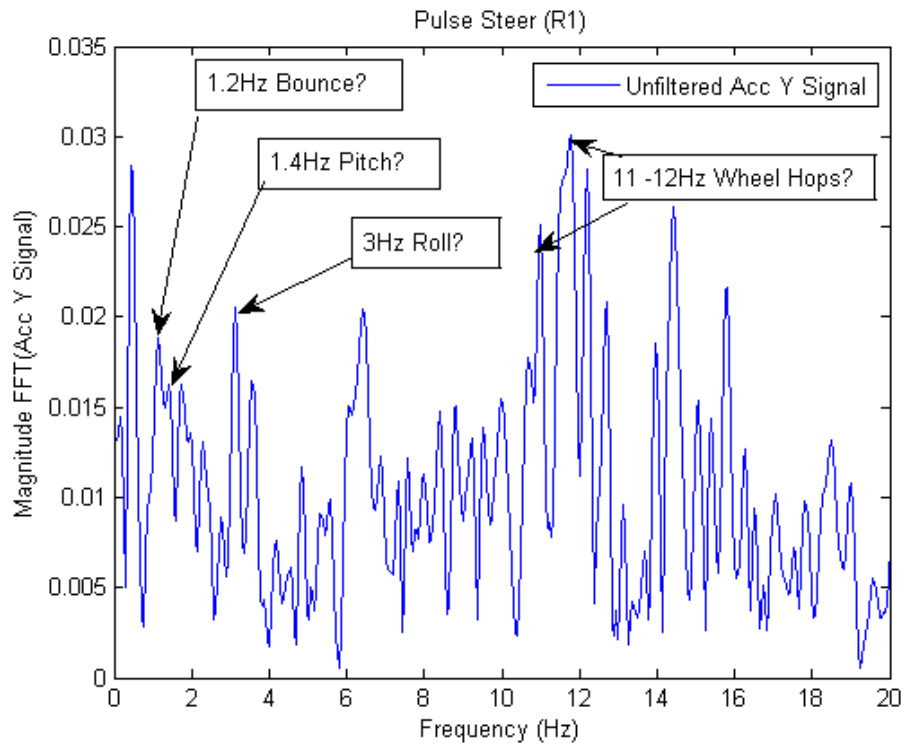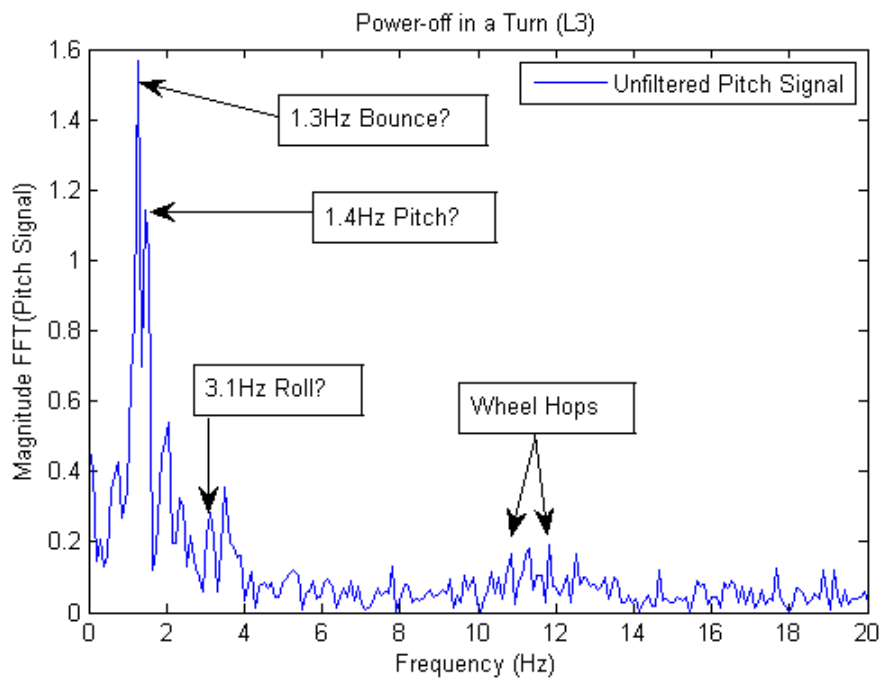
Figure D.1

Figure D.2

Figure D.3

Figure D.4

3. Bounce Natural Frequency

The MATLAB model gave a bounce and a pitch frequency for the laden test vehicle of 1.3Hz and 1.4Hz respectively, slightly higher at 1.35Hz and 1.57Hz for the less massive unladen Mondeo. The bounce mode is usually a response to bumps and undulations in the road surface but despite this the road tests seem to have produced a detectable bounce motion in the vehicle. Some of the tests conducted on the Mondeo were less likely to set the vehicle's bounce response into motion. Lane changing, steering inputs, braking and accelerating tend to excite other response modes more readily – roll and pitch, for example. However, the bounce and pitch frequencies are quite close to each other and, being functions primarily of the stiffness of the suspension springs only, these frequencies are inevitably coupled together and influence each other so that if one is excited so too is the other. The bounce motion may have been present at 1.2 - 1.3Hz or thereabouts in the *J Turn (Step Steer)* response (Figure D.1), in the *Pulse Steer* (Figure D.3), in the *Power-off in a Turn*
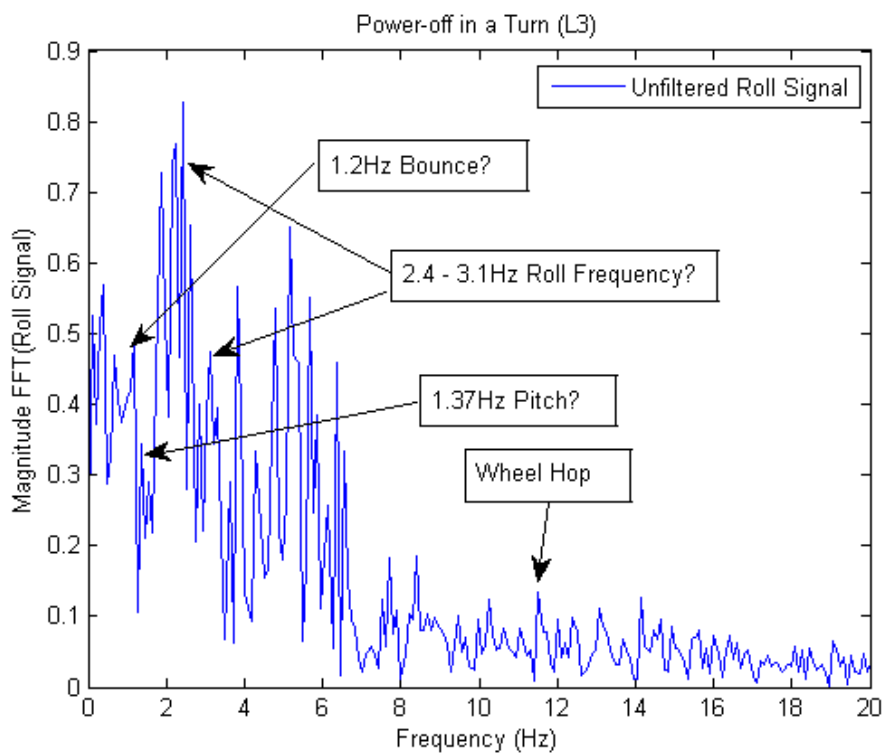

Figure D.5

manoeuvre (Figure D.4) and the *J Turn (Step Steer)* (Figure 6). This is apparent from an inspection of the FFT graphs where typical signatures of both can be seen.
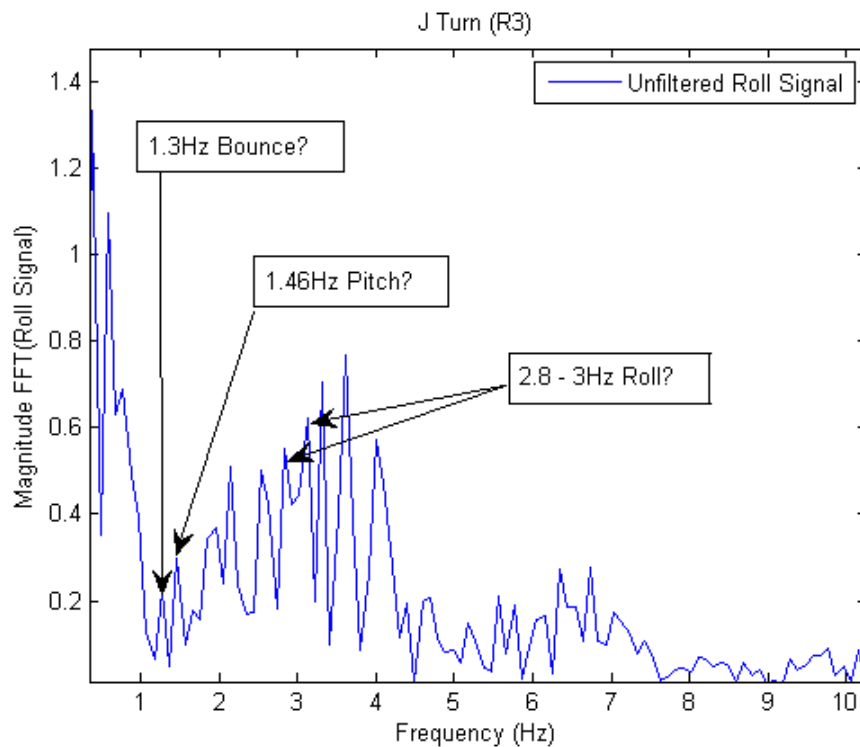

Figure D.6

In Figure D.2 (*Braking in a Turn*) and Figure D.4 (*Power-off in a Turn*) the signatures of the bounce/pitch event are almost identical. In both manoeuvres the car is executing a turn of small radius and the resulting sudden deceleration causes both a pitch and bounce reaction.

4. Pitch Natural Frequency

As noted, the MATLAB model analysis produced a value for the pitch natural frequency of about 1.4Hz for the heavier test vehicle. The pitch frequency of the unladen vehicle was about 1.6Hz. Of all of the tests conducted on the Mondeo, the two most likely to excite the vehicle's pitch motion were the *Braking in a Turn* and the *Power-off in a Turn* manoeuvres. The pitch frequency of 1.4Hz has already been mentioned with reference to Figure D.2 (*Braking in a Turn*) and Figure D.4 (*Power-*
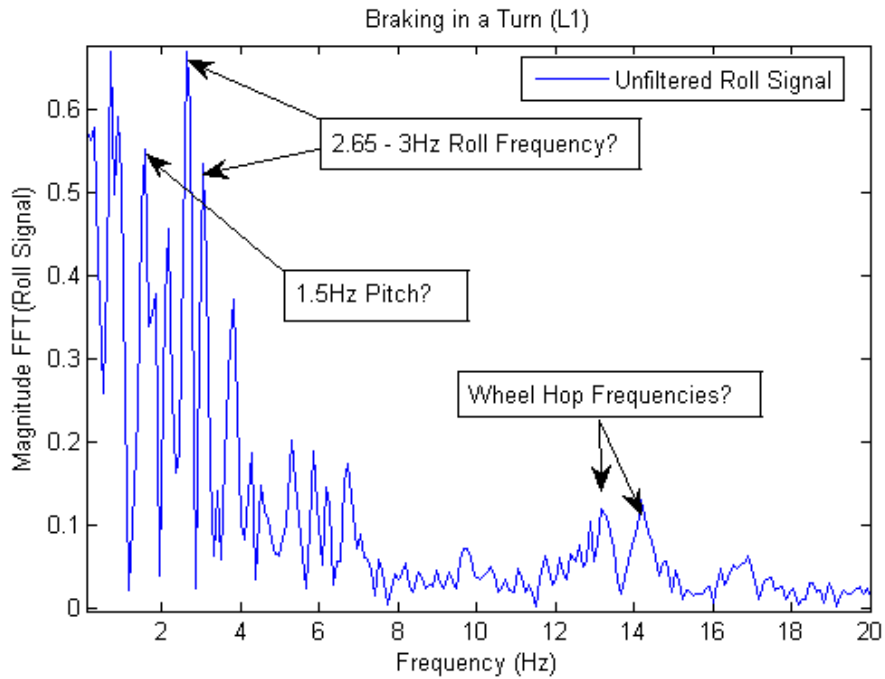
Figure D.7

off in a Turn). Its close association with a possible bounce frequency of 1.2Hz is also evident in Figure D.5 (another *Power-off in a Turn* manoeuvre). Here it appears as a 1.37Hz frequency. It may also be present at 1.3Hz in Figure D.1 (*J- Turn/Step Steer*) and either at 1.3Hz or 1.46Hz in Figure D.6 (another *J- Turn/Step Steer*). Inspection of Figure D.7 (*Braking in a Turn*) shows a possible pitch frequency at 1.5Hz and again in Figure D.9 (*Pulse Steer*) at 1.36Hz contributing to the roll vibration. Again, though not very pronounced, is the 1.4Hz frequency showing in Figure D.3 (*Pulse Steer*).

5. Roll Natural Frequency

All of the tests to which the Mondeo was subjected would excite the roll response of the vehicle to some extent, so it should be expected that evidence would be found of the roll natural frequency component in all of the FFT results. This would appear to be the case for all the roll sensor data except that in Figure D.9 (*Pulse Steer* test) unless the 2.54Hz can be attributed to it. All of the roll sensor data from the other tests show a frequency component at or below 3Hz: Figures D.5 (*Power-off in a Turn*), Figure D.6 (*J-Turn/Step Steer*), Figure D.7 (*Braking in a Turn*) and Figure D.8 (*Double Lane Change*). The nature of the test manoeuvres were such that the vehicle would have
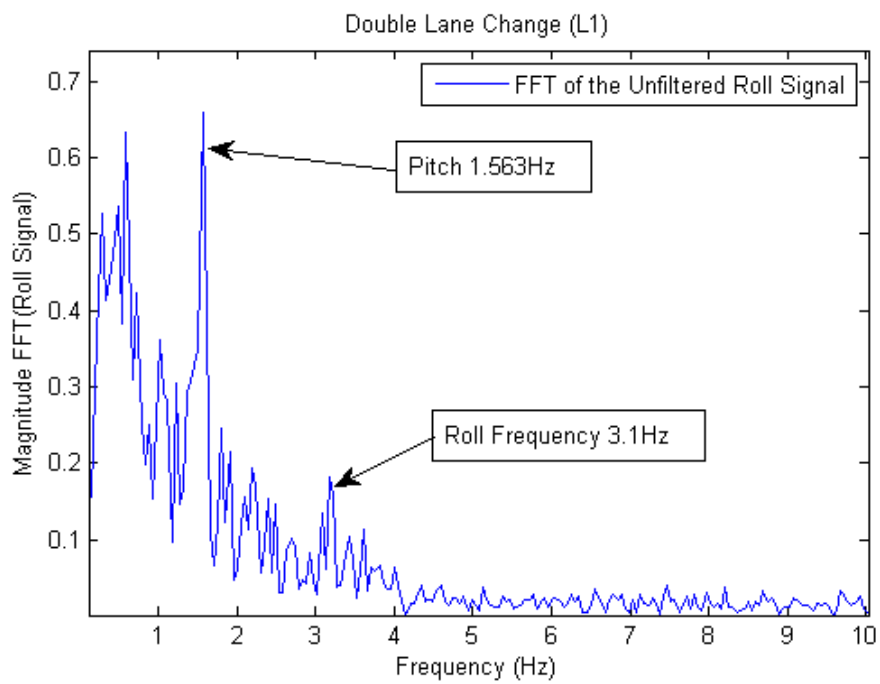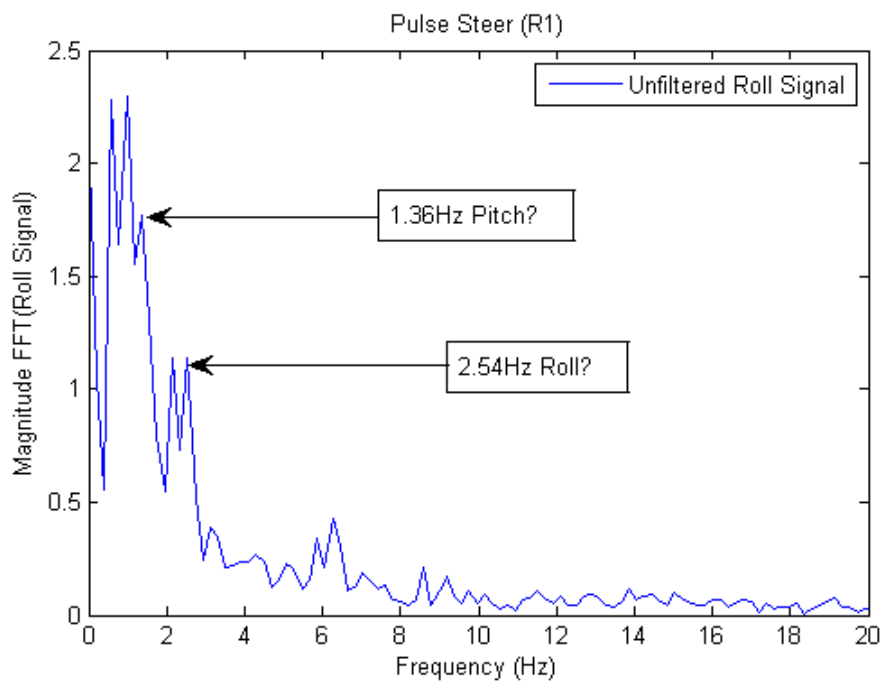
Figure D.8

Figure D.9

experienced both roll and pitch combined. The pitch sensor data also indicates the presence of a 3Hz component in Figure D.1 (*J-Turn/Step Steer*), Figure D.3 and Figure D.9 (*Pulse Steer* test), and Figure D.4 (*Power-off in a Turn*). These agree reasonably well with the results from the MATLAB Full Car Model (2.87Hz) allowing for the elements of error described in Chapter 6 and Chapter 7. Unfortunately, no information regarding roll frequency was obtained from Ford.
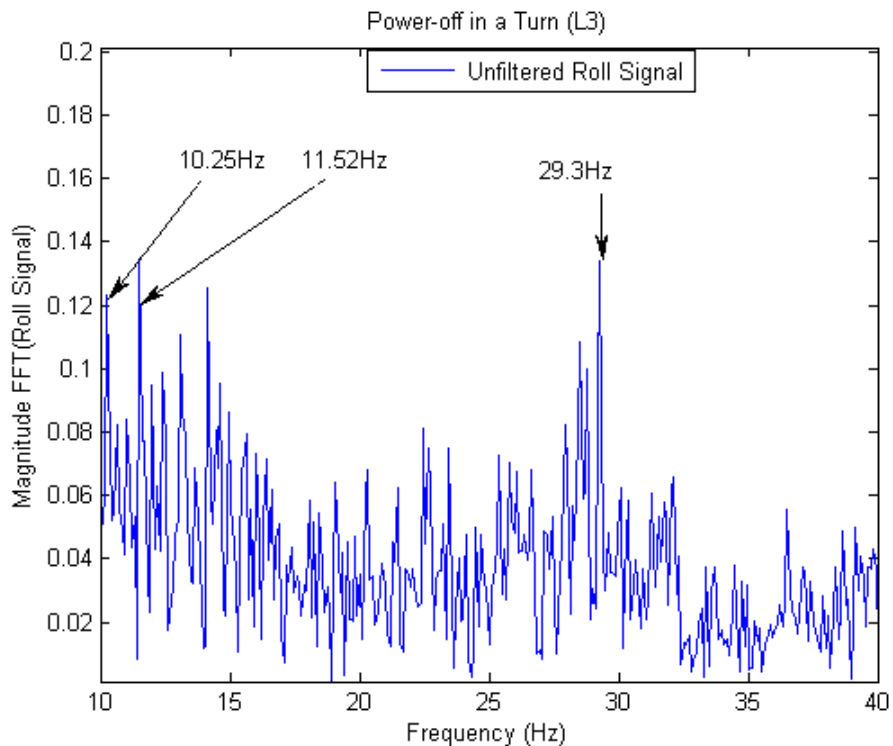

Figure D.10

6. Other Frequencies

Figure D.3 (*Pulse Steer*) shows evidence of all the vehicle natural frequencies discussed so far. There are many more frequencies than can be possibly accounted for and it is mere speculation as to their origin. The test vehicle was nearly ten years old. One possible source of vibration which has not been considered is static and dynamic imbalance in the Mondeo's wheels and wheel wobble associated with wear in bushings and other suspension parts. Wheel imbalance will manifest itself as a

hopping or wobbling vibration whose frequency will depend on the rotational speed, ω (rad/s), of the wheel. The velocities, v (m/s), at which some of the vehicle tests were carried out can be grouped as shown in Table 13 and since the effective rolling radius, r (m), of the wheels was 0.29m any associated vibration due to imbalance can be readily calculated. For example, at a velocity of 48km/hr a hopping frequency due to wheel imbalance would be calculated using equation (Eqn. A):

$$ f = \frac{\omega}{2\pi} = \frac{1}{2\pi}\left(\frac{v}{r}\right) \quad \Rightarrow \quad \frac{1}{2\pi}\left(\frac{48/3.6}{0.29}\right) = 7.3\,\text{Hz} \qquad \text{(Eqn. A)} $$

Similar calculations for the other velocities at which the vehicle was driven during particular tests produces the following frequencies:

Velocity Range (km/hr)	Vibration Frequency
20 – 32	3 – 5 Hz
48	7 Hz
100 – 113	15 – 17 Hz

Table 14: Possible Wheel Imbalance Frequencies related to Vehicle Velocity

The *J-Turn (Step Steer)*, the *Pulse Steer*, the *Power-off-in-a-Turn*, and the *Braking-in-a-Turn* test procedures were all initiated at a vehicle speed of 32km/hr (20mph). Inspection of some of the FFT plots already presented, Figures D.1, D.2, D.5 and D.7, all of which relate to some of these manoeuvres, reveals indications of a vibration occurring at a fundamental frequency of 7Hz or less with some possible harmonics at 14Hz and higher frequencies in Figures D.3 and D.5. Figure (D.12) also indicates the presence of a vibration around 5Hz and another possible at 3Hz. However, the strongest evidence of a wheel imbalance appears in Figure (D.12) which presents the FFT data from the *Double Lane Change* performed at 103km/hr. Here two very clear signals were apparent at 15.5Hz and 31Hz. This was the only set of results that showed so clear a signal and it would be expected that, if wheel imbalance was a

feature of the test vehicle, then its vibration signature would be consistently evident elsewhere in the analysed data.
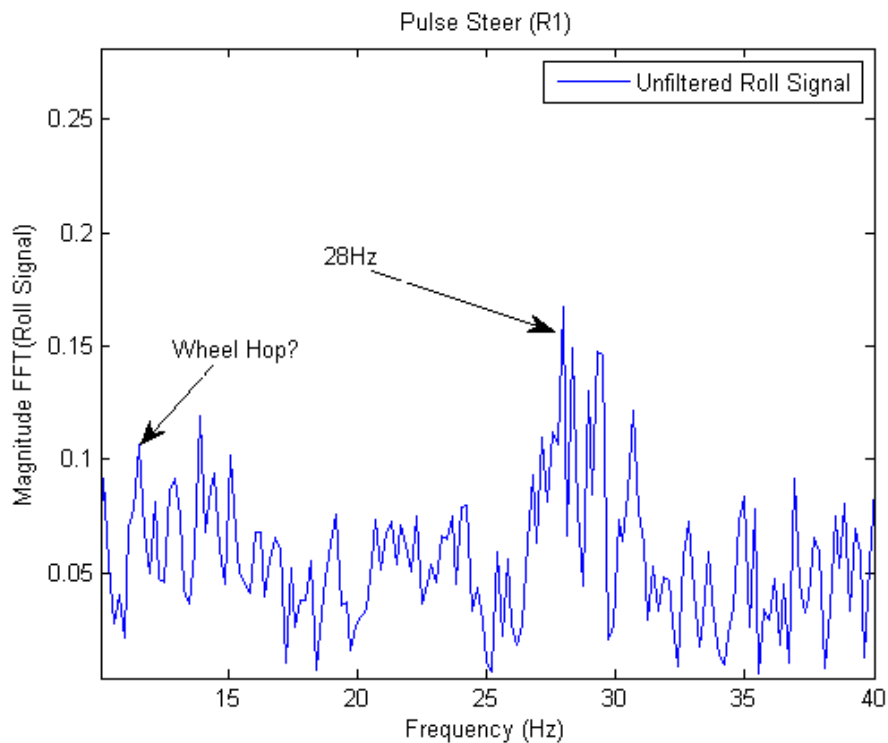

Figure D.11

Other frequency components, mostly less than 10Hz, which have not been mentioned so far have been evident in the figures presented in this chapter. It is a matter of pure speculation to attempt to explain the origin of these vibrations although it has been previously suggested that some possible sources might be the road surface, worn bearings and bushings, and aerodynamic ('booming') effects, for example. One a fairly consistent frequency component of 28-30Hz was evident in the data recovered from all of the tests that were performed. Its signature is clearly evident in Figure D.10 (*Power-off-in-a-Turn*), Figure D.11 (*Pulse Steer*) and Figure D.12 (*Double Lane Change*). This may possibly be due to a flexing vibration induced in the monocoque body of the test vehicle.
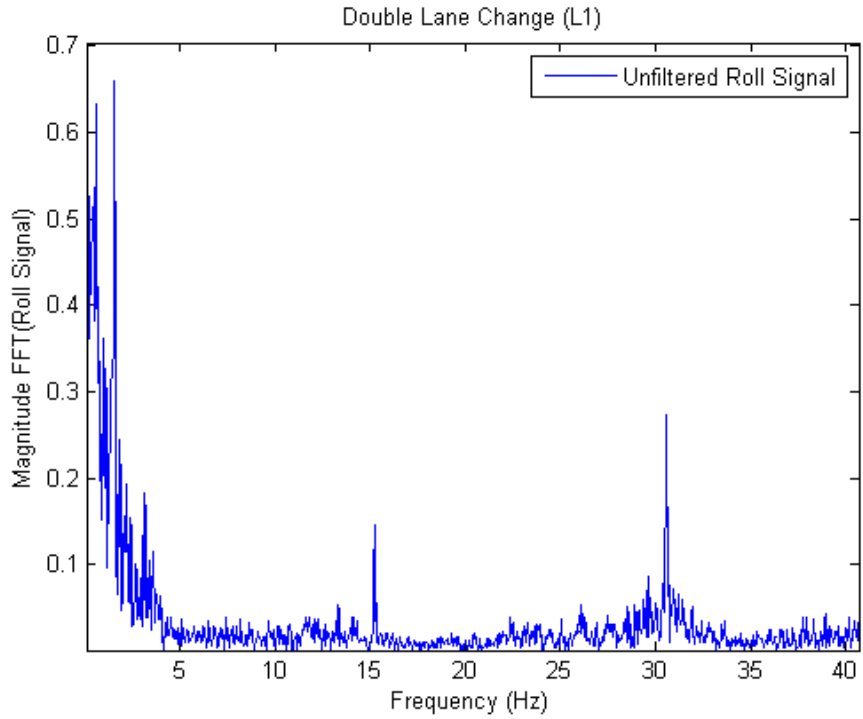
Figure D.12

A further set of FFT plots, Figures (D.13) to (D.17), are provided that show the frequency spectrum out to the filter corner frequency of 40Hz.
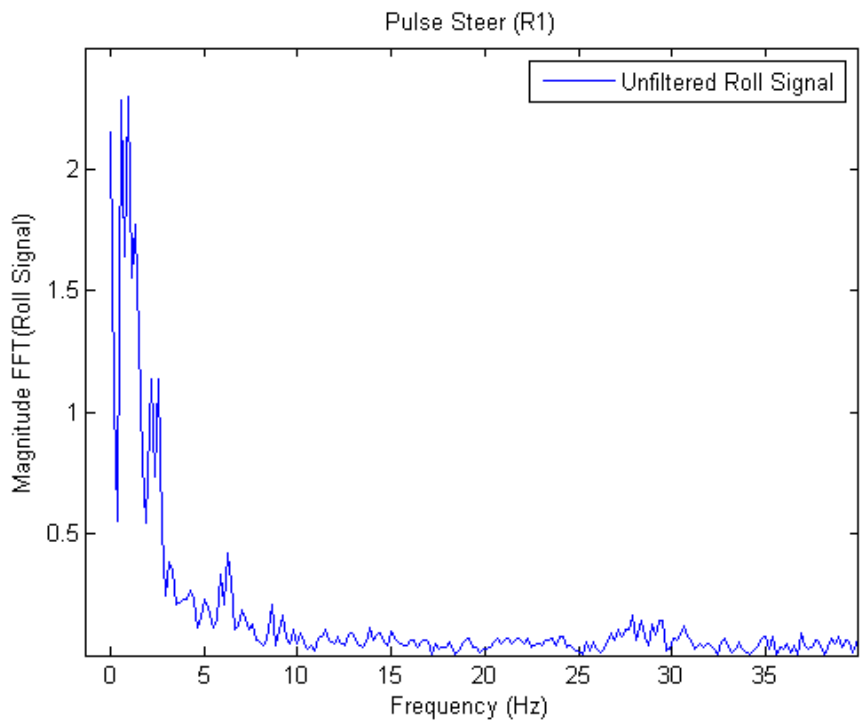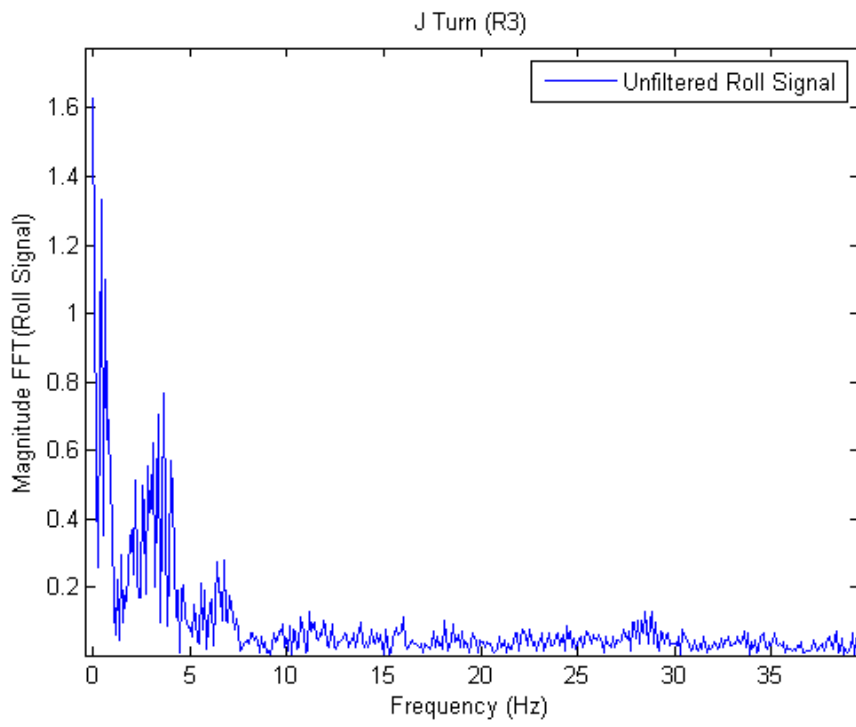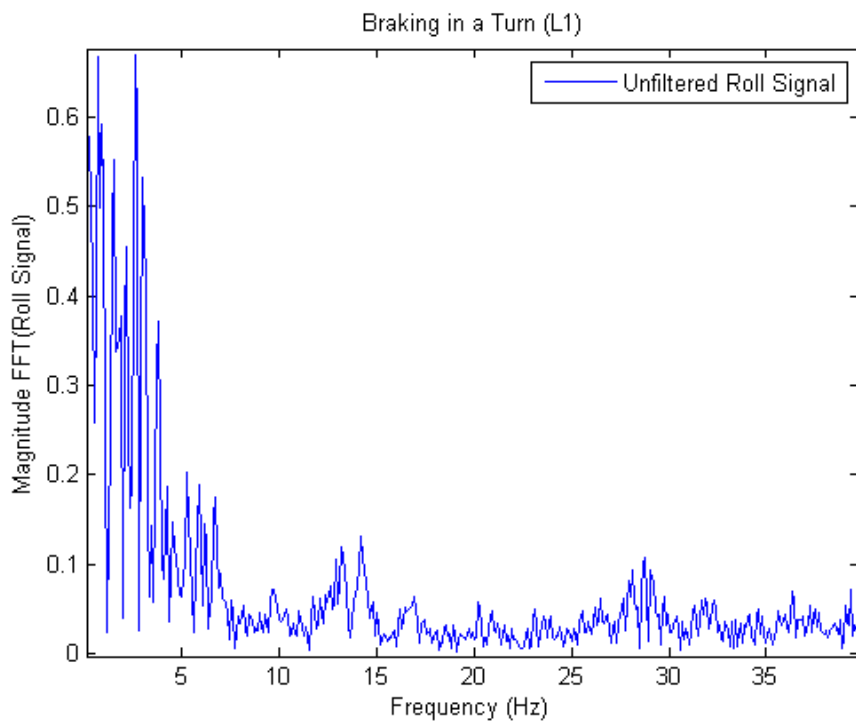

Figure D.13

Figure D.14

Figure D.15
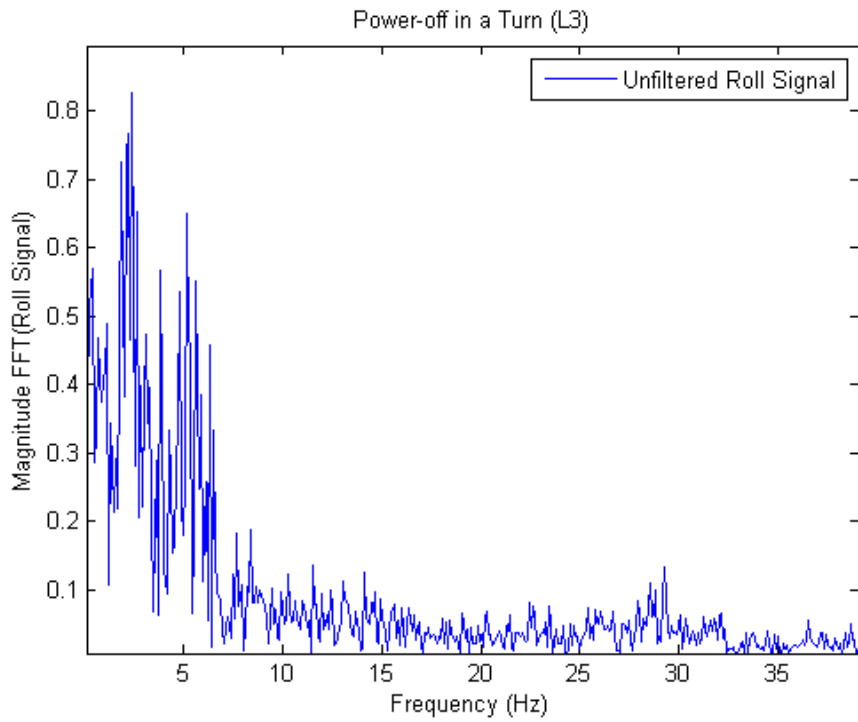
Figure D.16
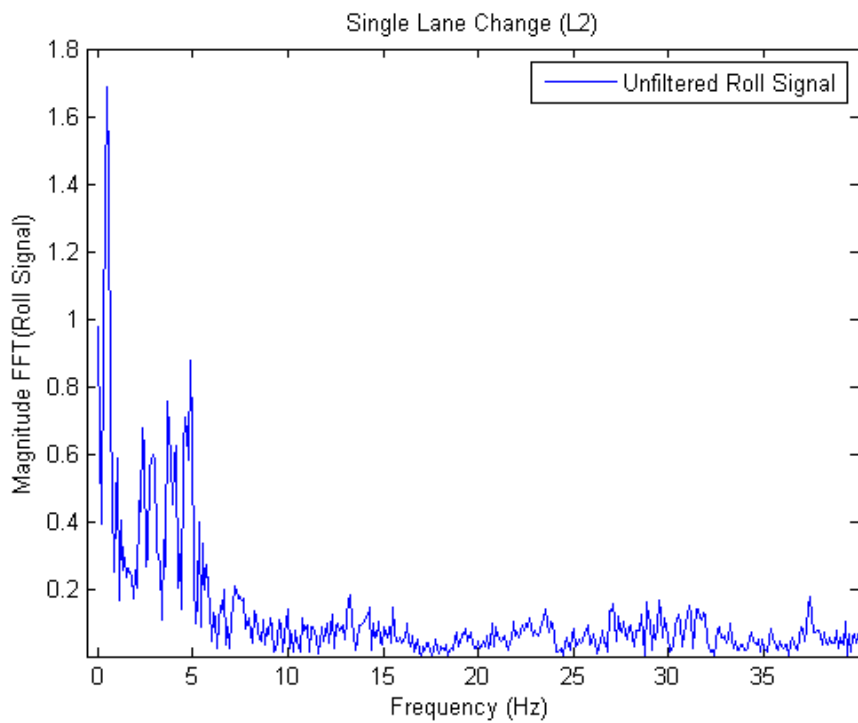
Figure D.17

Appendix E: Original Ford Mondeo Information

_____

GENERAL CHARACTERISTICS (Ford Mondeo)

_____

(PARAMETER)	(UNITS)	(TOTAL)	(LEFT)	(RIGHT)
Total weight	N	14.64E+03		
Front ground reaction	N	8791.74	4395.92	4395.82
Rear ground reaction	N	5852.29	2926.06	2926.23
Total roll inertia	Kg mm**2	512.9E+06		
Total pitch inertia	Kg mm**2	2.599E+09		
Total yaw inertia	Kg mm**2	2.769E+09		
Total product Ixy	Kg mm**2	1.268E+06		
Total product Ixz	Kg mm**2	-3.830E+06		
Total product Iyz	Kg mm**2	71.69E+03		
Sprung mass	Kg	1312.84		
Sprung roll inertia	Kg mm**2	396.7E+06		
Sprung pitch inertia	Kg mm**2	2.240E+09		
Sprung yaw inertia	Kg mm**2	2.331E+09		
Sprung product Ixy	Kg mm**2	1.269E+06		
Sprung product Ixz	Kg mm**2	6.491E+06		
Sprung product Iyz	Kg mm**2	71.27E+03		
Total c.g. height	mm	661.13		
Sprung c.g. height	mm	698.64		
Wheelbase	mm	2745.27	2745.27	2745.27
Bounce natural frequency	Hz	1.44		
Pitch natural frequency	Hz	1.68		
Ride frequency ratio	Hz	1.16		

_____

FRONT (Macpherson) SUSPENSION CHARACTERISTICS

_____

(PARAMETER)	(UNITS)	(AVERAGE)	(LEFT)	(RIGHT)
Unsprung mass (total)	Kg	97.91		
Unsprung c.g. height	mm	381.47		
Roll center height	mm	106.95		
Wheel center rise	mm	18.79	18.79	18.79
Static loaded tire radius	mm	379.00	379.00	379.00
Track width	mm	1521.44		
Axle distance from cg	mm	1097.11		

(PARAMETER)	(UNITS)	(AVERAGE)	(LEFT)	(RIGHT)
Wheel rate	N/mm	32.56	32.56	32.56
Single bump wheel rate	N/mm	46.45	46.45	46.45
Ride rate	N/mm	32.04	32.04	32.04
Tire rate	N/mm	2017.34	2017.34	2017.34
Roll rate - wheel	N mm/DEG	1.637E+06		
Roll rate - total	N mm/DEG	1.574E+06		
Wheel/spring ratio	mm/mm	954.1E-03	954.1E-03	954.1E-03
Wheel/shock ratio	mm/mm	925.7E-03	925.7E-03	925.7E-03
Wheel hop natural freq.	Hz	32.57	32.57	32.57
Wheel tramp natural freq.	Hz	N/A		
Front ride frequency	Hz	1.43		

_____

REAR SUSPENSION (QUADRALINK_with_STRUT) CHARACTERISTICS

_____

(PARAMETER)	(UNITS)	(AVERAGE)	(LEFT)	(RIGHT)
Unsprung mass (total)	Kg	82.52		
Unsprung c.g. height	mm	396.19		
Roll center height	mm	123.67		
Wheel center rise	mm	45.33	45.33	45.32
Static loaded tire radius	mm	379.72	379.72	379.72
Track width	mm	1527.71		
Axle distance from cg	mm	1648.16		
Wheel rate	N/mm	28.09	28.09	28.09
Single bump wheel rate	N/mm	38.88	38.88	38.88
Ride rate	N/mm	27.71	27.71	27.71
Tire rate	N/mm	2014.74	2014.74	2014.74
Roll rate - wheel	N mm/DEG	1.285E+06		
Roll rate - total	N mm/DEG	1.246E+06		
Wheel/spring ratio	mm/mm	950.7E-03	950.7E-03	950.7E-03
Wheel/shock ratio	mm/mm	1.01 1.01	1.01	
Wheel hop natural freq.	Hz	35.41	35.41	35.41
Wheel tramp natural freq.	Hz	N/A		
Rear ride frequency	Hz	1.65		